ABSTRACT

A Study on Radical Scavenging
and Magnetic Resonance Imaging
Characteristics of Stable Radical Nitroxides

by

Shiey-Shiun Horng

Several nitroxides have been prepared for study of their image enhancement capability. These nitroxides contain different nitroxyl moieties within one molecule. On MRI examination for the nitroxides prepared, TEMPO and HPTPO are better due to their better water solubility, even though some of the others have more nitroxyl centers available. The intensity response is linear with respect to concentration in the range studied in most of the cases except for HPTPO, whose intensity finally reaches maximum when its concentration is higher than 10 mM.

Three sources of biomass, namely, liver microsomes, whole-cell yeast and a bacterial activated sludge consortium, have been immobilized in calcium alginate gel. These beads are evaluated for contrast as measured on a clinical MRI machine with respect to time. This system is proposed as a hypothetical method to characterize the nitroxide behavior in porous beads containing active biological systems.

Furthermore, the prepared nitroxides are used as model inhibitors. Their inhibition characteristics are studied on styrene polymerization . Molecules with multinitroxyl centers within a single molecule possess stepwise radical killing reactivity. Their induction periods are also found to be proportional to their concentrations studied. Each of these nitroxyl centers exhibits slightly different inhibitory capabilities in terminating the growth of polymer chains. A kinetic model is developed to calculate individual inhibition constants for each molecule's nitroxyl center and to characterize kinetic behavior.

A STUDY ON RADICAL SCAVENGING AND MAGNETIC RESONANCE IMAGING CHARACTERISTICS OF STABLE RADICAL NITROXIDES

by

Shiey-Shiun Horng

A Dissertation
Summited to the Faculty of New Jersey Institute of Technology
in Partial Fulfillment of the Requirements for the Degree of
Doctor of Philosophy
Department of Chemical Engineering, Chemistry,
and Environmental Science
October 1992

APPROVAL PAGE

A Study on Radical Scavenging
and Magnetic Resonance Imaging
Characteristics of Stable Radical Nitroxides

by

Shiey-Shiun Horng

5-14-92

Dr. Sam S. Sofer, Dissertation Advisor
Professor of Chemical Engineering,
Chemistry and Environmental Science, NJIT

5/18/92

Dr. Ching-Rong Huang, Committee Member
Professor of Chemical Engineering,
Chemistry and Environmental Science, NJIT

5/20/92

Dr. Dana E. Knox, Committee Member
Professor of Chemical Engineering,
Chemistry and Environmental Science, NJIT

5/20/92

Dr. Barbara Kebbekus, Committee Member
Professor and Associate Chairperson of Chemical Engineering,
Chemistry and Environmental Science, NJIT

5/20/92

Dr. Arthur Greenberg, Committee Member
Professor of Environmental Science
Cook College, Rutgers University

BIOGRAPHICAL SKETCH

Author: Shiey-Shiun Horng

Degree: Doctor of Philosophy

Date: October, 1992

Undergraduate and Graduate Education:

- Doctor of Philosophy, New Jersey Institute of Technology, Newark, New Jersey, 1992
- Master of Science in Chemical Engineering, New Jersey Institute of Technology, Newark, New Jersey, 1988
- Bachelor of Science in Chemical Engineering, National Central University, Taiwan, 1980

Major: Chemical Engineering

Publications/Presentation:

Horng, S. and Huang, C. R. "Characterization of Viscoelastic and Thixotropic Properties of Blood in Diabetic Patients." will be presented in Beijing, China, August, 1992, at the *Satellite Symposium of the Eighth International Congress of Biorheology*. Beijing, China.

Horng, S. and Sofer, S. "Synthesis of Polyradical Nitroxides for MRI Contrast Agents." *Preceeding, Interphex-USA*, 1991.

Horng, S. and Sofer, S. "Studies of Multiradical Nitroxides as MRI contrast Agents" *Preceeding, Interphex-USA*, 1992.

ACKNOWLEDGEMENTS

The difficulties involved in this research were greater than had been expected. There are a number of contributors to this research, without whose support this work would have been impossible.

Dr. Sam S. Sofer, my advisor, has always stayed with me and strongly supported this work which I greatly appreciate.

My committee members are Dr. C. R. Huang, Dr. D. Knox, Dr. B. Kebbekus and Dr. A. Greenberg. I thank them for their time and effort through this long term research, in particular, Dr. Huang for his assistance in developing the kinetic model and for Dr. Kebbekus for her consultation in nitroxide analyses.

Many thanks are also due to Dr. D. K. Shen. His original proposal and early technical assistance were crucial to this research.

Prof. J. Potenza, Prof. G. Strauss and Dr. J. Yao (Rutgers University at New Brunswick) performed and interpreted ESR spectra. Dr. J. T. Cheng conducted the relaxivity experiment on NMR (Rutgers University, Newark) and Mr. S. Reantragoon measured MRI intensity at University Hospital, Newark, New Jersey.

The persistent strength to attain this degree is mainly from the support of my family members, my parents, my wife and my sons. Their encourangement and sacrifices make this happen. They deserve much credit for this work.

Finally, the author wishes to express appreciation for the timely help and valuable suggestions from the colleages in the Lab, including Emilia Rus, Fayaz Lahkwala and Tim Roche.

This work was partially supported by the state of New Jersey Sponsored Chair in Biotechnology Fund, and by the New Jersey Commission on Cancer Research Award #90-656-CCR-00.

TABLE OF CONTENTS

LIST OF TABLES

LIST OF FIGURES

CHAPTER 1

INTRODUCTION

Most organic free radicals have a very short lifetime, but sometimes the structural features can enhance the stability. The unpaired electron in the galvinoxyl radical is highly delocalized into its aromatic ring. Thus it is very stable and can be kept in air for several weeks at ambient temperature and pressure. Nitroxides without α-hydrogen are also stable in a variety of environments. They are extremely stable with regard to an oxygen atmosphere and to heating. Their steric hindrance also protects the nitroxyl group from dimerization and disproportionation. Such radicals, which have a long lifetime and are resistant to dimerization or bimolecular self-annihilation, are called stable free radicals.

Without losing their paramagnetism, stable nitroxides can dissolve in nonpolar and polar solvents. Reactions can be carried out on other functional groups without affecting the nitroxyl center. As indicated in equations (1) and (2), modifications of the functional groups in nitroxide molecules are easily performed at moderate conditions. The extensive studies of the functionalization of known carbocylic and heterocyclic nitroxides are discussed elsewhere [1-3].

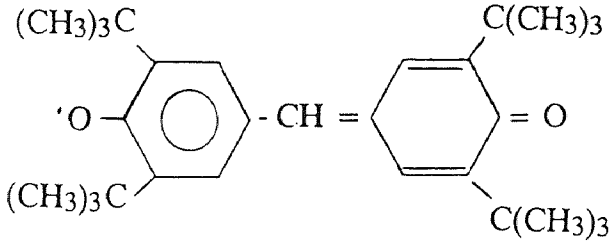

Galvinoxyl

The progress in the chemistry of nitroxides is largely stimulated by their fast expanding scientific and practical applications in many fields. Moreover, nitroxides can be easily identified and quantitatively determined by simple physical methods. Their paramagnetic property can be used to solve some special problems in structural organic chemistry. The progress of electron spin resonance (ESR) technology

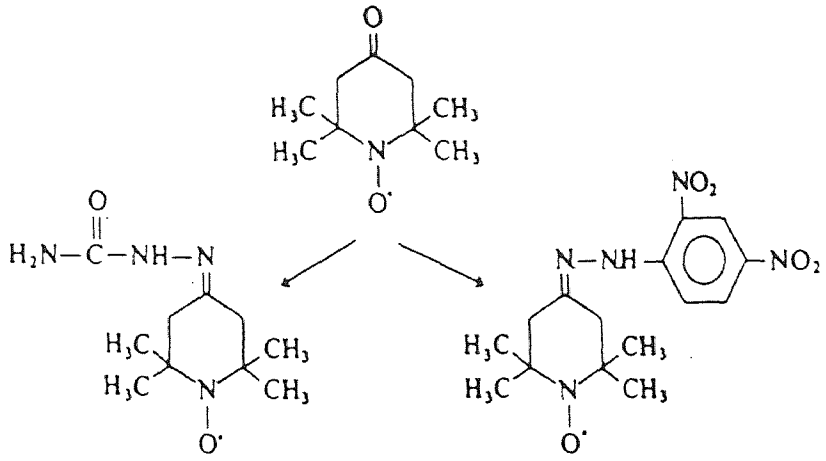

(1)

has further established the value of these radicals as spin labling and radical trapping agents. Their advantages have also been extended to the fields of cancer studies, medicine development and diagnostic improvements. However, the focus of this study will concentrate on the use of nitroxides as radical terminators. Also, they are found to be potential candidates for medical resonance imaging (MRI) contrast agents, and more results on this study are discussed as well.

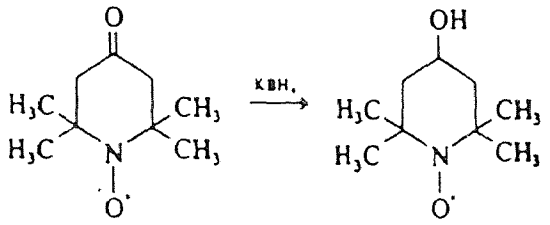

(2)

1.1 MRI Contrast Agents

1.1.1 Basic Principles

Atomic nuclei with an odd number of protons or neutrons, or both, have a magnetic moment. In a large external magnetic field, these atoms tend to precess about and align along the direction of the applied magnetic field. However, the alignment can be disturbed by applying a RF (radio frequency) wave, and on removal of the RF wave, the spins return to alignment. This return process is known as relaxation.

Since the frequency of the nuclear magnetic resonance (NMR) responding signal is proportional to the magnetic field strength and the local magnetic fields differ slightly but significantly for the same type of nuclei, the nuclei residing in different locations of the specimen will resonate at different frequencies after application of RF. In the production of MRI images, one can therefore apply gradient magnetic fields to the observed tissues and determine where in the field the signals from the relaxing spins emanate. As three orthogonal directions of magnetic field gradients are applied, spatial information on the tissues can be obtained.

MRI can measure and display image parameters that differ from tissue to tissue and which also change with disease. The NMR signal is proportional to proton concentration and exponentially proportional to two relaxation parameters (T_1 and T_2). T_1 is spin lattice relaxation which is a measure of how rapidly an excited atom can share energy with its surroundings. T_2 is spin spin relaxation time which is a measure of the homogeneity of the magnetic field. The signal intensity, SI, can be expressed [4] as follows:

$$SI = Hf(v)\,[\,1 - \exp^{(-b/T_1)}\,]\,[\,\exp^{(-a/T_2)}], \tag{3}$$

where H is the local hydrogen concentration; "a" and "b" are echo delay time measured in seconds and the repetition time measured in milliseconds respectively. They both are values under computer control for obtaining best image. Sometimes "a" is referred to as T_E and "b" as T_R. Different settings for a and b can yield different contrast tissue values on spin echo intensity images. The f(v) is the motion factor for protons. It is a function of both the speed with which the hydrogen nuclei move through the region being imaged and the fraction of the total number of nuclei that are moving. The intensity is computed directly from the signal received. T_1 and T_2 parameters can be calculated from the intensity data. This equation also demonstrates that reducing T_1 increases image intensity (SI), while decreasing T_2 decreases image intensity.

There are a number of methods to alter image contrast. These methods are primarily two types: the manipulation of physical characteristics and the manipulation of chemical characteristics of tissues. The former includes changes of tempera-

ture and viscosity and the latter the alteration of composition of a tissue, particularly the hydrogen concentration. Since it is not feasible to make dramatic changes in temperature and viscosity for a living system, manipulation of physical characteristics of tissues seems clinically impractical. The manipulation of chemical properties in tissues may be more practical to alter contrast. Water is a major tissue constituent and is rich in hydrogen. From equation (3), we can also see that the change of hydrogen concentration within tissues will directly influence NMR intensity. Thus, increasing hydration within a tissue by a proton relaxation enhancer (contrast agent) will not only influence the hydrogen concentration, but will tend to decrease both T_1 and T_2 for that tissue [5,9]. With greater concentrations of water, hydrogen density and the associated T_1 reduction will cause an increase in intensity, while the associated T_2 reduction should tend to reduce intensity.

1.1.2 Principle of Contrast by Paramagnetic Agents

All forms of matter may possess the magnetic properties. They are paramagnetism, diamagnetism, or ferromagnetism. A paramagnetic substance may be defined as one that is attracted toward and aligns with the stronger portion of a magnetic field; a diamagnetic substance is typically repelled by and aligns against the stronger portion of a magnetic field. A paramagnetic substance has its own magnetic moment and aligns in an external magnetic field, but loses this alignment and becomes randomly oriented when the field is removed. Ferromagnetic substances also align with an external magnetic field, but tend to retain that alignment after the external field is removed.

Substances that are paramagnetic possess one or more fundamental particles (proton, neutron or electron) with a spin that is not canceled by another particle with the opposite spin. There are numerous paramagnetic substances, but only a few show promise as clinical contrast media. The magnetic moments of unpaired electrons are about 700 times greater than those of protons or neutrons. Therefore, the local magnetic fields generated by unpaired electrons are proportionally much stronger. It is such paramagnetic compounds with unpaired electrons that elicit close attention as MRI contrast enhancers.

Paramagnetic compounds can catalyze the proton relaxation of the water in which they are dissolved [8]. As a result, T_1 and T_2 are both decreased, and the signal intensity (SI) is affected according to equation (3). But when paramagnetic compounds are involved in MRI measurement, the T_E and T_R can be chosen to make SI much more sensitive to T_1 than to T_2, so that the presence of the paramagnetic compound can increase SI.

Relaxivity (k_1, k_2) of paramagnetic compounds is defined as the difference in the reciprocal of the relaxation times measured in the presence and absence of paramagnetic compounds.

$$\frac{1}{T_{1p}} - \frac{1}{T_{1s}} = k_1 [P] \tag{4}$$

$$\frac{1}{T_{2p}} - \frac{1}{T_{2s}} = k_2 [P] \tag{5}$$

where [P] stands for the concentration of paramagnetic compound (p) and s represents solvent.

The relaxivity is generally used to describe each paramagnetic compound's ability to catalyze relaxation of bulk water protons. Each has a characteristic set of relaxivities. This kind of information is empirically derived.

1.2 Inhibition of Polymerization

Inhibitors are substances which are able to suppress the polymerization of monomers by reacting with the initiating and propagating radicals and converting them either to nonradical species or radicals of reactivity too low to undergo propagation. The inhibitors kill almost every radical and thus the polymerization is completely halted until they are consumed to an insignificant level. This phase preceding a polymerization period is called the induction period.

The other type of suppressors in polymerization are retarders, which behave less effectively and terminate only a portion of the reacting radicals. The difference between the two (inhibitors and retarders) is simply one of degree and not kind.

A typical inhibitor is benzoquinone. It almost completely stops free-radical induced polymerization during the induction period. At the end of the period, polymerization rate resumes as in the absence of inhibitor. Nitrobenzene is a typical retarder. It lowers the polymerization rate without an induction period. The inhibitors are preferentially added to commercial monomers to prevent premature thermal polymerization during their storage, shipment and processing.

1.2.1 General Concepts

Most vinyl and diene monomers were found to participate in spontaneous polymerization in late 1930s [6]. This observed polymerization, in many cases, was initiated by impurities present in these monomers or by traces of peroxides which were formed as they came in contact with air. As a result, the information on the rate of their polymerization was rarely consistent. Under the inert environment, the polymerization rates of styrene and methyl methacrylate have been extensively confirmed [7,8]. These types of polymerizations are free-radical in character.

Thermally initiated polymerization is another type of significant and important reaction in industry. It has been thoroughly investigated for many years. Generally, these processes are relatively easy to carry out and control. Usually they provide a very convenient route to polymers with a wide range of properties.

Figure 1 shows a typical chain polymerization curve. The polymerization is initiated by a reactive species R^*, which is produced from a thermal decomposition initiator. The reactive species R^* adds to a monomer molecule by opening the π-bond to form a new radical center. This process is then repeated as many more monomer molecules are successively added to the continuously propagating reactive centers. However, the polymer growth is terminated at some point by mutual destruction of the reactive centers, whose mechanisms depend on the type of reactive center and the particular reaction conditions.

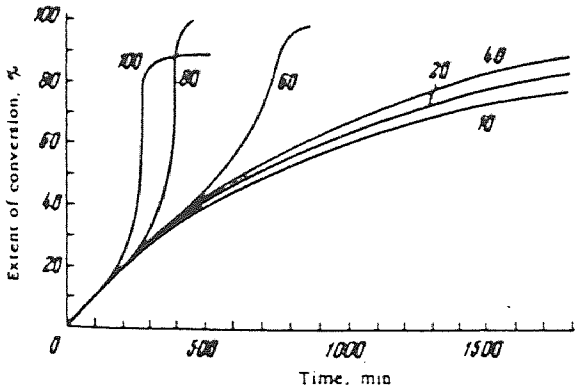

Figure 1: Styrene polymerization in benzene solution at various concentration (%). This graph is taken from reference [8].

Figure 1 also shows the shapes of the polymerization curves of styrene in benzene solution as a function of monomer concentrations. The polymerization rate does not increase rapidly at the initial stage of the polymerization. As a given degree of conversion has been attained, the polymerization rate then begins to increase rapidly, and decreases again when the degree of polymerization has become very advanced. The reason for this behavior is the formation of high molecular weight polymer molecules which increases the viscosity of the reaction medium and thereby diminishes the diffusion of polymeric radicals. The collisions between two active ends of polymeric radicals become less probable, i.e. the rate of chain termination decreases and then the reaction rate increases. Among the entire course of polymerization, the initial stage of polymerization (at low conversion) is the most appropriate for the accurate kinetic studies of the polymerization mechanism and determination of rate constants of elementary reactions. During this stage, the concentration of the high molecular weight reaction products is so low that they do not affect the course of reaction. Therefore, in this work, only the kinetic data at the early stage are taken for analysis of its kinetic behavior.

1.2.2 Kinetics and mechanism of polymerization

The kinetics of this type of free radical polymerization are usually considered to involve three essential processes : initiation, chain growth and termination by mutual destruction of propagating radicals.

Initiation

$$I \longrightarrow 2R_c^{\cdot} \quad (6)$$

$$R_c^{\cdot} + M \longrightarrow R_1^{\cdot} \quad (7)$$

Propagation

$$R_1^{\cdot} + M \longrightarrow R_2^{\cdot} \quad (8)$$

$$R_2^{\cdot} + M \longrightarrow R_3^{\cdot} \quad (9)$$

$$R_n^{\cdot} + M \longrightarrow R_{n+1}^{\cdot} \quad (10)$$

Termination

$$R_n^{\cdot} + R_m^{\cdot} \longrightarrow P_{n+m} \quad (11)$$

$$R_n^{\cdot} + R_m^{\cdot} \longrightarrow P_n + P_m \quad (12)$$

where I represents initiator, M is the monomer, $R_c^{\cdot}$ is the primary initiating radical from thermal decomposition of an initiator, $R^{\cdot}$ is the active radical and P is the inactive polymer.

The initiation step contains two reactions. The usual case in the first step, equation (6), is the homolytic dissociation of an initiator or catalyst species, I, to yield a pair of radicals $2R_c^{\cdot}$. The second part is their addition to the first monomer molecule to produce the chain initiating species $R_1^{\cdot}$, equation (7). Their corresponding rate constants are k_d and k_i.

Propagation consists of the growth of $R_1^{\cdot}$ by the successive additions of large numbers of monomer molecules. Each addition creates a new radical center, which also functions reactively as much as previous one. The process grows rapidly and almost simultaneously high molecular weight polymeric chains are produced.

At some point when the active radical concentration is relatively high, the propagating polymer chain stops growing and terminates. The termination usually occurs by bimolecular reaction between radicals. Two radicals react with each other by combination (coupling), or more rarely, by disproportionation. The final polymer product, P_n, is therefore formed.

Nonetheless, termination may also proceed through reaction of reactive radicals with some other species present in the reaction mixture such as inhibitors. They react with active radicals $R^{\cdot}$ to produce inactive species.

$$R^{\cdot} + Z^{\cdot} \longrightarrow \text{Inactive Products} \qquad (13)$$

This reaction is in direct competition with the chain growth process:

$$R^{\cdot} + M \longrightarrow RM^{\cdot} \qquad (14)$$

The consequence of the competition between them will depend on the relative values of their individual rate coefficients, the concentration of reagents and the properties of inactive products.

1.2.3 Kinetics of Inhibited Polymerization

Since the inhibitor can terminate the growth of reactive radicals, its kinetics can be simply analyzed using a scheme consisting of the usual initiation, propagation and termination reactions with the addition of the inhibition reaction, equation (15).

$$R^{\cdot} + Z^{\cdot} \longrightarrow P_n + Z^{\cdot} \qquad (15)$$

where $Z^{\cdot}$ is the inhibitor. The kinetics can be relatively simplified if one assumes that the inhibitor radicals $Z^{\cdot}$ do not reinitiate polymerization and that they terminate without regeneration of the original inhibitor molecule. The detailed kinetics of inhibition will be further discussed in later Chapters 2, 3 and 7.

CHAPTER 2

PREVIOUS WORK ON STYRENE POLYMERIZATION

2.1 Thermal Polymerization

Published kinetic data on purely thermally initiated polymerizations are not readily available. This is primarily due to slow thermal initiation and also masking by the initiation effects of peroxide impurities, atmospheric oxygen or other initiators which may be accidentally present. However, some reproducible data on thermal polymerization were obtained for styrene and methyl methacrylate. Schulz *et al.* [72] studied the polymerization of styrene in various hydrocarbons and found that the reaction rate is approximately second order, which led them to presume that the initiation was bimolecular. Their data for the temperature range of 100-130°C yields the following expression for the initiation rate:

$$V_{in} = 1.5 x 10^4 (M^2) \exp(\frac{-23300}{RT}), \quad (1)$$

where V_{in} represents the initiation rate and M is the concentration of monomer.

Mayo [10] studied the thermal polymerization of styrene in bromobenzene solution. He found that the thermal polymerization of styrene yields a low molecular weight fraction (dimers, trimers) in addition to the high molecular weight polymer. If the low molecular products are ignored, the order of the reaction is 5/2 with respect to monomer concentration, which is in agreement with the termolecular initiation (see section 2.1.2 for the detailed mechanism). He found the following equation for the initiation rate:

$$V_{in} = 1.32 x 10^6 (M^3) \exp(\frac{-28900}{RT}), \quad (2)$$

Parat and Kirchner [73] also found that the order of thermal polymerization of styrene was higher than two. The overall activation energy of styrene self

polymerization is about 21 Kcal/mol. When combined with reasonable activation energy for propagation and termination, it gives an activation energy for initiation step of about 29 Kcal/mol [11].

Many theoretical studies on the initiation mechanism of thermal polymerization were proposed, and they are discussed as follows: Biomolecular Initiation Theories and Termolecular Initiation Theories. It appears that no single theory is overwhelmingly satisfactory.

2.1.1 Bimolecular initiation theories

Early measurements of the rates of thermal polymerization of styrene suggested that the overall rate is second order with respect to monomer concentration [8]. Walling first proposed that the styrene initiation mechanism is the formation of two monoradicals from two molecules of styrene [12] as shown in equation (3).

$$2\ CH_2=CH\text{-}C_6H_5 \longrightarrow CH_3\dot{C}H\text{-}C_6H_5 + CH_2=\dot{C}C_6H_5 \qquad (3)$$

Even if equation (3) might be energetically feasible, it would of necessity involve the transfer of a proton from the α-position of a molecule of styrene. Such an effect was not observed in the polymerization of α-deuteriostyrene. The emphasis was then shifted to biradical theories.

Flory [13] proposed a biradical mechanism as shown in equation (4) for this self-initiated polymerization and expected the tail-tail biradicals to propagate in both ends and yield polymerization of high molecular weight.

$$2\ CH_2=CHCC_6H_5 \longrightarrow C_6H_5\dot{C}H - CH_2CH_2 - \dot{C}HC_6H_5. \qquad (4)$$

A great many objections to this theory have also been raised. Concerns about initiation and propagation capability in the course of polymerization both theoretically and experimentally have been raised, although the biradicals show considerable resonance stabilization. Statistically, the internal reactions of biradicals are more probable than interradical reactions. The great majority of biradicals formed would

cyclize before propagation has occurred. Zim and Bragg [14] have shown that with their mutual destruction, styrene biradicals cannot grow very large. The biradicals have too short a life span to contribute to the formation of high molecular weight polymer. If any biradicals are formed, fewer than 1% of them last long enough to grow one step. Therefore, this type of mechanism should result in a very broad and flat molecular weight distribution (MWD). Such distribution is not observed in practice and a normal MWD is obtained instead. On the other hand, if the biradicals are to be preserved, the addition of a small proportion of carbon tetrachloride, sufficient to terminate 60-90% of the polymer chains by transfer and to permit separation of most of the original biradicals, should accelerate the reaction. This gives no acceleration of the thermal rate.

It therefore appears that the attempts to formulate a second order process involving biradicals have been unsuccessful, not only in the propagation reaction for thermal polymerization of styrene, but in the initiation step.

2.1.2 Termolecular initiation theories

The termolecular theory of styrene self-initiation is based on the measurements of Mayo [7], who conducted thermal polymerization in various concentrations in refluxing bromobenzene. Mayo isolated two main products from the reaction. A polymer of high molecular weight for which the overall order of formation appeared to be 5/2, and oligomeric product of low molecular weight.

Mayo argued that 5/2 order agrees much better with the experimental results than the previous estimation of order 2. He attributed the failure of second order mechanisms to not recognizing the existence of two main types of products above.

An order of 5/2 indicates that the initiation step must be third order on monomer concentration. On this basis, Mayo proposed a mechanism that a pair of monoradicals from three molecules of styrene is formed as shown in reaction (5).

$$3\,CH_2=CHC_6H_5 \longrightarrow CH_3\dot{C}HC_6H_5 + CH_3C\dot{C}_6H_5=CH\dot{C}HC_6H_5 \qquad (5)$$

Since termolecular reactions in solution are rare, it might be more reasonable to suppose that initiation is a two-step process involving a reversible, inefficient bimolecular formation of a biradical followed by a rapid transfer reaction as follows:

$$2CH_2=CHC_6H_5 \longleftrightarrow C_6H_5\dot{C}HCH_2CH_2\dot{C}HC_6H_5 \quad (6)$$

$$C_6H_5\dot{C}HCH_2\dot{C}HCH_2C_6H_5 + CH_2=CHC_6H_5 \longrightarrow$$

$$CH_3\dot{C}HC_6H_5 + C_6H_5CH = CHCH_2\dot{C}HC_6H_5 \quad (7)$$

Both of these proposals received a number of objections. The Mayo scheme (Equation 5) is not supported by studies with labelled styrene, and neither is the second scheme (Equations 6 and 7). Once again, it must be remembered that much of the evidence against the participation of diradicals in a bimolecular initiation reaction will apply also in a termolecular reaction.

The more recent theory [7] of styrene thermal initiation stems from characterization of the low molecular weight products, formed concurrently with the high molecular weight products. This low molecular weight fraction mainly contains two dimeric products: 1,2 -diphenylcyclobutane (III) and 1-phenyltetralin (V). Mayo has proposed the following dimerization reactions (8) and (9), and compound IV is believed to take part in the initiation of the polymerization.

It is noted that such a scheme satisfies the apparent termolecular nature of the initiation step and it does not require the prior formation of a biradical. The mechanism (Equations 8 and 9) proposed below is consistent with the observed activation energy of 29 Kcal/mol for initiation. Support for this mechanism is also provided by the observation of the Diels-Alder dimer (IV) by Ultraviolet Spectroscopy [31]. Whether formation of the Diels-Alder dimer or its reaction with styrene is the rate - determining step in initiation is not completely established. However, the dependence of $R^{\cdot}$ on [M] being closer to third order than second order may indicate that equation(10) is the slowest step.

(8)

(III)

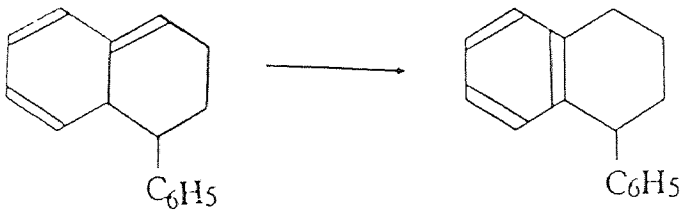

(IV) (V)

(9)

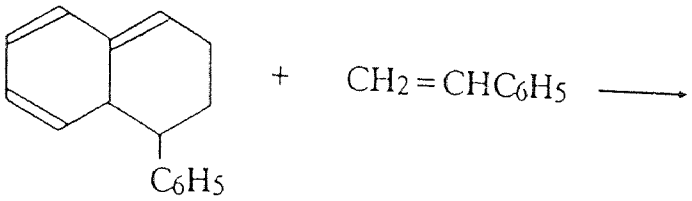

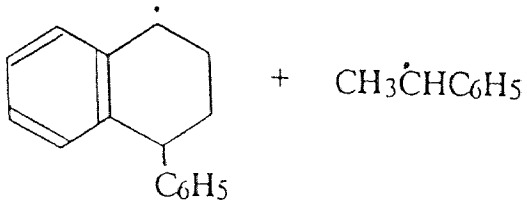

(10)

2.2 Initiator

A good initiator should be readily available, stable under ambient or refrigerated conditions, and possess a practical rate of radical generation at temperatures which are not excessive (less than 150°C). The thermal homolytic dissociation of an initiator to produce initiating radicals is most widely used in thermal initiated polymerization. Initiator compounds with lower or higher dissociation energies will dissociate too rapidly or slowly respectively. The appropriate bond dissociation ener-

gy is in the range 100-170 KJ/mol. Only a few classes of compounds such as O-O, S-S and N-O bonds meet these requirements. Other significant initiators are azo compounds such as 2,2'-azobis-isobutyronitrile (AIBN). Their facile dissociation is not caused by the presence of a weak bond. The C-N bond dissociation energy in AIBN is high (nearly 290 KJ/mol), but the driving force for homolysis is the formation of the highly stable nitrogen molecule.

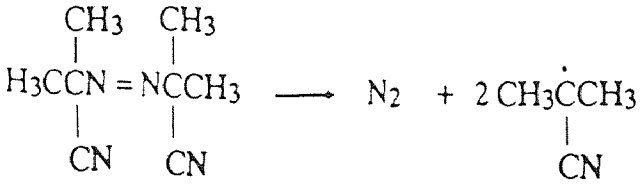

(11)

When heated in various solvents, 2,2'-azobis-isobutyronitrile decomposes with the evolution of a molecule of nitrogen and formation of dimethylcyanomethyl radicals. The existence of these radicals has been evidenced from electron spin resonance (ESR) studies [22]. Its decomposition kinetics is found to be first order [17-19], and it is considered solvent-independent [20]. For early data obtained in the temperature range of 40-100°C, Van Hook and Tobolsky [21,74] have suggested a "best value" of the decomposition rate coefficient, $k_d = 1.58 \times 10^{15} \exp(-30800/RT)$ sec^{-1}. Bretts *et al* [75] subsequently reported a value of $k_d = 1.7 \times 10^{15} \exp(-30700)$ sec^{-1}. In addition, AIBN has a long life time in solution (4.8 hours at 70°C) [46]. It is therefore chosen as an initiator during this study.

Despite the fact that most primary radicals are highly reactive, several studies have found that, when a material balance is performed on the amount of the initiator that is decomposed during a polymerization and compared with that which initiates polymerization, the initiators are not participating in the polymerization as much as expected. The reasons have been found to be due to two reactions. One is the attack of the primary radicals by the propagating radical. The second is the self recombination of primary radicals before they diffuse into the solution. The efficiency of AIBN to initiate styrene polymerization has been estimated from measurements of the uptake of radioactive fragments from C^{14}-labelled AIBN in the polymer and from the quantity of "wasted-radical" products from the AIBN decomposition [13].

It was concluded that only 70% of the radicals are available for capture by the monomer. These observations are further explained by postulating a cage effect [22,28], where a fraction of radicals is lost by geminate recombination inside the cage before they can diffuse into the solution.

The initiator efficiency **f** is then defined as the fraction of radicals formed in the primary step of initiator decomposition, which are successful in initiating polymerization. A popular method for estimating its value is from a comparison of the rates of reaction with radical scavengers to the overall decomposition rate of the initiator, if radical scavengers is powerful enough to capture all radicals. Most of reported values of **f** lie in the range 0.4 to 0.6 [22]. A summary of literature values of **f** is given in Table 1.

In pure styrene thermal polymerization, the walls of the cage are made up of styrene molecules. The efficiency factor could only be larger if styrene reacts with caged radicals. The reported data of efficient factors are: **f** (50^{o}C) = 0.73, and **f** (60^{o}C) = 0.8.

Table 1: Efficiency factor for radical production

T (^{o}C)	f	solvent	reference
40	0.522	benzene	10
50	0.477	benzene	10
60	0.437	benzene	10
70	0.417	benzene	10
78	0.37	benzene	10

2.3 Initiated Styrene Polymerization

As indicated in Chapter 1, the formed polymers are basically the successive stacking of many their corresponding monomers. These reactions contain three main processes which are represented as follows:

Initiation

$$I \longrightarrow 2R_c^{\cdot} \quad (12)$$

$$R_c^{\cdot} + M \longrightarrow R_1^{\cdot} \quad (13)$$

Propagation

$$R_1^{\cdot} + M \longrightarrow R_2^{\cdot} \quad (14)$$

$$R_2^{\cdot} + M \longrightarrow R_3^{\cdot} \quad (15)$$

$$R_n^{\cdot} + M \longrightarrow R_{n+1}^{\cdot} \quad (16)$$

Termination

$$R_n^{\cdot} + R_m^{\cdot} \longrightarrow P_{n+m} \quad (17)$$

$$R_n^{\cdot} + R_m^{\cdot} \longrightarrow P_n + P_m \quad (18)$$

In order to derive a kinetic expression pertaining to the reaction scheme shown above, it is necessary to discuss the following four traditional assumptions along with some experimental evidence:

1. The number of monomer molecules reacting in the propagation step is greater than those in the initiation step. The total rate of monomer consumption, which is synonymous with the rate of polymerization, is considered as:

$$-\frac{d[M]}{dt} = R_i + R_p \approx R_p. \quad (19)$$

2. The rate coefficients for both propagation and termination are independent of chain length, i.e. $k_{p1} = k_{p2} = k_{pn} = k_p$, and similarly for individual values of k_{tc} and k_{td}. A substantial body of experimental data has demonstrated that, although radical reactivity depends on molecular size, the effect of size vanishes after the dimer or trimer [24,25]. However, Gee and Melville [76] thought that a complete removal of this assumption is not practical. They then replaced this assumption by stating that, " although the velocity coefficients may be dependent on chain length, the ratio of the propagation coefficient to some quantity related to the termination coefficients is independent of chain length". But the results obtained for the form of the kinetic relations remain unaltered.

3. A stationary state in radical concentrations is established during the early stage of polymerization. Its theoretical and experimental validity have been extensively discussed in many polymerization experiments [25-27]. As a result, one may allow the rate of change of concentration of any radical intermediates to be equal to zero. Moreover, the radical concentrations are very difficult to measure quantitatively in the 10^{-8} M range. Therefore, it is desirable to eliminate [R·] during kinetic derivation. However, such a dynamic process can also be interpreted as that the concentration of radicals increases initially, but almost instantaneously reaches a constant , steady state value, and whenever the radical concentration builds up to some quantity, an increase in termination follows to maintain the constant values.
4. Termination involving primary radicals is negligible. This assumption is valid, since the concentration of $R^{\cdot}_{c}$ is small compared with the total radical concentration.

2.3.1 Kinetic Model

It is understood that reactions (12-18) constitute the relatively detailed mechanism for a polymerization system under study. Since the rate constants for all the propagation steps are assumed to be the same, one may rewrite them as follows:

Initiation

$$\text{AIBN} \longrightarrow 2\,f\,I^{\cdot} \qquad \text{rate} = 2\,f\,k_{di}\,[\text{AIBN}] \qquad (20)$$

$$I^{\cdot} + M \longrightarrow M_1^{\cdot} \qquad \text{rate} = k_{ii}\,[I^{\cdot}]\,m \qquad (21)$$

Propagation

$$R^{\cdot} + M \longrightarrow R^{\cdot} \qquad R_p = k_p\,r\,m \qquad (22)$$

Termination

$$R^{\cdot} + R^{\cdot} \longrightarrow X \qquad R_t = 2k_t\,r^2 \qquad (23)$$

where $r = [M_1^{\cdot}] + [M_2^{\cdot}] + \text{------} + [M_n^{\cdot}]$

$$\approx [M_2^{\cdot}] + [M_3^{\cdot}] + \text{-------} + [M^{\cdot}_{n+1}], \text{ and } m = [M].$$

At the condition of stationary state, $R_i = R_t$, therefore:

$$R_i = 2 k_t r^2 \quad , \quad \text{then} \tag{24}$$

$$r = \left(\frac{R_i}{2k_t} \right)^{1/2} \quad . \tag{25}$$

Combined with equation (22), we have:

$$R_p = k_p m \left(\frac{R_i}{2k_t} \right)^{1/2} \quad . \tag{26}$$

The initiation step in polymerization is composed of two steps and it is believed that the second step is much faster than the first one. Therefore, the homolysis of the initiator is the rate determining step in the initiation sequence and the rate of initiation can be given by

$$R_i = 2 f k_{di} [AIBN]. \tag{27}$$

When substituted into equation (26), we obtain:

$$R_p = k_p m \left(\frac{f k_{di} [AIBN]}{k_t} \right)^{1/2}. \tag{28}$$

Simultaneous determination of absolute values of both k_p and k_t from a single experiment has not been reported. The use of polymerization data under steady state conditions only allows the evaluations of the initiation rate constant, k_{di}, and the ratio $k_p/(2k_t)^{1/2}$, since R_p, m, and R_i are all measurable. Thus it might require nonsteady state experiments to evaluate the individual k_p and k_t rate constants.

In practice, $k_p/2k_t$ is determined from nonsteady state measurements of the average lifetime τ of the growing polymer chain on a photochemically initiated

polymerization. Here the radical lifetime τ is defined by the steady state radical concentration divided by its steady state rate of disappearance.

$$\tau = \frac{r}{R_t} \quad , \tag{29}$$

which yields from equations (22) and (23),

$$\frac{k_p}{2\,k_t} = \frac{\tau\, R_p}{m} \quad . \tag{30}$$

By combining equation (30) with $k_p/(2k_t)^{1/2}$, the individual propagation and termination rate constants can be calculated.

Details of the unsteady state theory and experiments are given elsewhere [28-32]. There is a variety of experimental techniques possible to measure the lifetime τ, such as using intermittent photoinitiation by a rotatory sector or a "flashing" laser, and using ESR for determination of the radical concentration.

Because of the influence of solvents on the rates, only data on bulk polymerization are considered in this study. Nonetheless, these data still maintain a wide scatter. A least squares analysis is performed, assuming all points of equal value, and the following expressions are obtained [8]:

$$k_p = 9.35\,x\,10^6 \exp\left(\frac{-7250}{RT}\right) \quad . \tag{31}$$

$$2k_t = 7.1\,x\,10^8 \exp\left(\frac{-1500}{RT}\right) \quad . \tag{32}$$

2.3.2 Kinetics of inhibition or retardation

We have also briefly described the kinetic model of inhibited polymerization in Chapter 1, in which an additional term describing radical scavenging is introduced. That is:

$$R^{\cdot} + Z \longrightarrow P_n + Z^{\cdot} \qquad \text{Rate} = k_z\, r\, z \tag{33}$$

Assuming that the radical concentration does not change with respect to time, we obtain:

$$\frac{d\,r}{dt} = R_i - 2\,k_i\,r^2 - k_z\,z\,r = 0. \tag{34}$$

This equation was then combined with with equation (22) to yield:

$$\frac{2\,R_p^{\,2}\,k_t}{k_p^{\,2}\,m^2} + \frac{R_p\,z\,k_z}{k_p\,m} - R_i = 0. \tag{35}$$

Equation (35) can be used to correlate the rate data of inhibited polymerizations, since R_p, k_p, R_i, m and z are all known or measurable. The rate constant k_z for inhibition can therefore be evaluated.

For the case that the retardation is very strong, i.e., $k_z/k_p >> 1$, the normal bimolecular termination can be neglected. Therefore, the first term of equation (35) is negligible and one has:

$$\frac{R_p\,z\,k_z}{k_p\,m} - R_i = 0\ , \tag{36a}$$

or

$$R_p = \frac{k_p\,m\,R_i}{k_z\,z} = -\frac{dm}{dt}\ . \tag{36b}$$

The inhibited polymerization usually accompanies an induction period, whose length is directly proportional to the inhibitor concentration. During this period, there is no polymerization. Only the inhibitor concentration decreases with time. Therefore the concentration of inhibitor at any time can be described by:

$$z = z_o - \frac{R_i t}{y}, \tag{37}$$

where z_o is the initial concentration of inhibitor, "t" is the time and "y" is the number of radicals terminated per inhibitor molecule.

Combination of equation (35), (36b) and (37) leads to:

$$-\frac{dm}{dt} = \frac{k_p R_i m}{k_z \left(z_o - \frac{R_i t}{y} \right)} \quad , \text{ and} \tag{38a}$$

$$\frac{-1}{\frac{d \ln m}{dt}} = \frac{k_z z_o}{k_p R_i} - \frac{k_z}{k_p} \frac{t}{y} \quad . \tag{38b}$$

A plot of the left hand side of equation (38b) versus time is linear and the values of k_z/k_p and y can be obtained from the intercept and slope respectively, if z_o and R_i are known.

If the inhibitor is very effective, the polymerization rate may be negligible until the inhibitor concentration is markedly reduced. As the inhibitor concentration becomes sufficiently low, propagation can become very competitive with the inhibition reaction. From equation (33) and equation (22), we can obtain:

$$\frac{dz/dt}{dm/dt} = \frac{k_z r z}{k_p r m} \quad , \text{ then} \tag{39a}$$

$$\frac{dz}{dm} = \frac{k_z z}{k_p m} \quad . \tag{39b}$$

Further integration yields:

$$\log \frac{z}{z_o} = \frac{k_z}{k_p} \log \frac{m}{m_o} \quad . \tag{40}$$

Considering equation (40), we may readily see that the inhibitor must be almost completely consumed before the monomer can be polymerized. Equation (40) can be used to determine the k_z/k_p from the slope of a plot of log z versus log m. Barlett and Kwart [39] use these model equations to evaluate the inhibition constants for the polymerization of vinyl acetate inhibited by 2,3,5,6-tetramethylbenzoquino (duroquine). Nonetheless, this method may involve difficult experimentation . The polymerization rate being measured is very small if the inhibitor is strong. Therefore, the monomer concentration may not be correctly quantified during the induction period.

A: The Bagdasar'yan - Bamford Equation [33]

The typical feature of the kinetics of polymerization is that the polymerization rate steadily increases as the inhibitor is consumed. It may be more convenient to find the inhibition constant, according to the inhibitor consumption rate.

Assuming the steady state relation to be valid for any instant during the induction period, we then have:

$$W_i = k_t r^2 + k_z r z, \tag{41}$$

where W_i is the rate of initiation. Also the consumption rate of the inhibitor obeys the equation

$$-\frac{dz}{dt} = k_z r z. \tag{42}$$

After solving for r from equation (41) and integrating equation (42), the following Bagdasar'yan - Bamford equation is obtained:

$$F_1 \equiv -\frac{1}{\varphi} + \ln\frac{1+\varphi}{1-\varphi} = \frac{k_z W_{\max}}{k_p m} t + A. \tag{43}$$

where φ is the ratio of the rate of the reaction at any instant to the steady rate of polymerization (W/W_{max}) and A is the intergration constant. Equation (43) describes the polymerization kinetics in the presence of an "ideal" inhibitor [32]. This equation is applicable only to inhibited polymerization in which side reactions do not disturb the inhibitor reaction and its contribution to the overall process kinetics is very small. The plot of the left hand side with respect to time give k_z from its slope k_z/k_p.

B: Inhibition Kinetics Taking into Account Chain Initiation by Inhibitor Molecules [34]

Polymerization may be influenced by the additional initiation from inhibitor molecules. Such radicals have been reportedly observed before and must be considered for derivation of their inhibition constants.

The steady state relation in equation (41) in this case is changed into:

$$W_i + k_i z m = k_z r z + k_t r^2, \tag{44}$$

where k_i is the constant for additional initiation, and again the consumption rate of the inhibitor obeys the equation:

$$-\frac{d z}{dt} = k_i z m + k_z r z. \tag{45}$$

At the end of the induction period, the reaction takes place at a steady state W_∞ and then,

$$W_i = k_t r_\infty^2 .$$

Similarly, the inhibition kinetics, after solving the rate equation (44), can be expressed as follows:

$$F_2 \equiv -2\theta \ln(\varphi + \theta) - (1-\theta)\ln(1-\varphi) + (1+\theta)\ln(1+\varphi) +$$

$$\frac{\sqrt{\theta} - \theta}{2} \ln \left| \frac{\varphi - \theta}{\varphi + \theta} \right| = \frac{k_x W_\infty}{k_p m} (1 - \theta^2) t + B, \text{ and} \tag{46}$$

$$\theta = \frac{k_i m}{k_x r_\infty}$$

Given the data of the inhibition consumption rate, it is possible to find k_z from this equation, if the character of inhibition initiation is known.

C: Kinetics Equation Taking into Account the Effects of the Secondary Inhibition (Retardation) of Polymerization

The effect of a highly efficient inhibitor of polymerization can produce not only an induction period but can also lower the rate of reaction with increasing concentration of inhibitor [33]. The decrease in the concentration of growing chains is usually associated with their interaction with the primary inhibitor products Y:

$$R^{\cdot} + X \longrightarrow Y \tag{47}$$

$$R^{\cdot} + Y \longrightarrow \text{polymer} \tag{48}$$

During the induction period, the stationary equation becomes:

$$W_i = k_t r^2 + k_y r [Y] + k_z r z, \tag{49}$$

At the end of induction period, the equation (49) changes to:

$$W_i = k_t r_\infty^2 + \alpha k_y r z_o, \tag{50}$$

where α is the stoichiometric secondary inhibition coefficient and k_y is the rate constant of the secondary inhibition reaction. The final equation obtained is:

$$F_3 = \frac{1}{\varphi} - \ln(1-\varphi) + (1 - \varphi_\infty^2)\ln\varphi +$$

$$\varphi_\infty^2 \ln\left(\varphi + \frac{1}{\varphi_\infty^2}\right) = \frac{k_z W_\infty}{k_p m} t + C. \qquad (51)$$

φ is the ratio of the rate of polymerization at any instant W_t to the steady state of inhibited reaction W_∞ and φ_∞ is the ratio of W_∞ to the steady state of the non-inhibited process W. The primary inhibition constant k_z/k_p can be determined from the slope of the linear time variation of F_3.

The secondary inhibition (retardation) rate constant k_y can be calculated from the relation obtained from a calculation for the polymerization scheme in the presence of a relatively ineffective inhibitor (Y) and equation (50).

CHAPTER 3

PREVIOUS WORK ON INHIBITORS

The most commonly used inhibitors in the radical polymerization of vinyl monomers are oxygen, quinones, phenols, aromatic amines, nitrocompounds and transition metal salts. Each has its own inhibiting characteristics and functions through different mechanism. A highly effective inhibitor usually is accompanied by an induction period, during which there is no polymerization. As the end of this period is reached, steady state polymerization resumes and its rate can be identical or a little lower than that in the absence of the inhibitors. This character depends on the structure of monomers and inhibitors, the method and mechanism of initiation, the nature of initiator and other physiochemical conditions in polymerization.

3.1 Common Inhibitors:

Oxygen can act as an effective inhibitor as well as initiator. It reacts with polymeric radicals to form the relatively stable peroxy radicals:

$$R^{\cdot} + O_2 \longrightarrow R\text{-}OO^{\cdot} \qquad (1)$$

This peroxy radical can react with itself or another propagating radical to form inactive products by coupling and disproportionation [35-37]. The peroxy radical is also capable of initiating polymerization. The occurrence of polymerization is due to the initiating radicals that can be produced from the thermal decomposition of the peroxides and hydroperoxides formed with monomers. Many commerical processes for ethylene polymerization involve initiation by oxygen. Whether it favorably functions as an initiator, inhibitor, or both, is highly temperature and monomer dependent. Initiation will occur at temperature where the peroxides are unstable. The interrelationship between polymerization processes and monomer oxidation has been studied in detail by Tseitlin and Medvedev [77] for styrene.

In the kinetic study of polymerization, it is extremely important to remove oxygen dissolved in the monomer and contained in the reaction vessels. A common laboratory practice is to follow the freeze/thaw cycles or to bubble nitrogen into monomers for an extended period.

Quinones such as benzoquinone and chloranil are widely used as inhibitors in radical polymerization. The mechanism which describes the chemical reaction between the propagation radicals and quinones is not yet clear. Its inhibiting behavior is also very complex. However, the reported mechanisms are described elsewhere [32,38]. If the attack of a propagating radical is on the oxygen in quinones, aryloxy radicals (I) will be produced. If the attack is on the ring carbon, radical (II) will be produced as shown below:

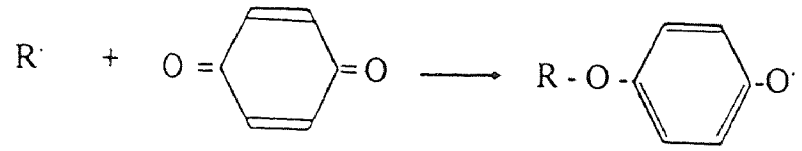

(2)

(I)

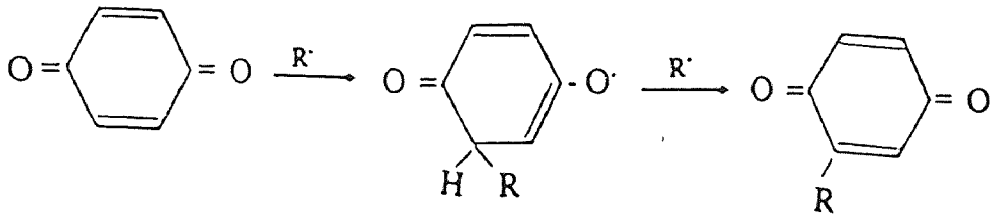

(3)

(II)

+ RH

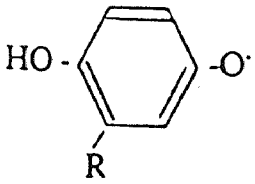

(4)

Both intermediate radicals can still continue to behave as inhibitors in further polymerization. An alternative route might occur as shown in reaction (4). The obtained radical also has the inhibiting capability to continue as active radical killer by coupling reaction in the polymerization medium.

Early analysis of the kinetic data in polymerization of methyl methyacrylate and methyl acrylate with different quinones as inhibitors indicates that one molecule of quinone terminates two kinetic chains. On the other hand, some studies of quinones inhibited thermal polymerization at 100°C show that the termination of one kinetic chain is accompanied by the consumption of 17 molecules of quinones. This result indicates effective kinetic chains were regenerated. Tudos *et al.*[78,79] systematically investigated the inhibition mechanism of quinones and demonstrated that their stoichiometric coefficients should be lower than two.

An interesting result was obtained in the study of the inhibition mechanism of quinones in styrene thermal polymerization at 60°C. The rate of its consumption is 61 times more than that in the initiated styrene polymerization. Hiattand and Bartlett have suggested that quinones could participate in the styrene polymerization. The relatively high temperature and low concentration of free radicals may provide better opportunity for their addition into styrene molecules easily.

In comparison to quinone, **phenols** are relatively poor inhibitors. Their inhibiting mechanism involves hydrogen abstraction followed by coupling of the phenoxyl radical with other polymeric radicals. Their typical mechanism can be represented as follows:

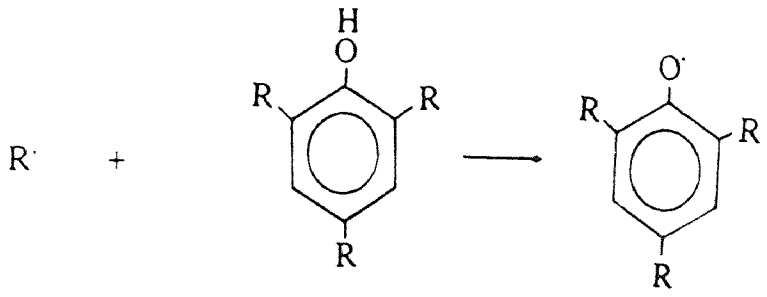

(5)

Some phenols act as effective inhibitors in the presence of air, owing either to their oxidation to quinones [25], which are active inhibitors, or to conversion of propagating radicals to peroxy radicals, which undergo autoxidation by the hydroxybenzene compound. The detailed studies are described in references [8, 28].

Nitrocompounds act as effective inhibitors in polymerization at suitable concentrations and temperatures. Their inhibiting activity is strongly monomer dependent. They will inhibit vinyl acetate and retard styrene polymerization, but have little

effect on methyl methacrylate and methyl acrylate, and do not inhibit the polymerization of acrylonitrile in dimethylformamide solution. Also their effectiveness increases rapidly with the increasing number of nitro groups in the molecules. The mechanism of radical termination usually contains two pathways. Free radicals may attack either aromatic ring or nitro group. If the attack is on the aromatic ring, radical (V) will be produced. If the attack is on the nitro group, then it produces radical (VI). Again both formed intermediate radicals can further react with and terminate other propagating radicals.

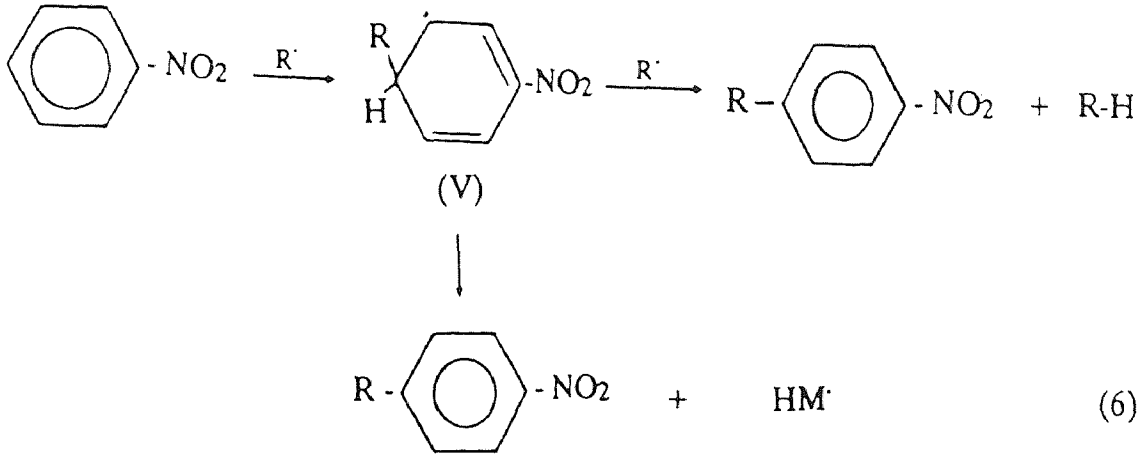

(6)

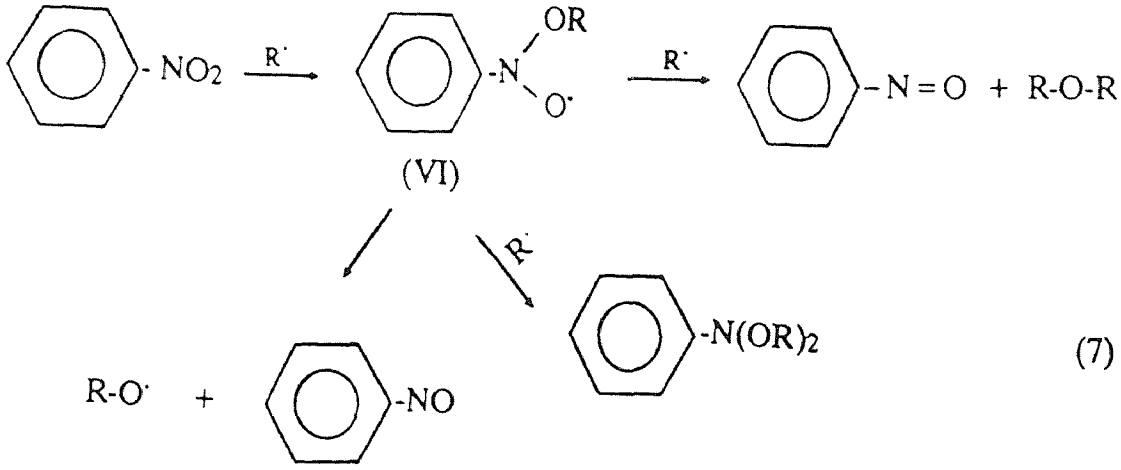

(7)

Aromatic Amines. Bevington and Troth [25] made a detailed study of the behavior of diphenylamine by the method of tagged atoms. A substitution of

deuterium for the amine hydrogen led to the conclusion that the cleavage of amine hydrogen is the primary reaction. Then the polymeric radical reacts with diphenylnitrogen radical. The active radical is then inactivated.

Metal Salts. Oxidants such as $FeCl_3$ or $CuCl_2$ are strong inhibitors. They terminate radicals by receiving an electron from radicals [41].

$$\text{--- } CH_2CHC_6H_5 + FeCl_3 \begin{cases} \nearrow \text{------}CH=CHC_6H_5 + FeCl_2 + HCl \\ \searrow \text{---- } CH_2CHClC_6H_5 + FeCl_2 \end{cases} \quad (8)$$

3.2 Radical Inhibitors

Systematic investigations on the kinetic and mechanism studies for different classes of stable radicals are discussed in references [39, 42-45]. Typically, six groups of radicals received more attention. The features of these stable radical inhibitors are greatly compound dependent. The nature of solvents and monomers plays an important role as well. Five among the six will be discussed in this section. They are as follows:

- Hydrocarbon Radicals
- Verdazyl Radicals
- Nitroxyl Radicals
- Hydrazyl Radicals
- Aryloxy Radicals

3.2.1 Hydrocarbon Radicals

Gomberg's radical [46] (triphenylmethyl radical) was found present in the thermodynamic equilibrium with its dimer (hexaphenylethane). At room temperature, only 2% of the dimer dissociated into free radicals in benzene solution. As expected, it inhibits the thermal polymerization of styrene. Nonetheless, the measured induction period (τ) of the polymerization reaction is much shorter than the value calculated from the consumption of the inhibitor.

$$\tau = \mu \frac{[X]_o}{W_i}, \tag{9}$$

where W_i is the rate of initiation, $[X]_0$ is the initial inhibitor concentration and μ is the stoichiometric coefficient, which indicates the number of reactive chains broken by one inhibitor species. According to Mayo and Gregg's data [82], μ is equal to 0.013 for Gomberg's radical.

Benzyl and diphenyl methyl radicals are more reactive than Gomberg's radical. But they react with monomers. As they were added to the polymerization reaction of acrylonitrile and methyl methacrylate as inhibitors, the induction period was not observed. And the rate of polymerization is comparable to the rate of the initiated reaction.

3.2.2 Hydrazyl Radicals

Probably the best known hydrazyl radical is 1,1-diphenyl-2-picrylhydrazyl (DPPH). The compound was first obtained by Goldschmidt [83]. It is highly stable in the solid state and also in dilute solution at moderate conditions. Thus, the possibilities of using it to study the kinetics of photolysis and radiolysis of various compounds, cage effect, and the decomposition of initiators was extensively examined. As for an inhibitor, DPPH behaves both as a strong inhibitor and a weak initiator in the radical polymerization of vinyl monomers.

Bengough [16] observed that the time required for the complete disappearance of the stable radical from the reaction system is different from the induction period using equation (9). The stoichiometric coefficient is less than 1. With the increase of DPPH concentration in the reaction, the induction period is shortened [42-45]. It was later estimated that about 10% of DPPH was involved in the chain initiation. Therefore, at the DPPH inhibited polymerization, the stationary polymerization falls after the end of the induction period.

Matheson [25], and Bartlett and coworkers [47] used this radical for the determination of the kinetic characteristics of the polymerization reaction, by assuming

that one radical terminates one kinetic chain. Their result of $k_p / k_t^{1/2}$ was very close to literature data. It was later established that the ratio of [DPPH] to [initiator] should be less than 0.5 when DPPH was used as a radical counter in the kinetic study of the initiated polymerizations [39].

Multiradical inhibitors based on DPPH are also investigated in the literature. In the presence of the multiradical 2-(2,6-dinitrophenyl)-1,1-diphenylhydrazyl [39], no additional initiation was observed and the decrease of the stationary polymerization rate was also observed to be much smaller than in the case of DPPH. This slight retardation is due to the inhibition effect of the presence of the nitro group in the molecule rather than from the influence of its participation in initiation reaction.

3.2.3 Verdazyl Radicals

The 1,3,4-triphenylverdazyl radicals was the first verdazyl radical used as radical terminators in the polymerization of styrene. Since then, the studies on its inhibitory effectiveness for the polymerization of methyl methacrylate and other vinyl monomers was initiated [48]. But, since the product (VII) formed with propagating radicals can homolytically dissociate back to the original verdazyl radical, the use of this radical in the kinetic studies is not appropriate.

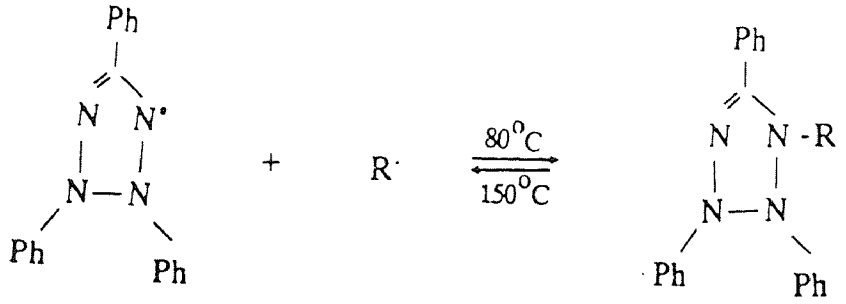

(10)

where R· is the active radical.

In the polymerization of certain monomers (for example, oligourethane acrylate), the regeneration of the verdazyl radical was not observed, but the inhibition efficiency was appreciably decreased as the reaction temperature was increased.

Moreover, the triphenylverdazyl radical is capable of reacting with the double bond in acrylonitrile molecule. The verdazyl radicals are also relatively easily oxidized by the presence of peroxy compounds at low temperatures (10-20^{o}C) [84].

The above characteristic features of the behavior of verdazyl radicals limit their application to the reliable estimation of the various kinetic parameters. However, when a verdazyl radical is to be employed, the ratio of [verdazyl] / [initiator] should not exceed two.

3.2.4 Aryloxy Radical

Galvinoxyl radical [49] is the only one stable radical considered as an inhibitor in polymerization in the literature. However, owing to its low photochemical and thermal stability, and its ability to react with oxygen, it cannot be used in the accurate kinetic measurements for vinyl polymerization.

3.2.5 Nitroxyl Radicals

It was not until the beginning of the 1960s that only one classical nitroxyl radical (Banfield's radical or nitroxylnitroxide) was used as polymerization inhibitor. This compound is relatively unstable in air, and in inert environment it is appreciably stable. As an inhibitor in the polymerization of styrene and methyl methacrylate [50], its induction period was shorter than the value calculated from the equation(9). This was first explained by the fact that the compound undergoes partial decomposition during the reaction. Later, Tudos [61] suggested that this compound may be involved in chain initiation reactions. However, only the kinetic data obtained from the latter hypothesis agree satisfactorily with the literature data. Banfield's radical was found to react with acrylonitrile. It is not a suitable radical counter for determination of the quantitative characteristics of the polymerization

reaction of acrylonitrile. There are more applications of Banfield's radical as discussed in references [39].

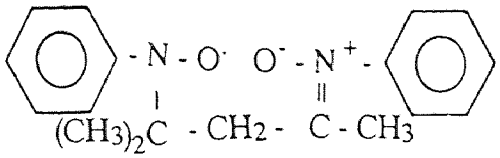

Banfield's radical

In the 1970s, a new class of extremely stable non-aromatic nitroxyl radicals (iminoxy radical) with a localized free radical center was successfully developed [51,52]. Initially, these radicals were used as radical counters and antioxidants. An interesting feature of these radicals is that the non-aromatic nitroxyl radicals recombine rapidly with alkyl radicals but, in general, do not interact with peroxy radicals, whereas the aromatic nitroxyl radical reacts with the peroxy radical ROO·.

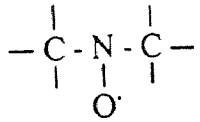

(iminoxy radical) (11)

Using these nitroxyl radicals as inhibitors in the polymerization of styrene was first attempted by Ruban and coworkers [53]. They studied the inhibition of monoradical nitroxyl in the styrene polymerization initiated by AIBN and benzoyl peroxide. The inhibition rate constants were calculated based on the assumption that the chain termination took place in 1:1 proportions. Further, this study was extended to the reaction of biradicals with alkyl radicals produced from the thermal homolytic dissociation of AIBN initiator in the solution of ethylbenzene and dioxane. It was observed that the recombination of the radical centers with alkyl radicals depends on the residual unpaired electron in the biradical. The first radical center within the biradical proceeds more readily than the second. The reason, according to the authors, is that the spin reactivity in the biradical exceeded that in the monoradicals in terms of the adiabaticity of the recombination reactions.

The study on the addition kinetics of mono-, and bi-radicals to the double bond of the styrene and α-methylstyrene at 100-170°C was also attempted by Ruban *et al.* [53]. The following mechanism was proposed to characterize the reaction kinetics for monoradicals:

$$CH_2=CHC_6H_5 + X^{\cdot} \xrightarrow{k_m} X\text{-}CH_2\text{-}CHC_6H_5 \ (R^{\cdot}), \text{ and} \qquad (12a)$$

$$R^{\cdot} + X^{\cdot} \xrightarrow{k_X} \text{products} , \qquad (12b)$$

where $R^{\cdot}$ represents the active radicals and $X^{\cdot}$ is the monoradical. The k_m and k_X are the rate constants for their corresponding reactions.

Under the above conditions, the addition reactions were fairly significant. The polymerization was then initiated by both styrene itself and this addition reaction. Therefore, the nitroxyl radical functions both as an initiator and an inhibitor simultaneously. But the authors did not take into account the fairly high rate of styrene thermal polymerization in their model. Thus, the addition constants they evaluated are not appropriate. Later, this factor was considered in two other investigations [86,87]. Assuming that the thermal initiation takes place in accordance with Mayo's mechanism [7], the authors proposed the following equations for the rate of consumption of the nitroxyl radical in the monomer.

$$-\frac{d[X]}{dt} = 2k_{da}[M]^2 + 2k_m[M][X] , \qquad (13)$$

where k_{da} is the rate constant for the reaction of the iminoxy radical with the Diels - Alder adduct and [M] is the monomer concentration.

The latest data illustrate that the validity of this model requires additional evidence, in view of the uncertainties of the mechanism of the initiation of styrene thermal polymerization and of the influence of iminoxy radicals on the rate of its thermal polymerization.

The 2,2,6,6-tetramethyl-4-hydroxypiperidin-1-yloxy (TEMPO) radical was one of the first iminoxy radicals used as the counter of active centers in the polymeriza-

tion of tetrafluoroethylene. Its induction period was found proportional to the inhibitor concentration and the polymerization rate was not retarded at the end of the induction period. The stoichiometric coefficient was 1, which implies one nitroxyl radical terminates one active radical during the course of inhibited polymerization.

The 2,2,6,6-tetramethyl-4-oxopiperidin-1-yloxyl (TMPO) radical was also used to study the influence of the reaction product of nitroxyl radical with primary and polymeric radicals on the inhibited polymerization of styrene and methyl methacrylate. It was found that its final products (VIII) did not effect induction period and the rate of stationary polymerization. Only the product hydroxylamines, which were obtained from the reactions between propagating radicals and inhibitor, could retard the steady state polymerization. But, since their amount is very small and the reaction curve does not indicate any significant retardation at the end of the induction period, this effect can be excluded.

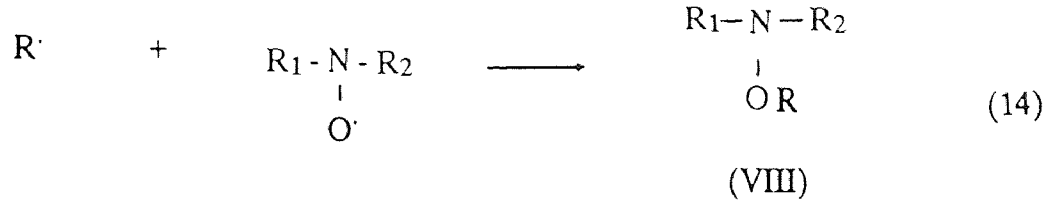

(VIII) (14)

Trubnikov [54] investigated the effect of nitroxyl radical-plus-initiator products on the reaction rates of the polymerizations of different monomers. He confirmed that most of the end products do not affect the polymerization kinetics except for hydroxylamine, whose presence can lower the rate of the process. In certain cases, some iminoxy radicals disproportionate with active radicals and form nitroso compounds, equation (15), [55]. These nitroso compounds are capable of terminating two kinetic chains per molecule. Therefore, the stoichiometric coefficients of iminoxys can be larger than 1.

The progress in the chemistry of nitroxyl radicals led to successful synthesis of polymeric free radicals. Such macromolecular stable radicals effectively inhibit the polymerization of styrene and methyl methacrylate, initiated by AIBN. These polymeric inhibitors also suppress the unwanted thermal polymerization during the synthetic processes of unsaturated ester, allylmethylacrylate, and glycol bismethacrylate. As a result, their reaction yield was increased from 52% to 92% (allylmethylacrylate). Nonetheless, the authors did not consider the kinetic behavior of

these macromolecular inhibitors during their synthetic reactions. Only experimental results demonstrating the improvement of reaction yield were reported.

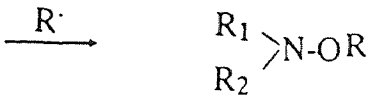

(15)

The influence of aromatic nitroxyls on the polymerization was also investigated in the literature. Gol'dfein and coworkers [52] use di(4-ethoxyphenyl)nitroxy radical as an inhibitor in the polymerization of styrene initiated by benzoyl peroxide (BP). The linear dependence of the induction period on the concentration of this additive was observed. But the rate of the reaction was slowly increased during the induction period and a decrease of the steady state rate with the increase of this aryl nitroxyl radical concentration was also observed. It was shown that this is due to the interaction of the benzoate radical with the aryl nitroxyl radical. When AIBN was used, this side effect was not revealed. Trubnikov et al. [88] proposed the following mechanism to explain this phenomenon:

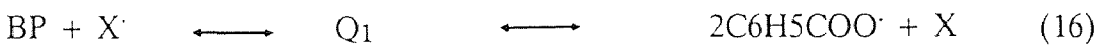

(16)

The effective activation energy (19 Kcal/mol) for the decomposition of the BP formed complex is appreciably lower than that of its initiation (29.87 Kcal/mol). Thus, BP is not a suitable initiator for determination of chain initiation when iminoxy or aryl nitroxyl radicals are used.

Many studies on the effect of the substituents in the iminoxy radical on the inhibition constant were investigated [54,55]. The main distinction was only on the

pre-exponential factor, not on the activation energy. Nonetheless, the kinetics and mechanism of the polymerization inhibited by nitroxyl radicals change significantly on passing from initiation by azo compounds to initiation by peroxy radicals. The nature of inhibition characteristics is also determined by the chemical structure of the initiator and the properties of solvents. The steric factor is not very significant.

CHAPTER 4

PREVIOUS WORK ON MRI CONTRAST AGENTS

Since the first observation of nuclear magnetic resonance (NMR) in 1946, developments in NMR spectroscopy have progressed at a rapid pace. In four decades, NMR has become a powerful analytical method in chemistry and biochemistry, and most recently in the field of medicine. Magnetic resonance imaging (MRI) has shown exceptional promise as a useful diagnostic modality for human disease. Unlike computerized X-ray tomography (CT), MRI does not use ionizing radiation, but yields two dimensional images of the body with quality usually equal to and in some cases exceeding that of CT images. It has many features when account for its rapid clinical acceptance: high soft tissue contrast sensitivity, high anatomic resolution, the ability to image detail in any arbitary direction, freedom from ionizing radiation, the ability to view and measure flow, and the availability of contrast agents to help measure perfusion in normal and diseased tissue. In this study, the focus is on the contrast agents. Such pharmaceuticals are capable of altering the intrinsic contrast between tissues and therefore improving the diagnostic confidence. A tumor over one hundred times smaller than the smallest a gamma ray system can detect can be observed by MRI.

The limits of MRI usefulness in assisting diagnosis are presently unknown. Nonetheless, early clinical reports greatly recognized this modality in human disease [55-57]. The use of appropriate contrast agents may further its effectiveness in detection sensitivity and disease selectivity. Therefore, its efficacy, and its extent of clinical acceptance and utilization could considerably rely on the additional clinical information afforded by appropriate contrast-enhancing pharmaceutical agents.

Two kinds of paramagnetic imaging pharmaceuticals have been developed in recent years, transition metal complexes and nitroxyl radicals. The first oral administration was $FeCl_3.H_2O$, and later $MnCl_2$ was used in injection into mice. However, the unmodified metal ions remained too toxic to be considered as MRI contrast agents for human use [58,59]. Metal ions are metabolized by the liver and display slow biological clearance. To reduce the toxicity of the agents, some organic

metal complexes have been used. In particular, metal complexes with polyaminocarboxylate ligands, EDTA and diethylenetriaminepentaacetic acid (DTPA) have received widespread attention [60]. Gadolinium-DTPA has been used to provide image enhancement of normal kidney tissue in animals. There are also some reports of the use of Gd-DTPA in Europe and the U.S. for the detection of cerebral tumors, hepatic tumors, and transitional cell carcinoma of the bladder. Nonetheless, the biggest problems encountered with this metal chelated complex is that the starting materials are known to be highly toxic. The LD_{50} values for free DTPA ligand and the free Gd^{3+} ion are 25 to 100 times more toxic than the complex itself.

An alternative class of paramagnetic agents that possess unique characteristics for contrast enhancement of MRI is those compounds containing nitroxyl radicals. In effective doses nitroxides are relatively non-toxic and they meet several requirements for being good contrast agents: prolonged stability at varying pH and temperature; feasible preparation and long shelf life; chemical flexibility permitting utilization either alone as nonspecific contrast agents or after modification as a highly specific agent, and longer spin relaxation times compared with inorganic ions. For these reasons in recent years attention has been focused on nitroxides used as MRI agents.

Currently, there are two classes of nitroxides being tested for NMR imaging. They are five membered heterocyclic compounds such as pyrrolidine nitroxides, and six membered heterocyclic compounds such as piperidine nitroxides. For example, 4-[3-(carboxy-1-oxopropyl) amino]-2,2,6,6-tetramethyl-1-piperidinyloxyl (TES) has been used to characterize the hydronephrosis, renal artery and vein ligations and sterile subcutaneous abscesses, and 3-carboxy-2,2,5,5-tetramethyl-1-pyrrolidinyloxyl (PCA) has been used to improve tumor/soft tissue contrast.

The design of nitroxides for *in vivo* bioreduction and for use as MRI contrast agents has been well documented in the literature. Valvis *et al.*[61,62] of this laboratory have demonstrated that nitroxides such as TMPNO(4-hydroxy-2,2,6,6-tetramethyl-piperidine-1oxyl), TMONO (2,2,4,4-tetramethyl-1,3-oxazolidine -3-oxyl) and DPNO (diphenylnitroxide) can be easily produced as well as reduced by hog liver enzyme. Eriksson and coworkers [63] examined the metabolic fate of nitroxide PCA in dogs and showed that ninety-four percent of either the unchanged

nitroxide or its corresponding hydroxylamine was recovered in urine within three days, and no other metabolic transformations were observed. These results imply that nitroxides in general are more compatible with animal and human metabolic system than metal chelated complexes.

In vitro spectroscopic measurements and osmotic load determination for a variety of nitroxides have demonstrated that greater relaxation and less toxicity with increased number of paramagnetic centers can be obtained. The six-membered ring piperidine nitroxides are relatively more powerful relaxing agents than the five-membered ring pyrrolidine nitroxides.

The factor viewed as the main drawback against the use of nitroxides is the possibility of their reduction to the nonparamagnetic hydroxylamine *in vivo*. But this tendency can turn out to be an advantage with proper imaging techniques. Recent progress in the chemistry of nitroxides has stimulated their scientific and practical applications. Their structures are easily altered synthetically [1,2] for different purposes. The preparation of persistent paramagnetic nitroxides and multinitroxides has become routine.

In this work, we synthesized a series of structurally diverse stable nitroxides which consist of mono, bi,and tri-nitroxyl radicals within a single molecule. The water molecule can directly access the paramagnetic centers of these molecules. As a comparison, two oligomers were also prepared. Each contains large quantities of nitroxyl radicals within a single molecule. At a given concentration, they might perform as effectively as a high concentration of equivalent monoradical or biradical nitroxyls. If they are relatively applicable, these polymeric nitroxides should have an expanded margin of safety in the sense that their intensity per molecule is higher.

CHAPTER 5
OBJECTIVES

- Prepare a series of structurally diverse stable nitroxides with multiple nitroxyl centers within a single molecules.

- Use styrene as a model monomer and evaluate their (nitroxides) inhibiting characteristics in terms of the length of the induction period in its polymerizing reaction.

- Develop kinetic models to calculate inhibition constants and further compare their stepwise radical killing capability.

- Evaluate the imaging enhancement characteristics of these nitroxides when used as contrast agents on NMR or MRI.

- Demonstrate their image enhancing capability in biological system. Use immobilized beads of liver enzyme, yeast and bacterial consortium as model systems.

CHAPTER 6

EXPERIMENTAL METHODS

6.1 Materials

All reagents were of spectrophotometric grade* (GC, HPLC or puriss) and were commercially available. All solvents were distilled prior to use. 4-hydroxy-2,2,6,6-tetramethylpiperidine (TEMP, purum), 2,2,6,6-tetramethyl-4-piperidone hydrochloride (purum), methyl acrylate (purum), methyl methacrylate (purum), pyrrolidine (puriss), oxalyl chloride (purum), adipoyl chloride (purum), sebacoyl chloride (purum), phthaloyl chloride (purum), phosphorus trichloride (pract.) and trimesic acid trichloride(purum) were used as purchased from Fluka Chemical Corporation (Ronkonkoma, New York). The catalyst, magnesium methanoxide (8% in methanol), was obtained from Aldrich Chemicals.

The 2,2'-azobis-isobutyronitrile (AIBN, assay (UV/VIS): 99%) obtained from Eastman Kodak Company (Rochester, New York) was recrystalized twice from petroleum ether. Its melting point is 100°C. The styrene used in bulk polymerization was purchased of high quality (puriss) from Fluka Chemical Corporation. It was purified by repeated washings with 10% sodium hydroxide followed by water washings till the final solution was not alkaline. After drying over anhydrous sodium sulfate, it was then distilled at reduced pressure (~ 25mmHg/ 45°C) and the middle fraction was collected for this experiment . The distilled styrene, after being sealed under nitrogen, was then refrigerated at - 4°C and used within 3 days.

6.2 Methods and Analysis

The analyses of synthetic compounds were performed by Thomas Hoover Capillary Melting Point Apparatus 6427-H10, IR (Perkin-Elmer Spectrometer 1310 or 1600 series FTIR), NMR on a Varian VXR 400 at Rutgers University (Newark, NJ), and

*: The detailed information of the reagent purity grades are described in the catalogs of Alltech Associates Inc. (for GC and HPLC grades) and Fluka Chemicals Corporations, 1991-1992 (for puriss, purum and pract. grades).

Mass Spectra on a HP 5988. The E.S.R. spectra were obtained with a Varian E-12 Spectrophotometer at Rutgers University (New Brunswick, NJ).

The relaxation times were recorded on NMR (Varian VXR 400) at Rutgers University (Newark, NJ). The image intensity was measured on a clincial MRI machine (GE Signa II) at University Hospital (Newark, NJ)..

Evaporations under vacuum were carried out with Buchi Rotoevaporator R110 apparatus. E. Merck TLC sheets (silica gel 60 F254, thickness 0.2mm) were used for detection with visualization using UV light and/or iodine chamber. Column chromatography was performed on Silica 60 (70-230 mesh, Fluka).

The dilatometer used to determine the rate of polymerization was obtained from Lab Glass LG 5618 (Vineland, New Jersey). It reaction volume is 10.75 cm^3 and its fitted capillary is graduated from 0.000 to 1.400 ml in 0.005 ml subdivisions.

The UV spectrophotometer used to measure the concentration of nitroxides was from Perkin-Elmer (Model C618-6437, Lambda 3B).

6.3 Synthesis of Nitroxides

The detailed procedures for the preparation of nitroxides (TEMPO, HPTPO, biradicals, triradicals and polyradicals) used in this study were described in literatures [3,64-66]. They are also briefly described as follows:

A. 4-hydroxy -2,2,6,6-tetramethylpiperidine-1-oxyl (TEMPO) [3]

The 4-hydroxy -2,2,6,6-tetramethylpiperidine (TEMP) (5 g) and sodium tungstate (0.07 g) were dissolved into 40 ml water and the solution was then cooled to 0-5^{o}C. The 30% hydrogen peroxide (5.4 g) was added to it slowly and left for one day for reaction. After being saturated with sodium chloride, extracted with ethyl acetate and dried over anhydrous sodium sulfate, the solution was stripped of solvent. The residue was further purified on column chromatography with a mixture of ethyl acetate/ hexane (1:1,v/v). After evaporation of eluting solvent, the pure red solid was obtained, which weighed 4.5 g. MP: 70-71^{o}C (literature: 71.5^{o}C [3])

The IR and ESR spectra are shown in Figures 1a and 1b respectively.

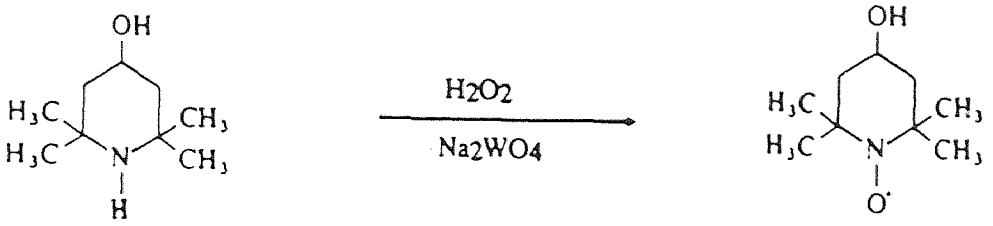

Scheme I

B. 4-hydroxy-3-hydroxypropylene-2,2,6,6-tetramethyl-piperidine-1-oxyl (HPTPO) [64]*

- **Neutralization of 2,2,6,6-tetramethyl-4-piperidone hydrochloride(II):**

Fifty (50) grams of (I) was dissolved in 50 ml distilled water and treated with 25 ml of cold 30% NaOH solution by adding dropwise with continued stirring. The resulting sludge was extracted with 240 ml benzene (3 x 80 ml). After evaporation of benzene, a white solid (2,2,6,6-tetramethyl-4-piperidone, II) was obtained which weighed 32 grams.

IR: 1700 cm^{-1} (C = O) and MP : 37 ^{o}C (Fig 2)

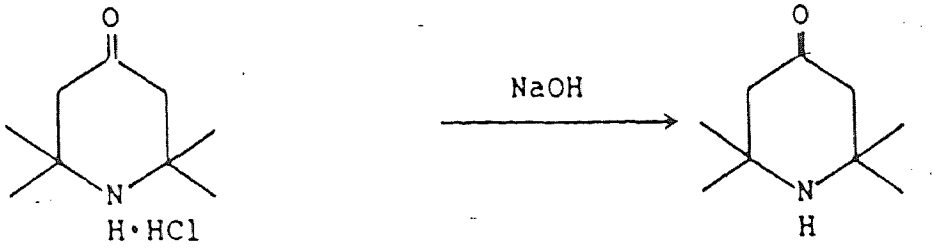

(I) (II)

Scheme II

* This work was under the supervision of Dr. D. K. Shen during 1989 and 1990, without whose proficient technical support it would become less probable.

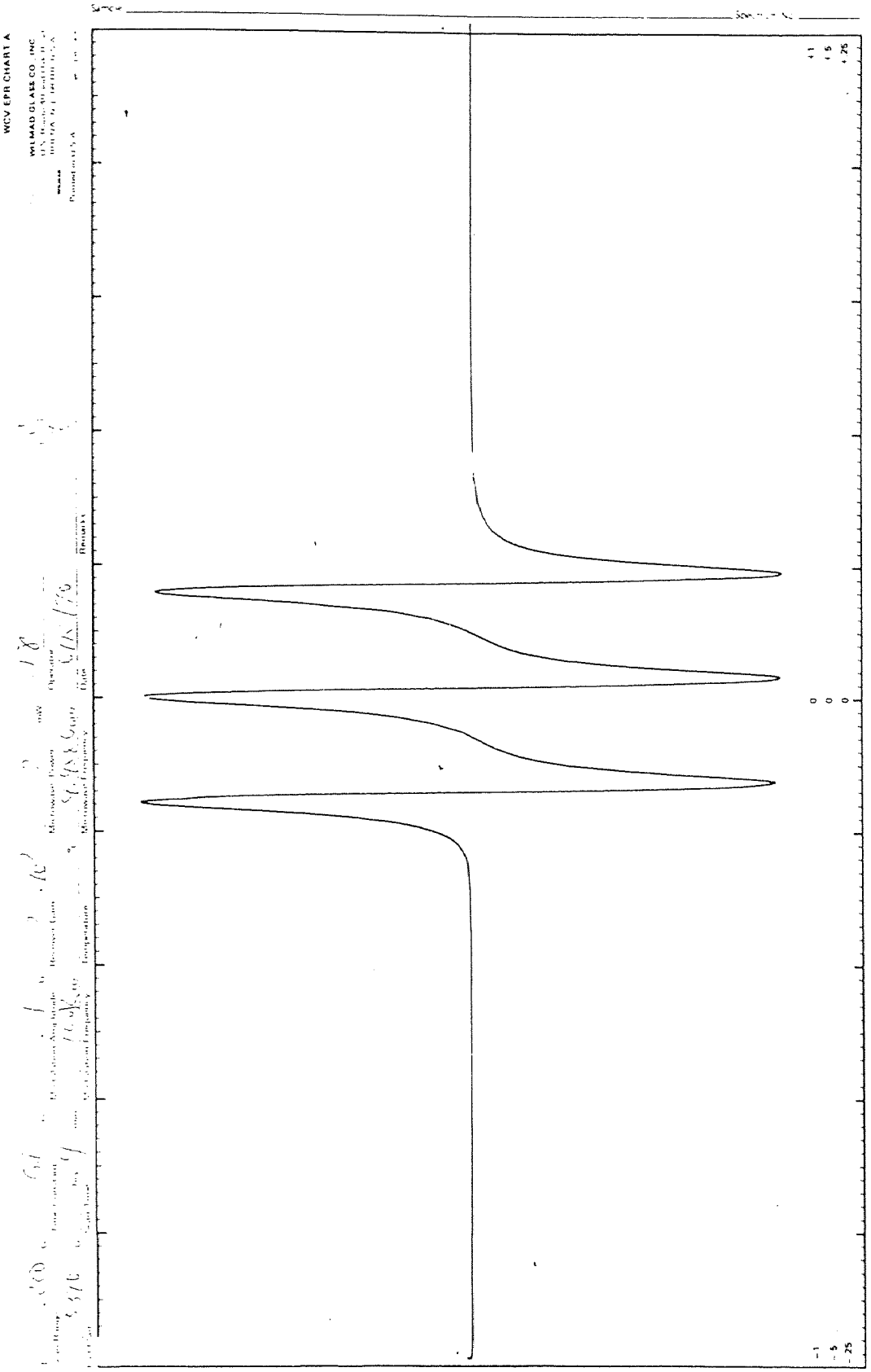

Fig 1a : ESR spectrum of TEMPO

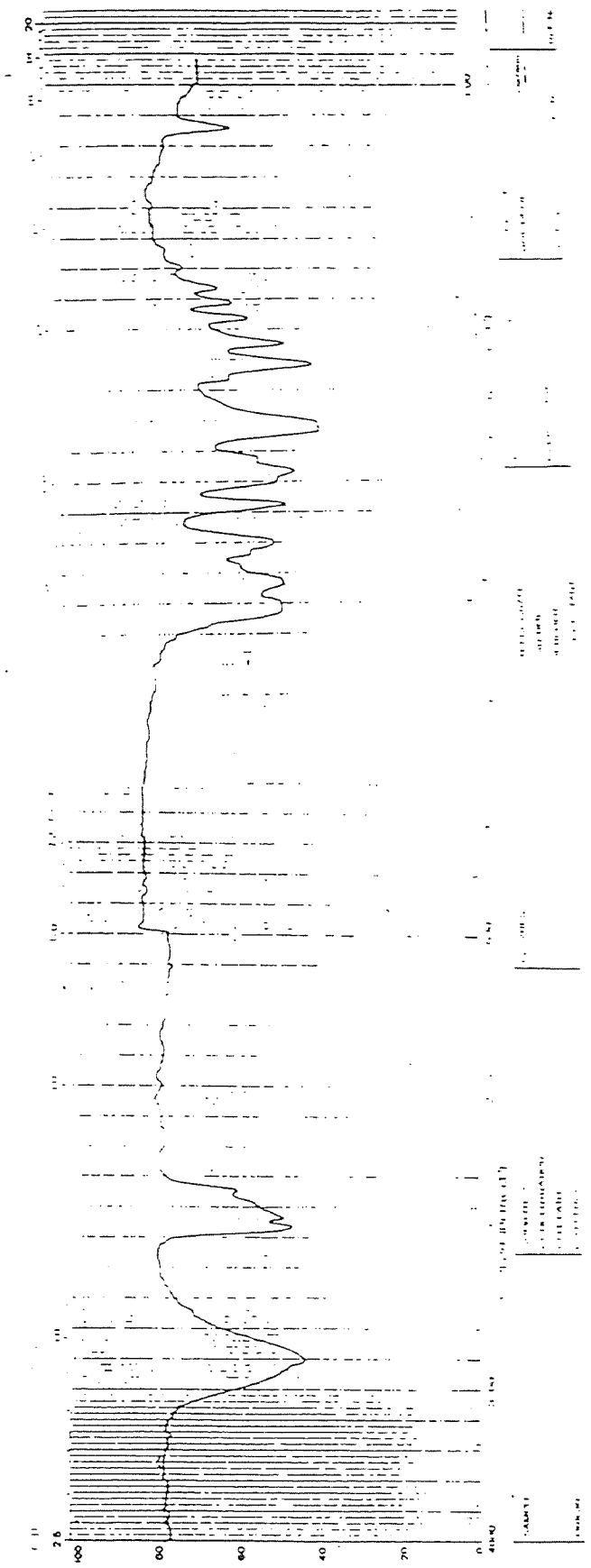

Fig 1b: IR Spectrum of TEMPO

OH: 3400 and 1050 cm^{-1}.

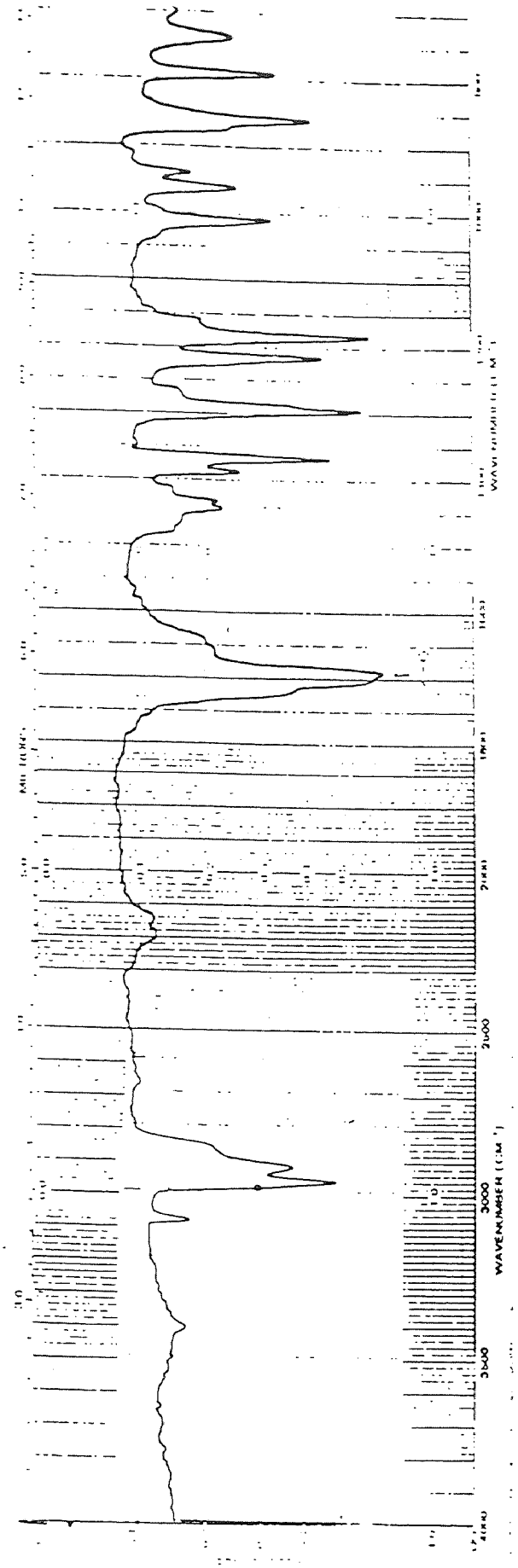

Fig 2: IR Spectrum of 2,2,6,6-tetramethyl-4-piperidone (II)

C=O : 1700 cm^{-1}

- **Preparation of 2,2,6,6-tetramethyl-4 (N, N-tetramethyleneimine)-piperidine-3-ene (III):**

Thirty four (34) grams of (II) and twenty two(22) grams of pyrrolidine were added to 50 ml benzene. The solution was refluxed for seven hours until no further water was generated in a Dean-Stark trap. Benzene and excess pyrrolidine were removed under reduced pressure. The crude enamine was distilled under vacuum to yield a yellow liquid. (bp: 80 ^{o}C/0.05mmHg).

IR:1630 cm^{-1} (C = C) and (C = O) 1700 cm^{-1} trace (Fig 3).

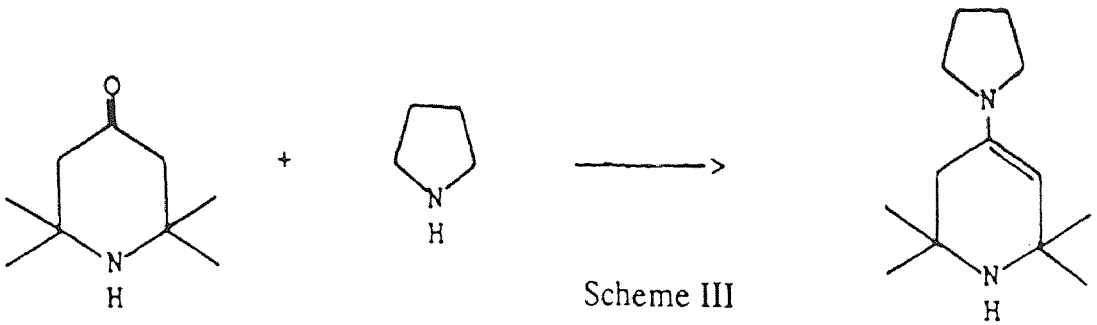

Scheme III

(II) (III)

- **Preparation of 2,2,6,6-tetramethyl-3 (2'-methoxycarbonyl)-4-piperidone (IV):**

A solution of 21.7 g of enamine (III) in 50 ml absolute ethanol was combined with 23.5 g of methyl acrylate (23.5 g). The mixture was then refluxed for 6 hours and an additional hour was followed after the addition of 16 ml water. Then the solvent was removed under reduced pressure. The crude product was purified by column chroma-tography with silica gel using ethyl acetate/hexane(1:1, v/v) mixture. Removal of solvent gave 15.6 g of (IV).

IR:1737,1707 cm^{-1} (C = O) and 1640 cm^{-1} (C = C) disappeared (Fig 4a).

Mass spectrum: m/e 242 (M + 1)(Fig 4b).

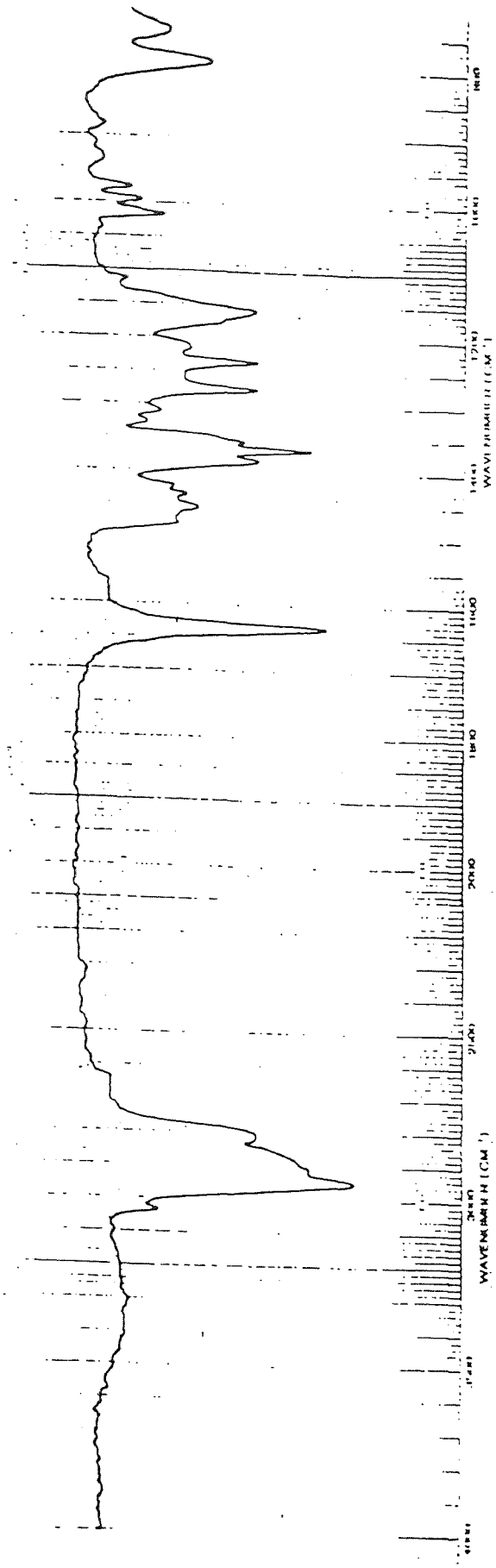

Fig 3: IR Spectrum of **2,2,6,6-tetramethyl-4(n,n-tetramethyleneimine)-piperidine-3-ene** (III)

C=C 1630 cm^{-1} and C=O 1700 cm^{-1} disappeared.

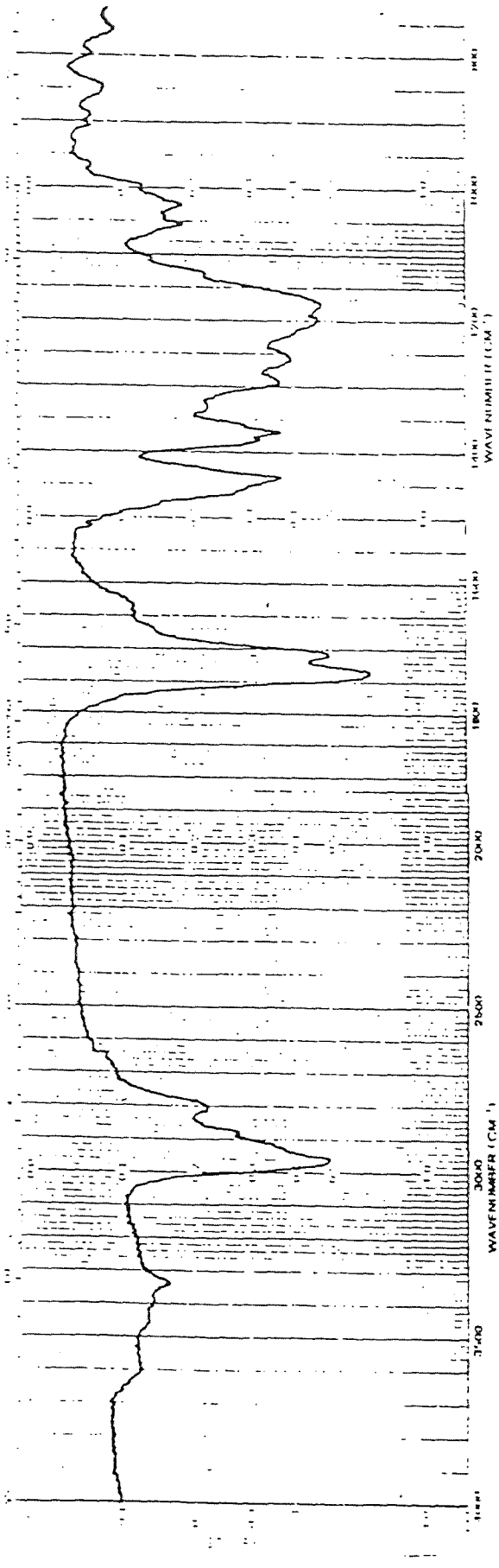

Fig 4a: IR Spectrum of **2,2,6,6-tetramethyl-3(2'-methoxycarbonyl)-4-piperidone (IV)**

C=O 1737 and 1707 cm^{-1}
C=C 1630 cm^{-1} disappeared.

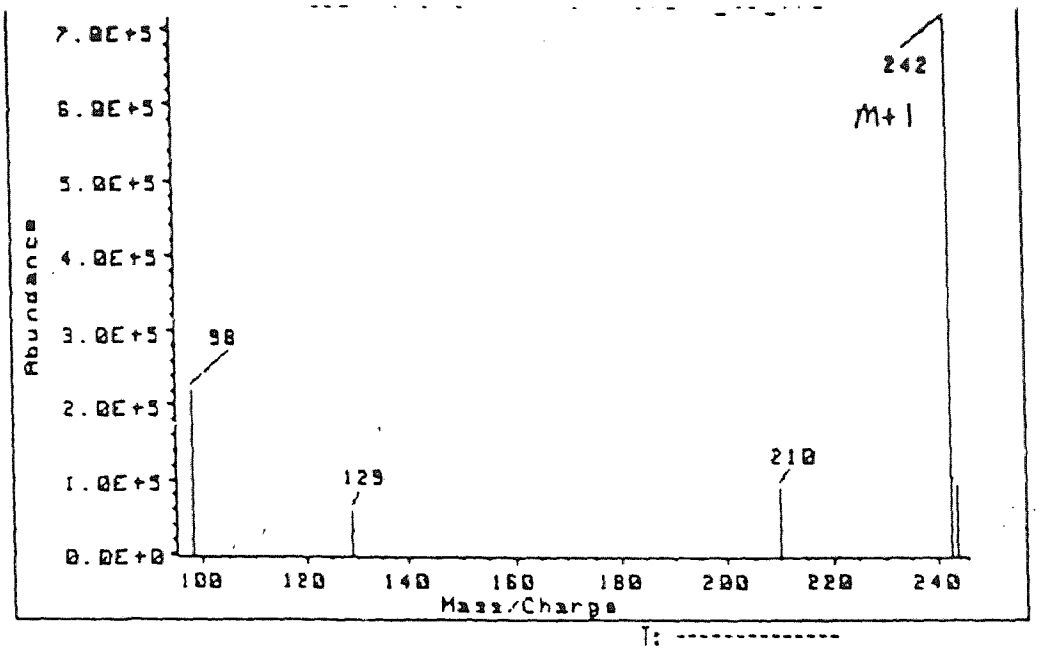

T:
Z: Scan 1.414 min. of V3:SAM_
Y: TIC of V3:SAM_CI_1.D
X: Scan 0.942 min. of V3:SAM_

[DE]

U

Scan 0.942 min. of V3:SAM_CI_1.D

AMU.	Abundance	AMU.	Abundance	AMU.	Abundance
97.95	218496.00	210.05	89232.00	243.20	94128.00
128.95	57832.00	242.20	715712.00		

Fig 4b: Molecular weight confirmation of compound (IV) by Mass Spectrometry using Chemical Ionization.

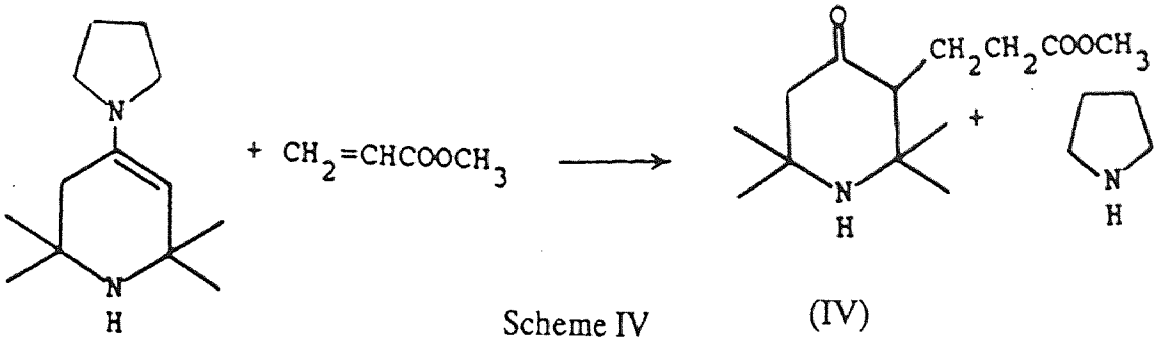

(III) Scheme IV (IV)

- **Preparation of 4-hydrozyl-3-hydroxypropylene-2,2,6,6-tetramethyl-piperidine (HPTP, V):**

1.5 g of sodium borohydride in 30 ml dry methanol was added to 3.3 grams of (III) dropwise in 10 ml dry methanol at 0-5°C. The reaction mixture was stirred for 24 hours and then refluxed for 12 hours following addition of 1.5 gram of sodium borohydride in 30 ml dry methanol. The solvent was removed in a rotary evaporator and the residue was dissolved in acetone and refluxed again for 1.5 hours. Acetone was evaporated at reduced pressure. The resultant solution was then rendered alkaline with 10% sodium carbonate and extracted with chloroform (4 x 50 ml). It was then dried with anhydrous sodium sulfate, filtered and concentrated at reduced pressure. The yellow sticky residue was distilled (126°C/2mmHg) and 1.8 g of product was obtained..

IR: 3300,1050 cm^{-1} (OH) and 1737,1704 cm^{-1} (C=O) disappeared (Fig 5a).

Mass spectrum: m/e 215 (Fig 5b).

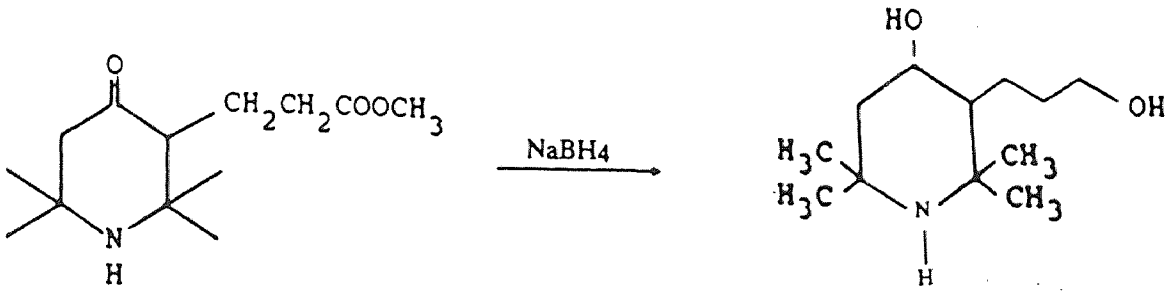

(IV) Scheme V (V)

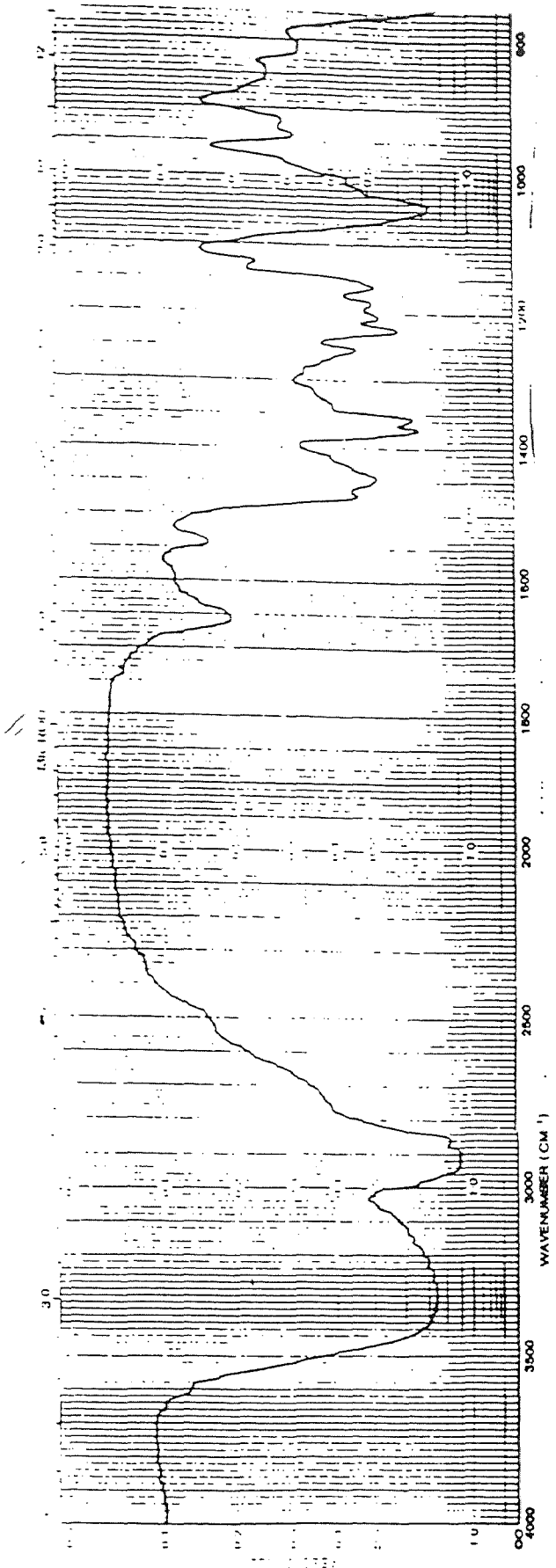

Fig 5a: IR Spectrum of **4-hydroxyl-3-hydroxypropylene-2,2,6,6-tetramethyl-piperidine (HPTP, V).**

OH: 3300 and 1050 cm^{-1}.
C=O 1737 and 1707 cm^{-1} disappeared.

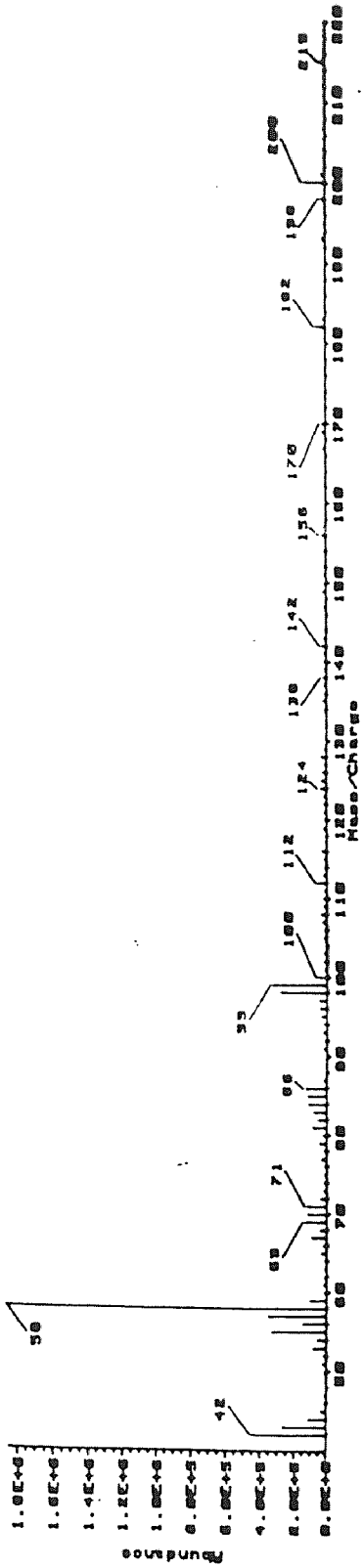

Fig 5b: Mass Spectrum of HPTP.

- **preparation of 4-hydroxyl-3-hydroxypropylene-2,2,6,6-tetramethyl-piperidine-1-oxyl (HPTPO, VI):**

Sodium tungstate dihydrate (0.03 g) in 3.5 ml of 30% hydrogen peroxide was added dropwise to one gram of (IV) in 10 ml water at 0-5°C, and the resultant mixture was stirred for 24 hours at room temperature. Ammonium carbonate (1.9 g) was then added and the mixture was extracted with methylene chloride (3 x 30 ml), and later dried with anhydrous sodium sulfate. The solvent was removed at reduced pressure and the product was purified by column chromatography on silicagel using ethyl acetate/hexane (1:1, v/v) mixture. The product (HPTPO) was obtained, which weighed 0.61 g.

IR:3390 and 1050cm^{-1} (Fig 6a).

Mass Spectrum: m/e 230 (Fig 6b).

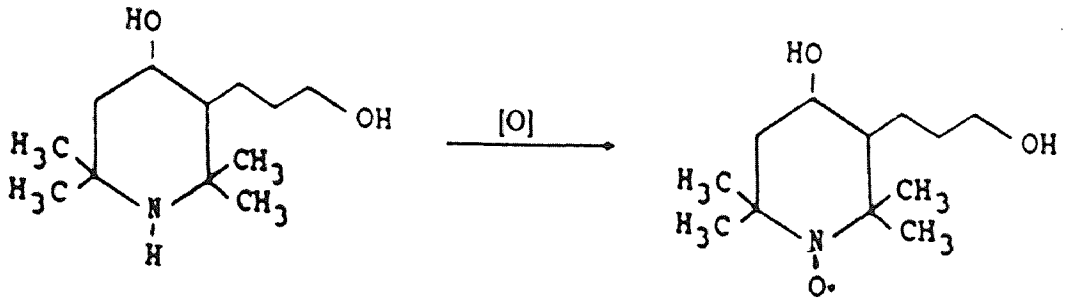

Scheme VI

(VI)

C. Synthesis of Biradicals and Triradicals [3]

The TEMPO (0.02 mole) was first dissolved in absolute pyridine and then cooled to 0-4°C. After slowly adding the dicarboxylic acid dichloride (0.01 mole), the resulting solution was kept stirring and cold for another 1.5 hours and for 14 hours at room temperature. This mixture was then poured into ice water (200ml) and then acidified with 10% hydrogen chloride to pH 4. The precipitate in this mixture was filtered off, washed with water and then dried at reduced pressure. The obtained raw solid product was again chromatographed on a column filled with silica gel 60 and eluted with ethyl acetate/hexane (1:1,v/v). The bright zone mixture was collected and

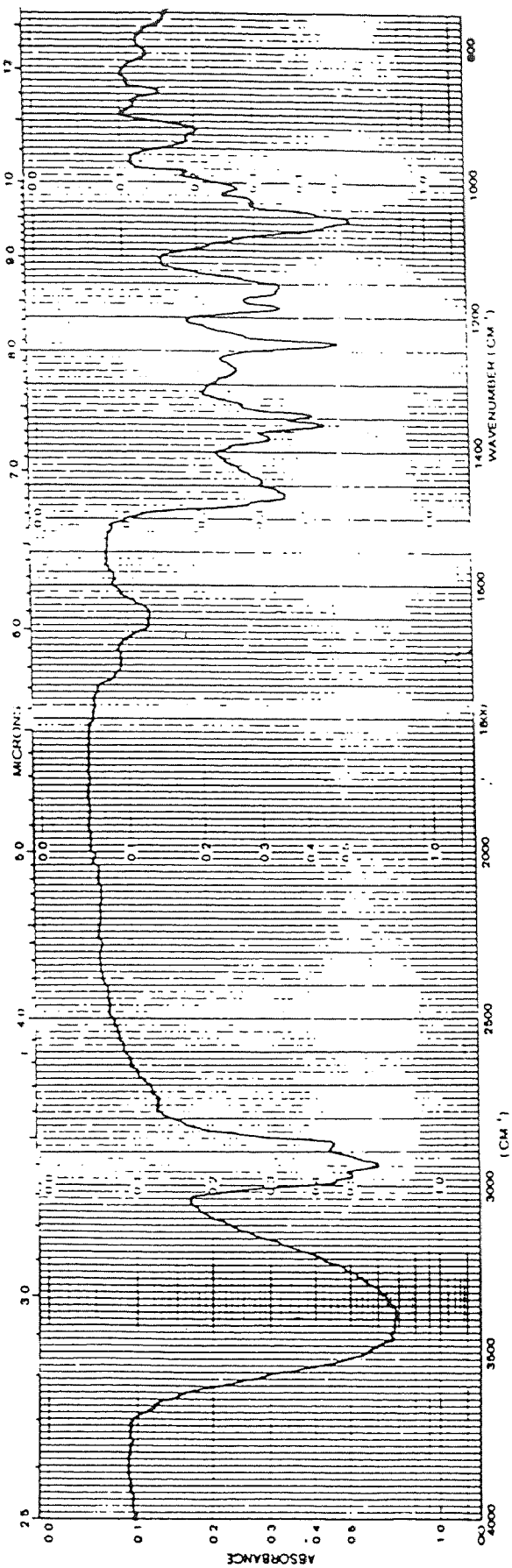

Fig 6a: IR Spectrum of **4-hydroxyl-3-hydroxypropylene-2,2,6,6-tetramethyl-piperidine-1-oxyl** (HPTPO, VI)

OH: 3300 and 1050 cm^{-1}.

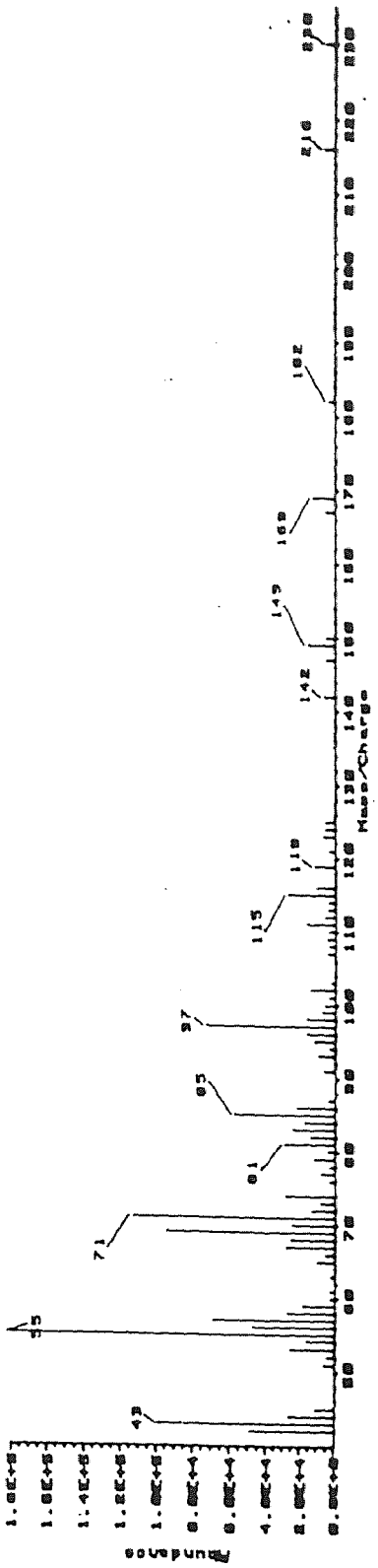

Fig 6b: Mass Spectrum of HPTPO

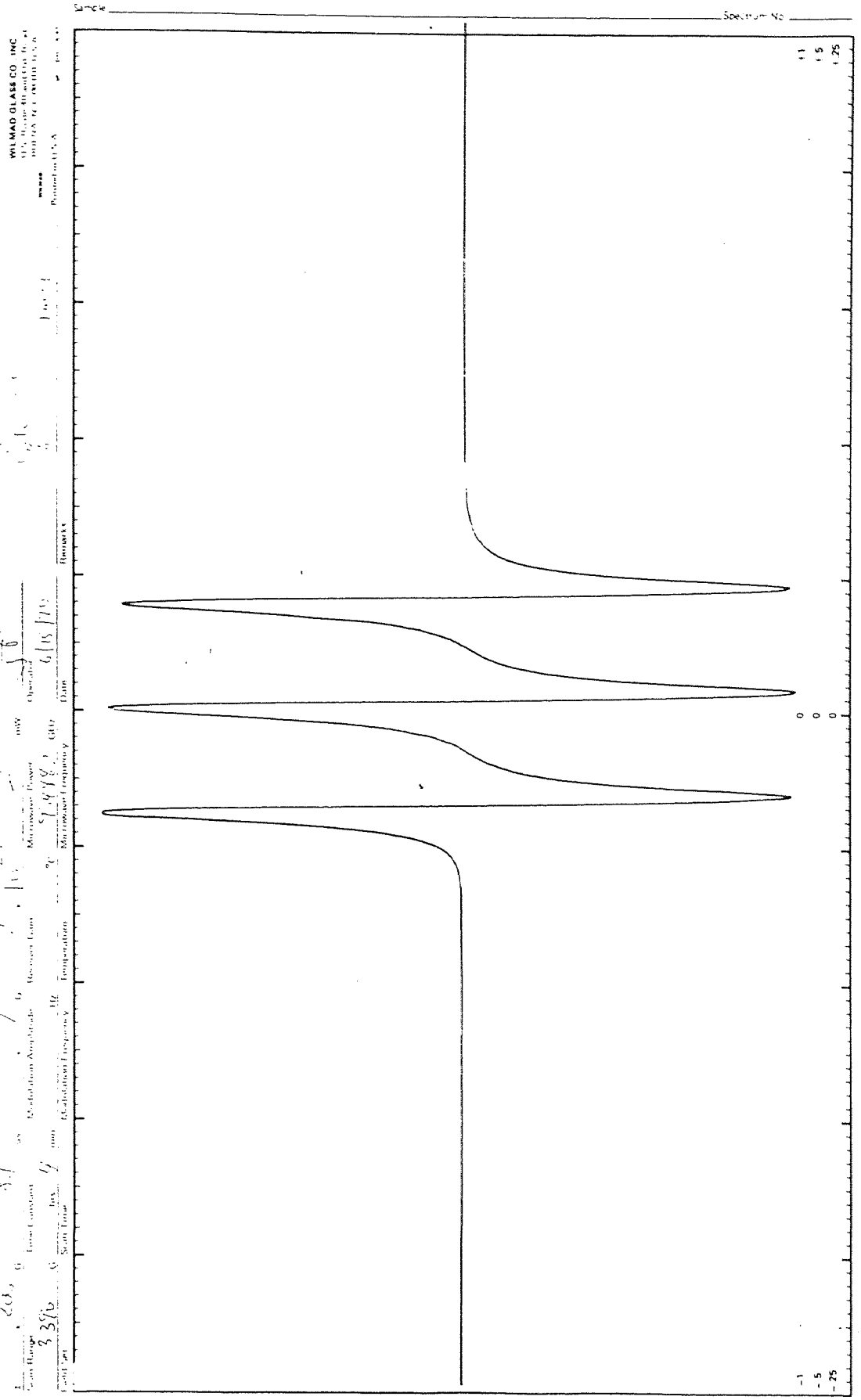

Fig 6c: ESR spectrum of HPTPO

its solvent was evaporated. The obtained solid was further recrystallized from dichloromethane and hexane and thus yielded pure biradicals.

VII: bis (2,2,6,6-tetramethyl-1-oxyl-4-piperidyl) oxalic acid (Fig 7a and 7b).

VIII: bis (2,2,6,6-tetramethyl-1-oxyl-4-piperidyl) adipic acid.

IX: bis (2,2,6,6-tetramethyl-1-oxyl-4-piperidyl) sebacic acid.

X: bis (2,2,6,6-tetramethyl-1-oxyl-4-piperidyl) terephthalic acid.

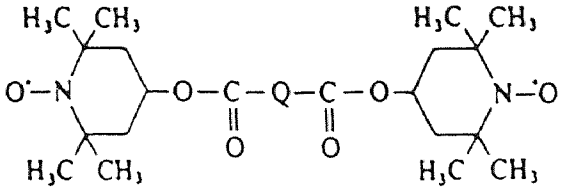

Q = — VII

$(CH_2)_4$ VIII

$(CH_2)_8$ IX

$p\text{-}C_6H_4$ X

The **triradical (XI)** was also prepared by using the above procedure, except that the molar ratio of reactants TEMPO and trimesic acid trichloride were 3:1.

XI: tris (2,2,6,6-tetramethyl-1-oxyl-4-piperidyl) trimesate (Fig 8a and 8b).

Another **triradical (XII)** was prepared as follows: Three grams of TEMPO and 1.8g of triethylamine were dissolved in the 15 ml benzene. This solution was then cooled to 0-4 ^{o}C. The solution of 0.8g of phosphorus trichloride in 10 ml benzene was then added to it very slowly. The resulting mixture was stirred for another 2 hours with ice cooling and kept overnight at room temperature. The solid precipitate was discarded and the solvent was removed by rotary evaporator. The residue was chroma-tographed on a column filled with silica gel 60 and with ethyl acetate and hexane as eluant. The red zone mixture which contained trichloride was collected. Following the evaporation of the solvent, further recrystallization was performed by using the solvent mixture of dichloromethane and hexane. The product thus obtained was :

(XII): tris (2,2,6,6-tetramethyl-1-oxyl-4-piperidyl) phosphite

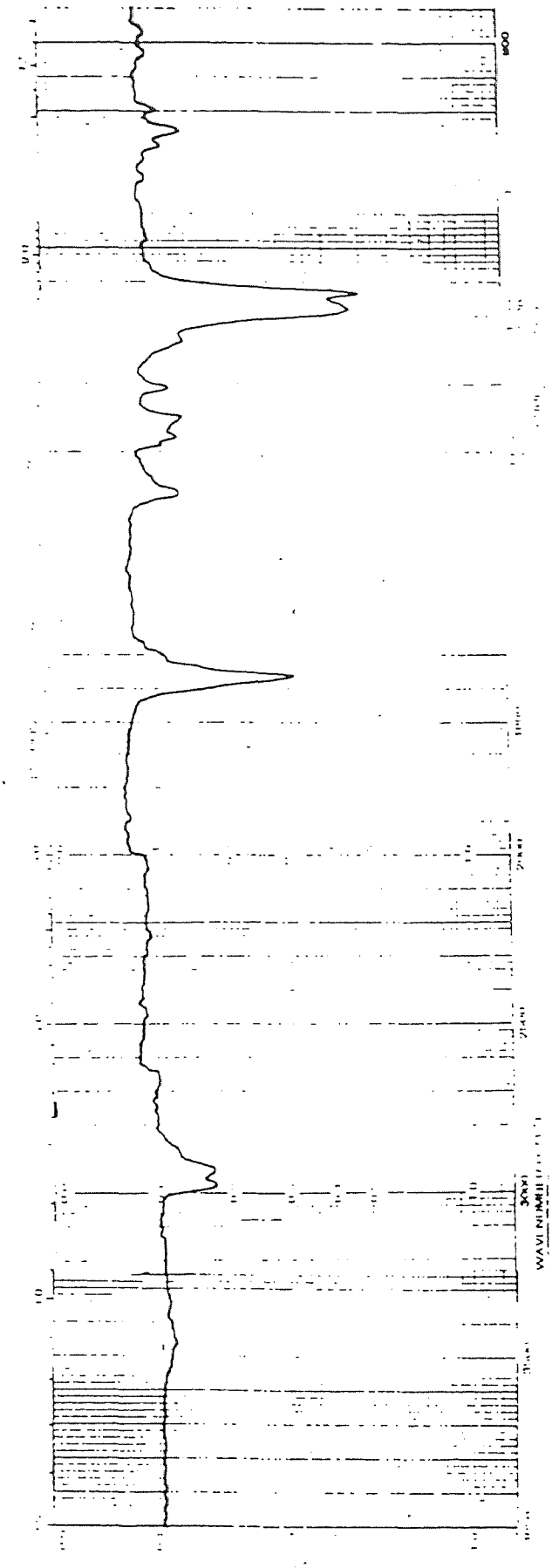

Fig 7a: IR Spectrum of bis (2,2,6,6-tetramethyl-1-oxyl-4-piperidyl) oxalic acid

C=O 1730 cm^{-1}

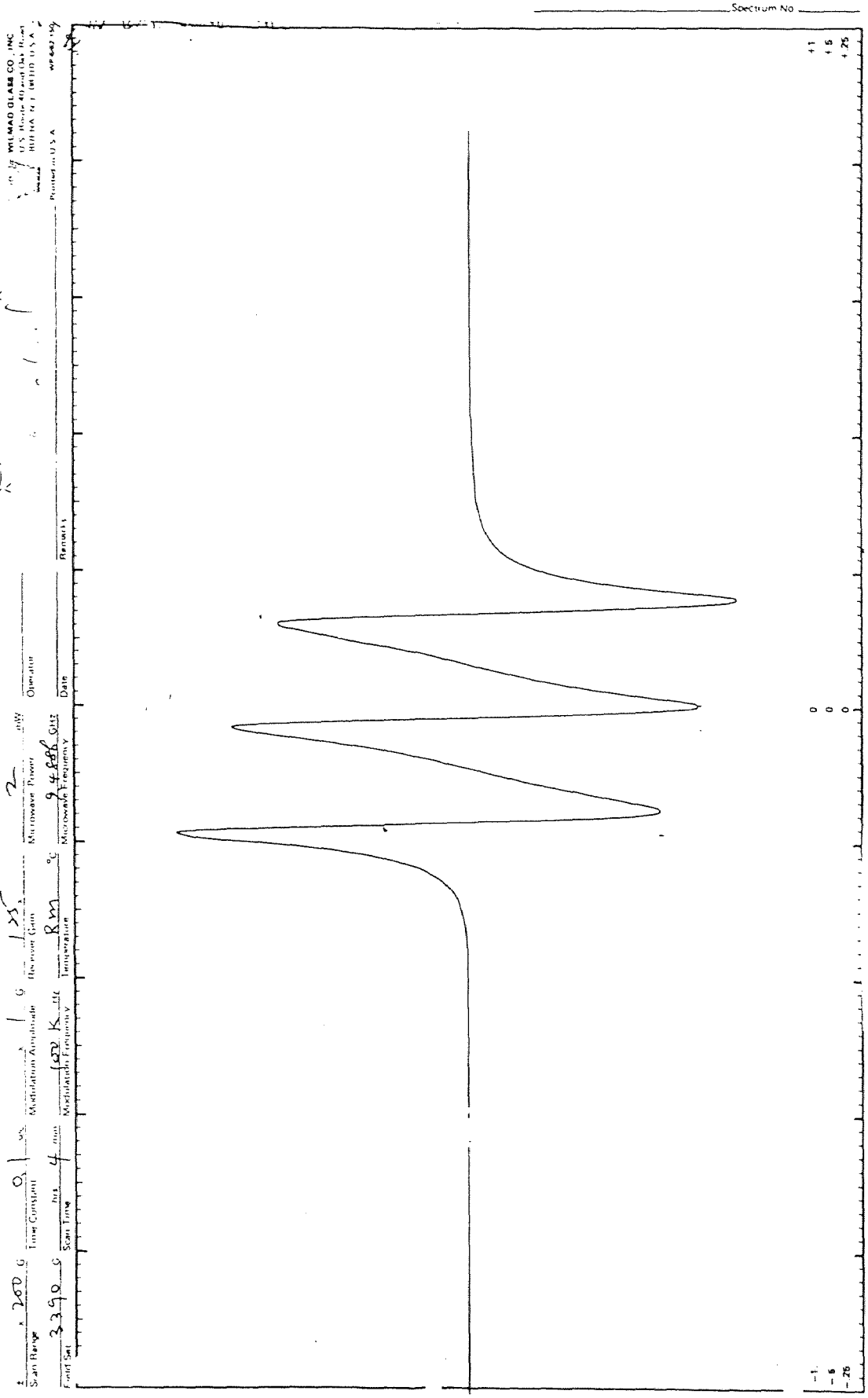

Fig 7b: ESR spectrum of bis(2,2,6,6-tetramethyl-1-oxyl) oxalic acid

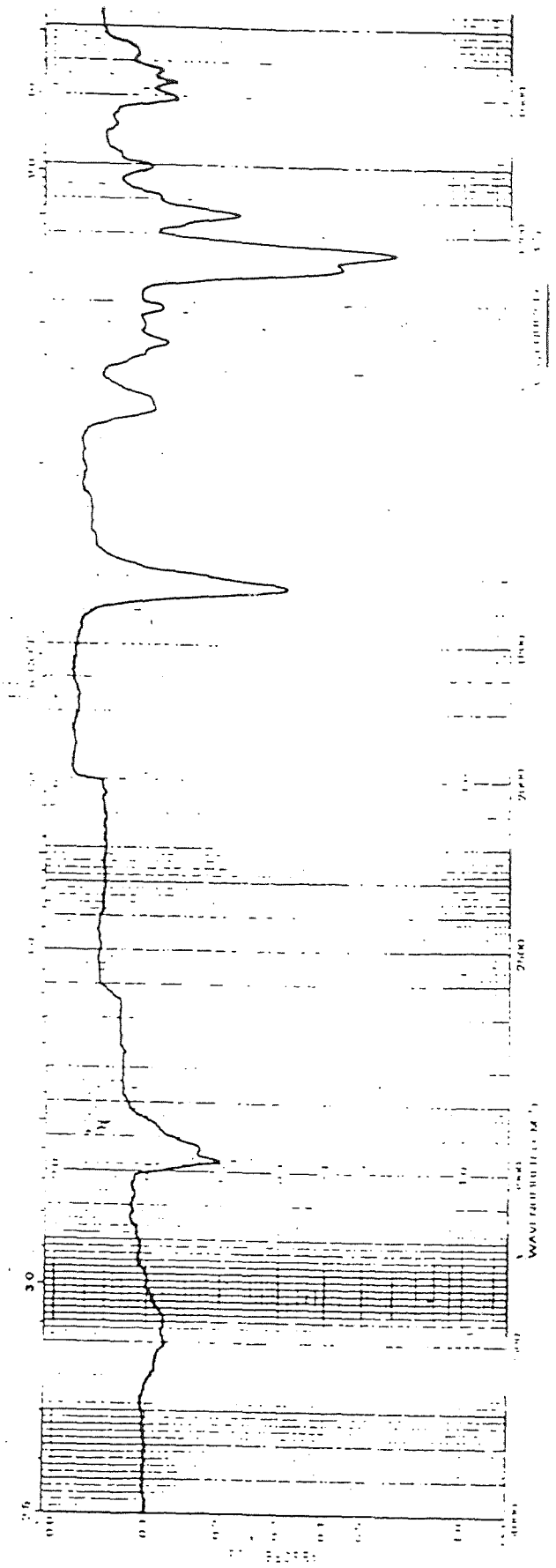

Fig 8a: IR Spectrum of tris (2,2,6,6-tetramethyl-1-oxyl-4-piperidyl) trimesate

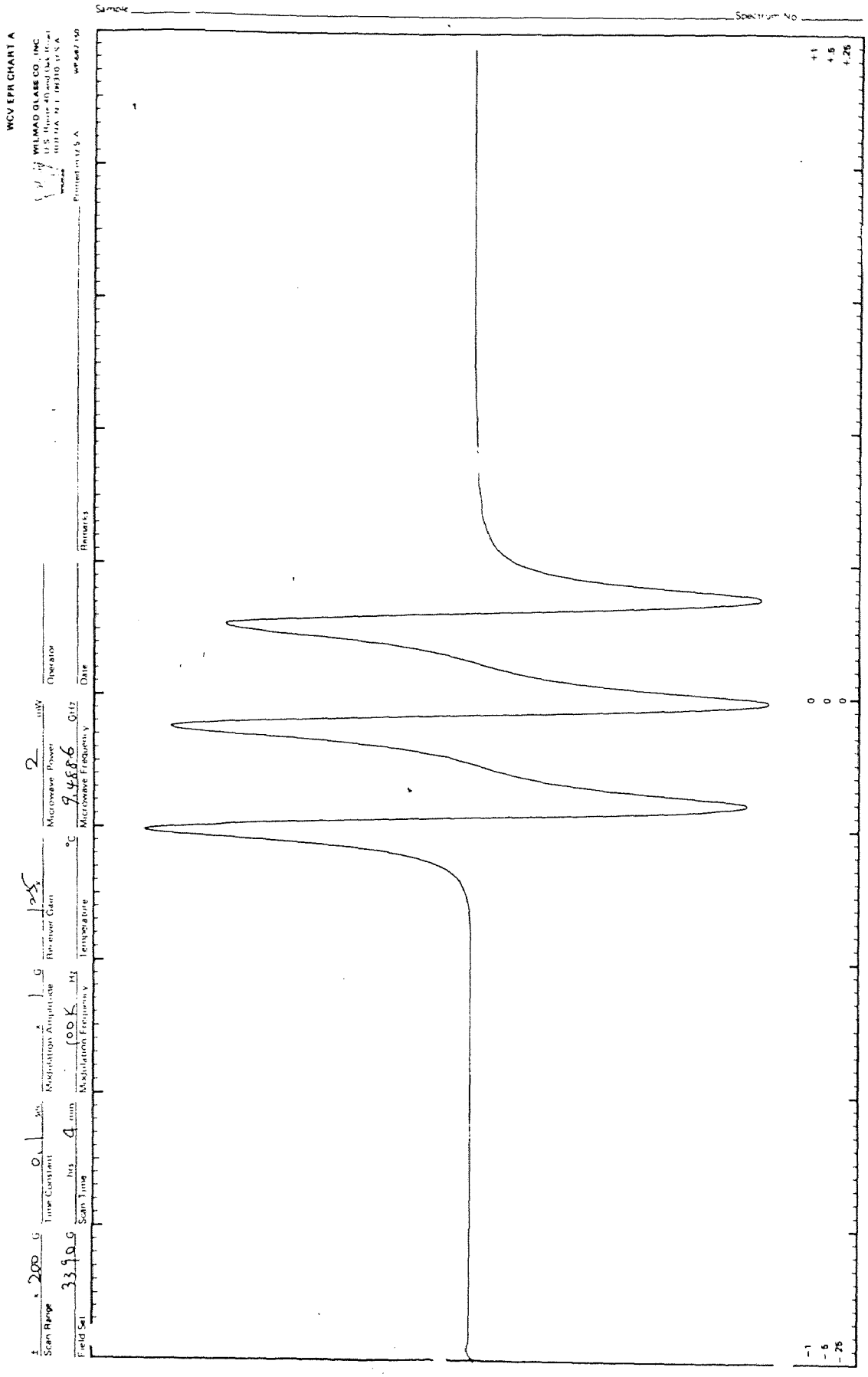

Fig 8b: ESR spectrum of tris(2,2,6,6-tetramethyl-1-oxyl) trimesate

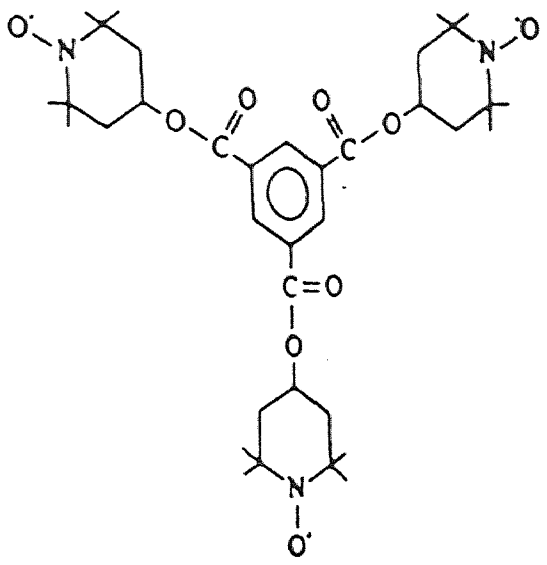

XI

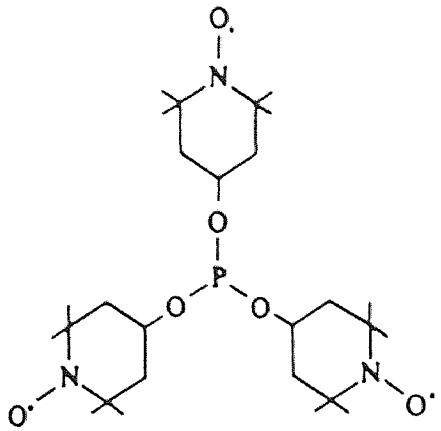

XII

D. Preparation of Polyradical Nitroxides [65,66]

- **Preparation of 4-methylacryloyl-2,2,6,6-tetramethyl-piperidine-1-oxyl(MTMP):**

Ten(10) grams of 4-hydroxy-2,2,6,6-tetramethyl-piperidine was dissolved in 13 ml of 8% magnesium methanoxide (in methanol). The combined solution was then added to another solution containing 50 ml of methyl methacrylate and 0.015g of 4-hydroxy-2,2,6,6-tetramethyl-piperidine-1-oxyl (used as inhibitor) in a 50 ml round bottom flask. The flask was equipped with a fractionation column and a distillation head. The temperature was increased and methanol was removed as top distillate. When the temperature at top of the column was maintained at 100°C for an hour, heating was stopped, 13 ml of water was added and magnesium hydroxide was filtered out. The organic filtrate was again washed with 25 ml distilled water and dried with anhydrous sodium sulfate. Excess methyl methacrylate was evaporated and the residue was purified by vacuum distillation. The product obtained weighed 6.2 g.

Mp:57-59°C (literature 57-58°C)

IR:1696 cm^{-1} (C=O) and 1625(C=C) cm^{-1} (Fig 9).

- **Homopolymerization of MTMP:**

The solution of 0.03 g of AIBN in 1 ml benzene was added to 2 grams of monomer MTMP in 10 ml benzene. The mixture was bubbled with nitrogen at 70°C

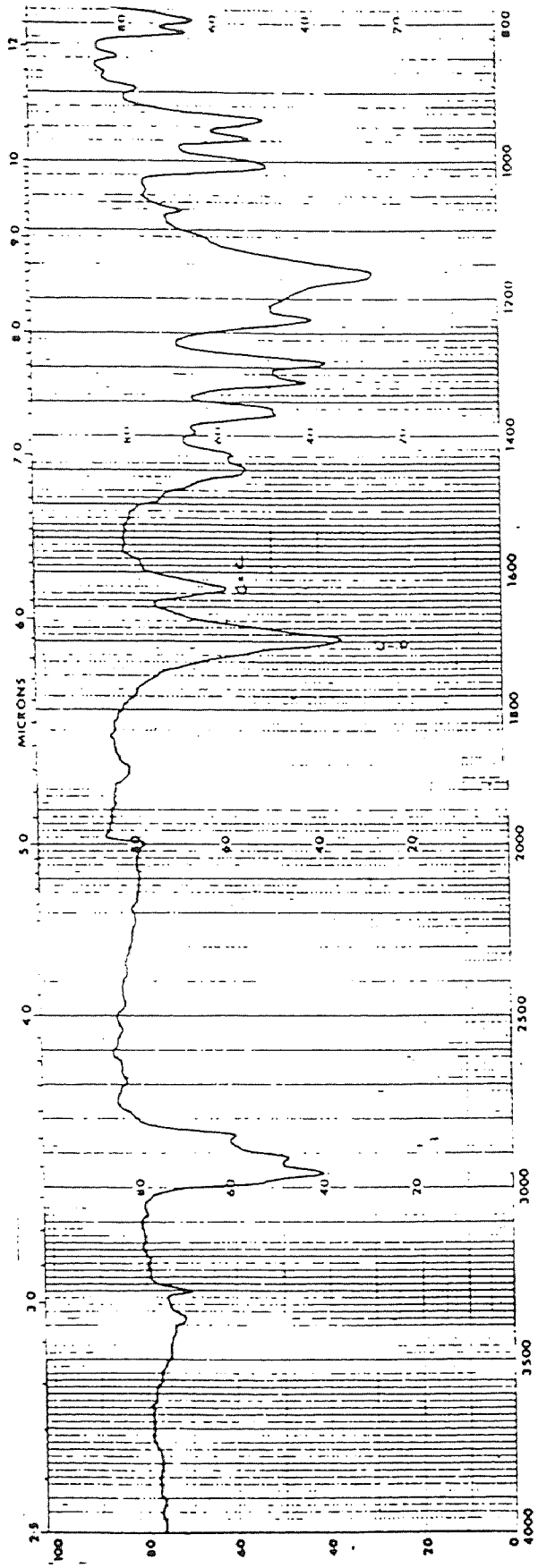

Fig 9: IR Spectrum of 4-methylacryloyl-2,2,6,6-tetramethyl-piperidine-1-oxyl (MTMP)

C=O 1696 and C=C 1625 cm^{-1}

for 10 hours. After reducing volume by rotary evaporator, 50% methanol was added to precipitate polymer, which was then dried under reduced pressure. The solid product obtained was 0.85 g in weight.

IR:1710 cm^{-1} (C=O) and 1625 cm^{-1} (C=C) disappeared.

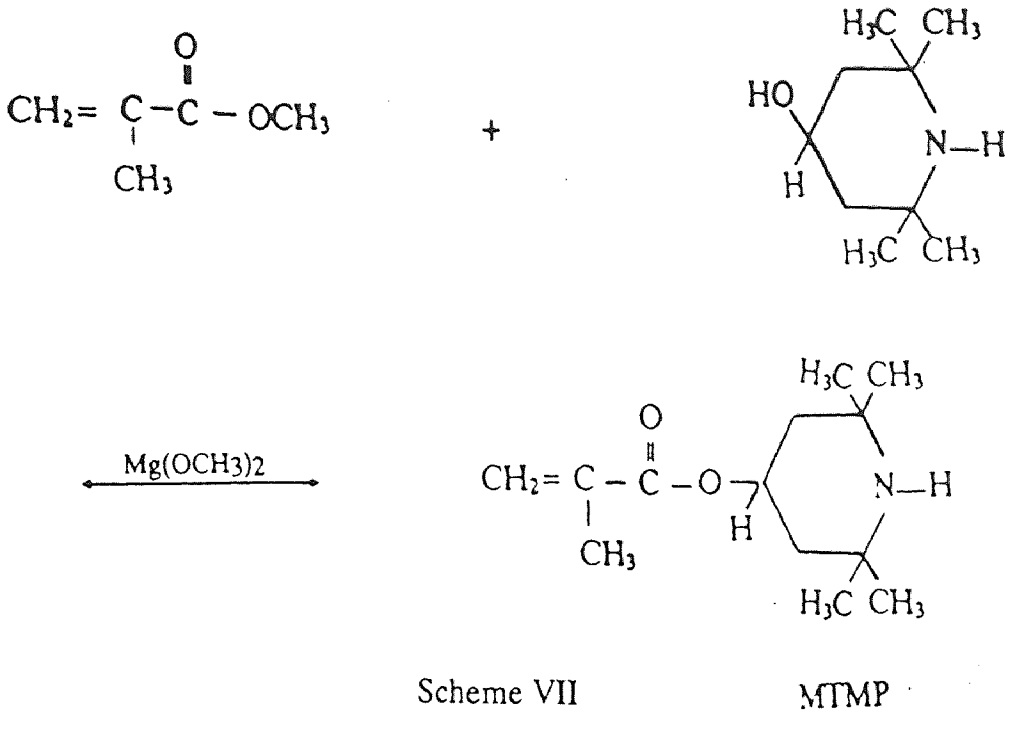

Scheme VII MTMP

- **Copolymerization of MTMP with styrene (PMS):**

The solution of 0.03 g of AIBN in 1 ml benzene was added to the mixture of one gram styrene and one gram MTMP in 10 ml benzene. The mixture was stirred at 70°C for 10 hours under a nitrogen blanket. The volume of mixture was again reduced by rotary evaporator, and methanol was added for precipitation. The precipitate was dried in the vacuum oven and afforded 1.4 g of product.

IR: 1710 cm^{-1} (C=O) and 1625 cm^{-1} (C=C) disappeared.

- **Preparation of polyradical nitroxides:**

Two grams of m-chloroperbenzoyl acid (MCPBA) in 10 ml CH_2Cl_2 were added dropwise to one gram of PMTMP (or PMS) in 20 ml CH_2Cl_2 at 0-5°C. The mixture was stirred for 24 hours and then its volume was reduced, and the product was precipitated by 50% methanol. The residue was dried under reduced pressure and yielded 1g PMTMPO (0.7g PMSO) nitroxide (Fig 10a, 10b, 11a and 11b).

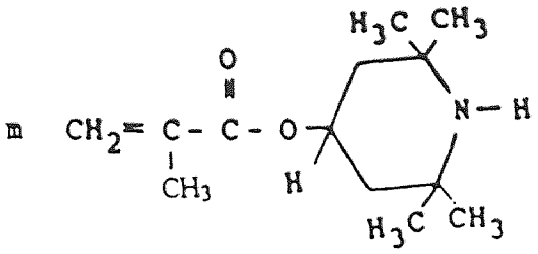

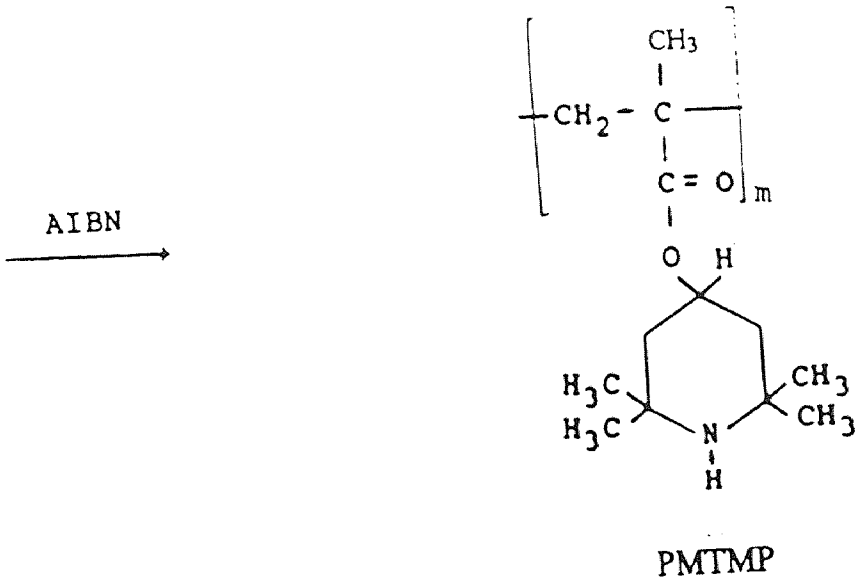

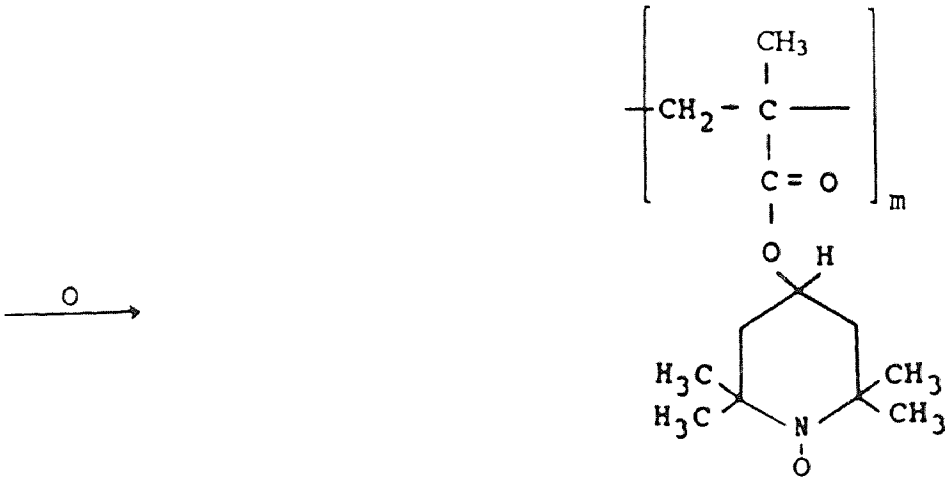

Scheme VIII

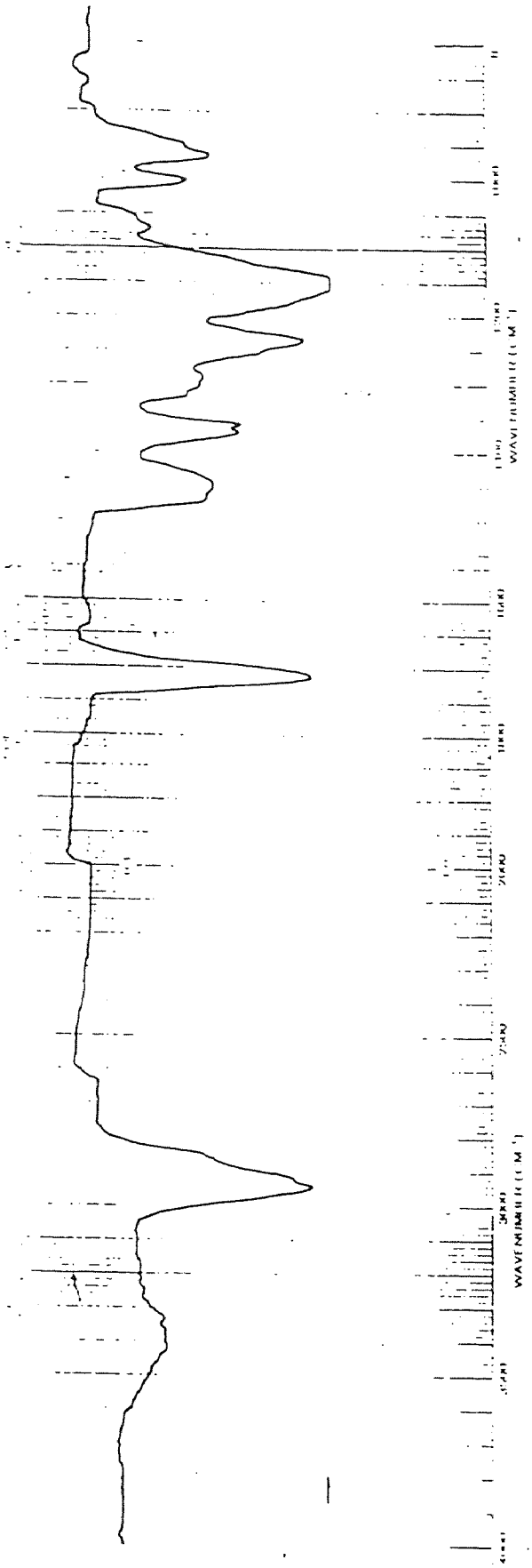

Fig 10a: IR Spectrum of **PMTMPO**

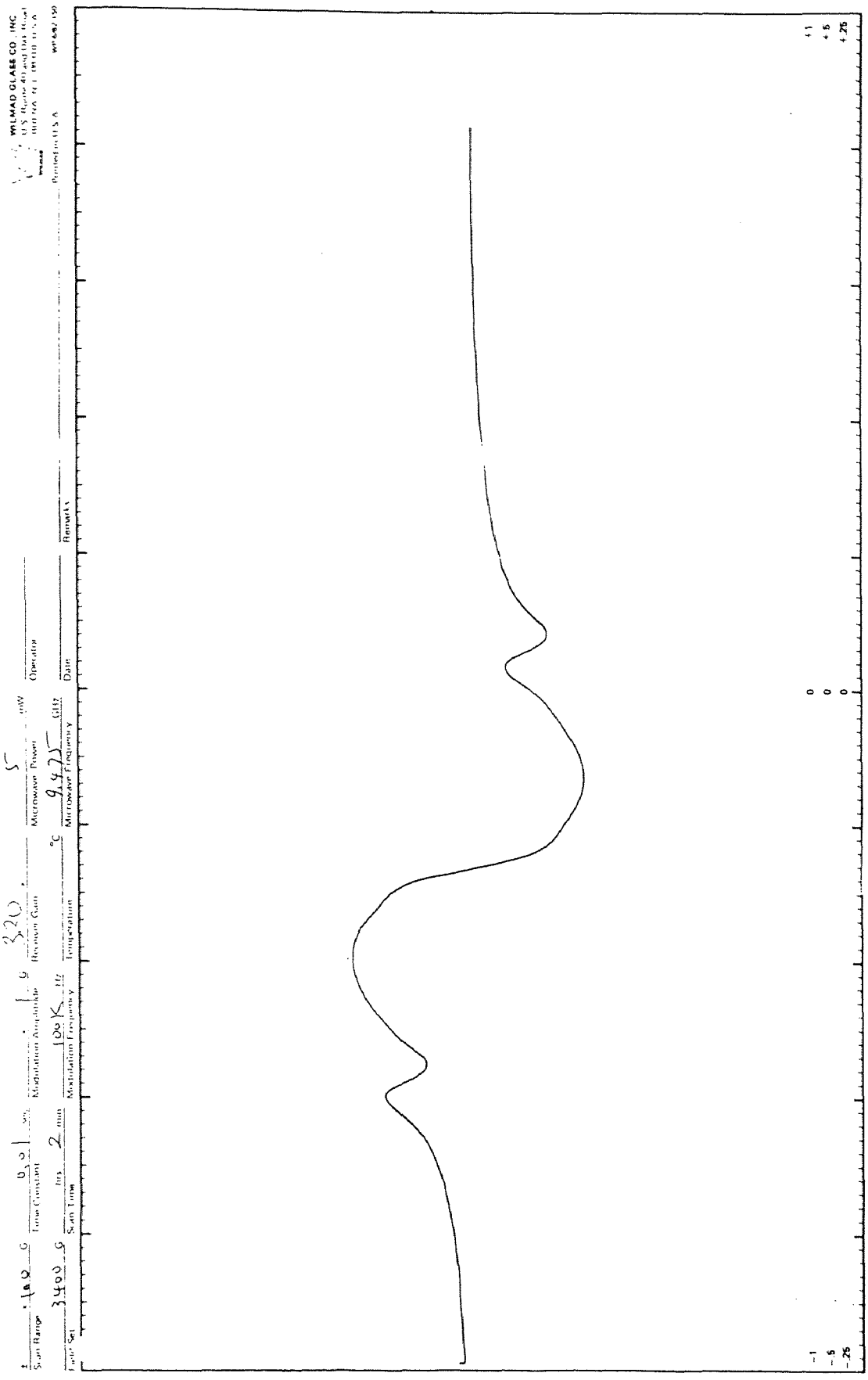

Fig 10b: ESR spectrum of PMTMPO

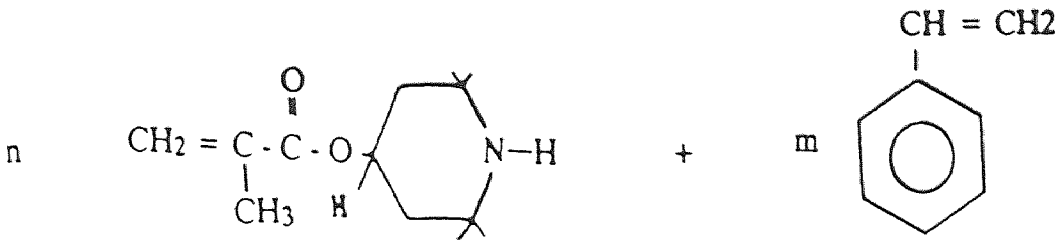

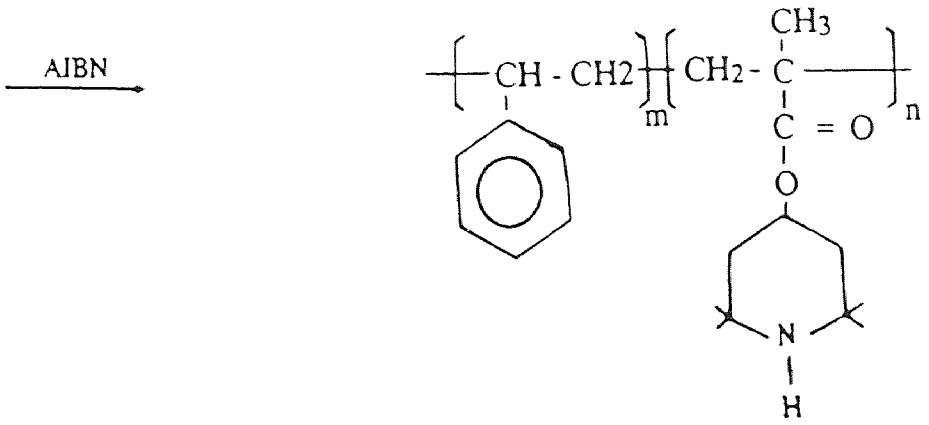

PMS

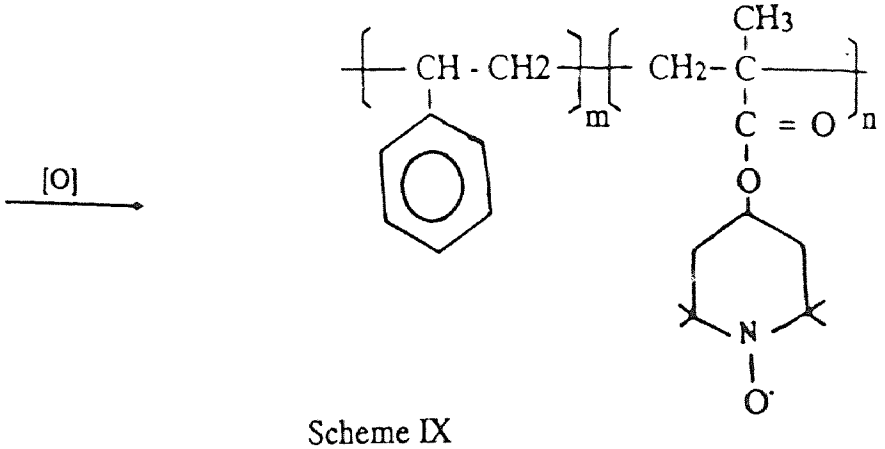

Scheme IX

PMSO

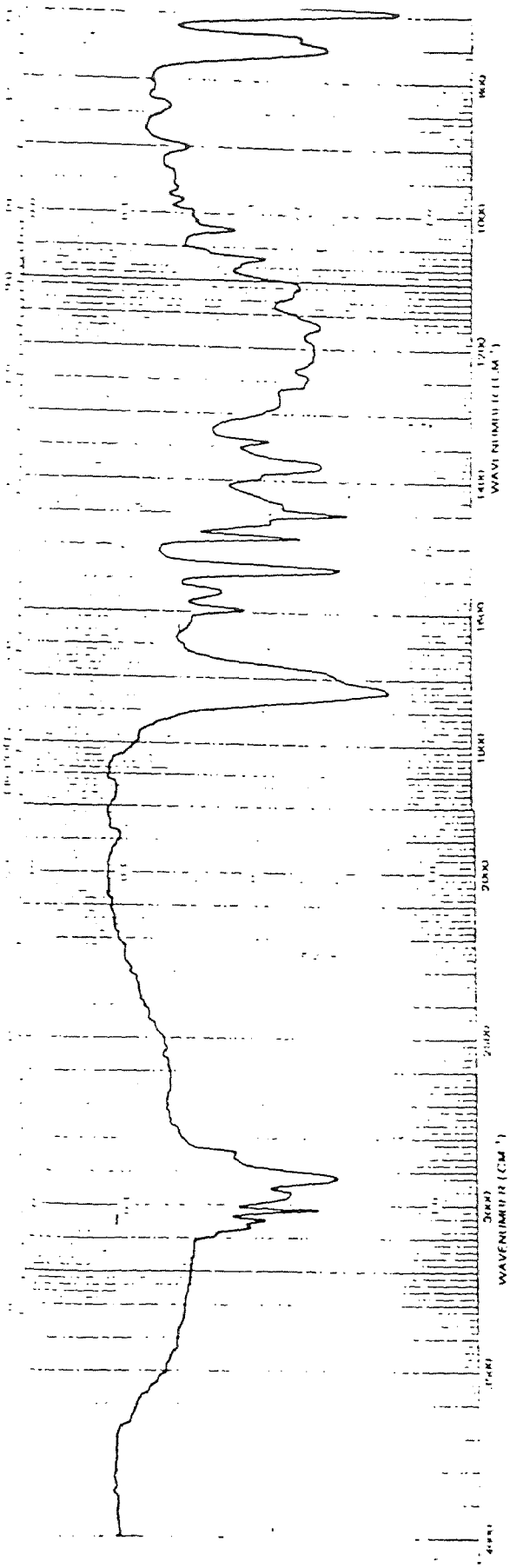

Fig 11a: IR Spectrum of PMSO

C=O 1718 cm^{-1}

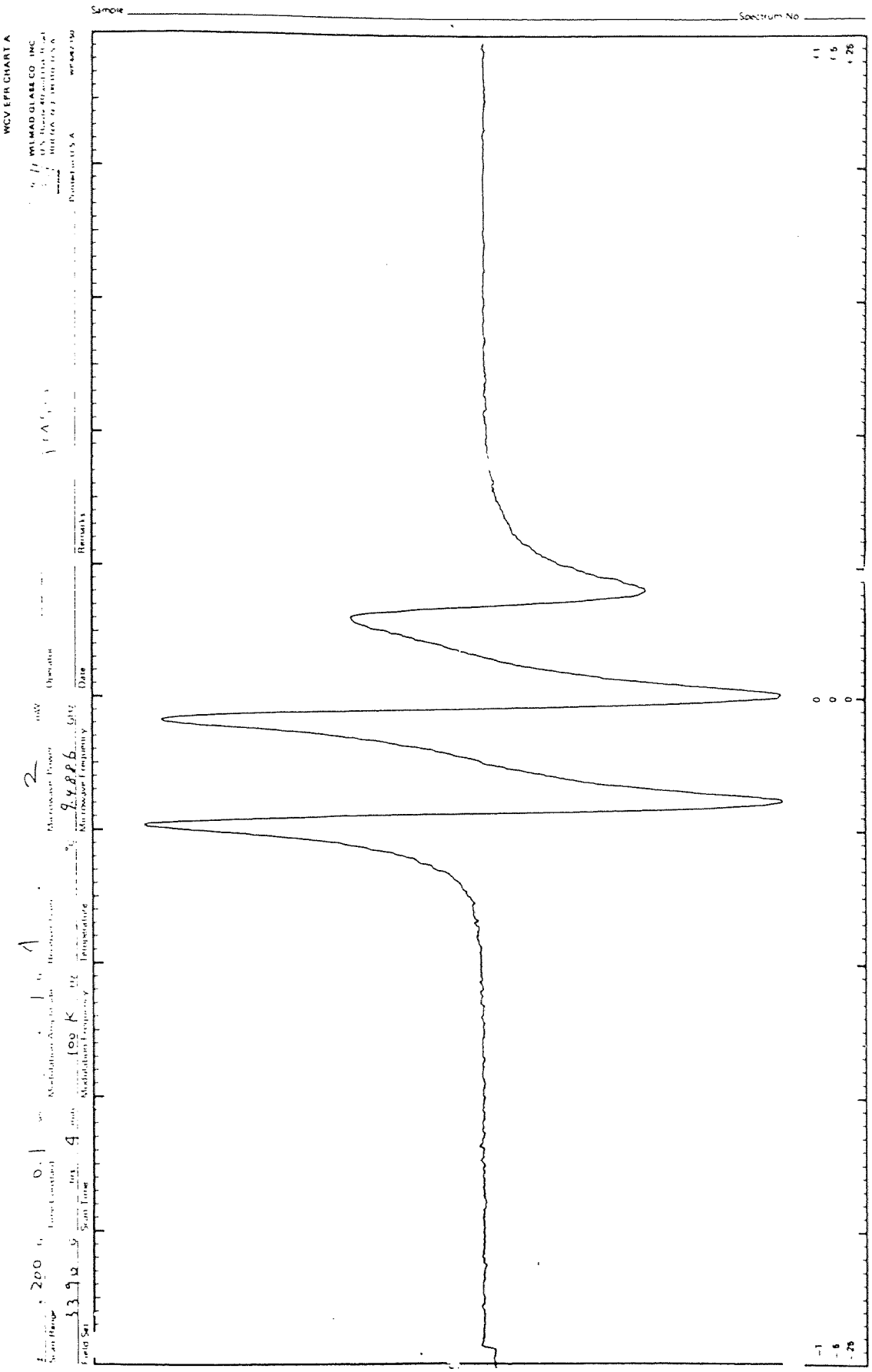

Fig 11b: ESR Spectrum of PMSO

6.4 The Bead Preparations

The details are described in reference [67]. Briefly, the wet bacterial, yeast or microsomal pellets and 0.5% saline solution are mixed in a ratio of 2:5 by weight in a blender. Sodium alginate (0.75% w/w) is then added slowly to the mixture with continuous stirring over a period of 2 to 3 minutes to obtain a homogeneous suspension. With the help of a syringe pump the cell suspension solution is then extruded as discrete droplets in a slowly stirred solution of 0.1 M calcium chloride. Upon contact with calcium chloride, the droplets harden to form uniform beads about 2 to 3 mm in diameter. The beads are then cured in calcium chloride for 24 hours at $4^{o}C$ before use.

6 .5 Procedures for the Rate Measurement of Styrene Polymerization in Bulk

The desired concentrations of nitroxides (TEMPO, HPTPO, Compounds VII and XII, PMTMPO and PMSO) and AIBN in styrene were prepared in different vessels and appropriate amount of them for a desired concentration were taken and combined into a vessel connected to a vacuum line and a nitrogen bulb with a three-way valve. The polymerization solution was then degassed by continued vacuum to 25 mmHg for about an hour and during which dry nitrogen was flushed frequently. The reactor was wrapped with aluminium foil to prevent exposure to UV radiation.

After the dilatometer was purged with dry nitrogen, the reaction medium was transferred to the dilatometer under nitrogen environment. It was then immersed into a thermostat with an accurate temperature control at $70 \pm 0.05\ ^{o}C$. As soon as the meniscus in its capillary stablized, the height of the meniscus was recorded in properly chosen time intervals. When approximately 10% of the conversion was reached, the reaction was stopped.

6.6 Procedures for the Measurement of Nitroxides' Disappearance Rate in Styrene Polymerization.

The styrene samples are prepared by the same procedures as described above. The known concentration of mixture containing nitroxide, AIBN and styrene is separated into 10 test tubes under N_2 blanket. These tubes are again immersed into the temperature controlled bath. Samples were taken periodically to analyze the concentration of nitroxide by using a UV/VIS spectrophotometer at wavelength 450 nm.

CHAPTER 7

DISCUSSION AND RESULTS

7.1 Nitroxides Synthesis

The reaction schemes (2)-(4) in Chapter 6 are the published procedures for the alkylation of carbonyl compounds via enamines. This method was first proposed by G. Stork [68]. The usefulness of this method is that the produced enamine contains nucleophilic carbon. The unshared pair of electrons on nitrogen are available for nucleophilic attack by carbon of the enamine. After it reacts with methyl acrylate, the intermediate, iminium ion, is readily hydrolyzed to regenerate the carbonyl group (product IV in Chapter 6).

To produce HPTPO, further hydrogenation and oxidation are necessary. For product IV in Chapter 6, the ketone group is found easier to be reduced to the hydroxyl group by sodium borohydride, whereas its carboxylic ester is relatively difficult. While monitoring the presence of its C = O group by IR, we found that the first 10-fold excess of sodium borohydride did not reduce all C = O, The second 10-fold excess of sodium borohydride was then added. HPTP was finally obtained after the mixture was heated under reflux for 12 hours.

The oxidation takes place in the water phase in the presence of hydrogen peroxide and sodium tungstate. The yield was higher (62%) than the corresponding oxidation by peracid (m-chloroperbenzoyl acid or MCPBA, 55%). Oxidation in the organic phase by means of MCPBA was attempted in the beginning. Unfortunately, the result was not very satisfactory. The obtained HPTPO was not pure enough to allow only one observable spot (HPTPO) on the TLC plate. It is believed that many chromatographic separations are required and consequently the yield will be lower.

Rozantsev prepared the polyradicals by using carboxylic acid chlorides as well as chlorides of phosphorus. The multiradicals obtained are completely stable [3]. He further prepared PMTMPO by reacting TEMP with polyacrylic acid chloride. Nonetheless, in this work, Shen improved the synthetic routes of PMTMPO and PMSO by suggesting that the synthesis of polymerizable functional groups in

heterocyclic amines can be accomplished by esterification. In the presence of magnesium methanolate, the reaction takes place between TEMP and methyl methacrylate. In order to shift the reaction to the desired direction, low - boiling methyl methacrylate was also used as solvent, and simultaneously the distillation is performed to remove the produced methanol from top of the distillation head. As the top temperature rose gently to 100°C for 2 hours, the reaction stopped. The whole process took about 3 days.

7.2 Inhibition: Experimental Results

Various stable free radicals have been used as inhibitors for kinetic studies in radical polymerization, but many of them have side reactions that make the kinetic analysis much difficult. This work utilizes stable free radical nitroxides for such use and almost no side effects are observed.

This group of inhibitors has a clearly defined inhibition period and no retardation after the period. They also have a peculiar advantage in the polymerization of styrene or methyl methacrylate. The reaction can be followed by the intensity change of the characteristic absorption of nitroxide at 450 nm.

7.2.1 Background

- Data Treatment

The polymerization rates were measured in the dark at 70°C by dilatometer. The monomer with desired concentration was charged into the reactor in the dilatomer, volume 10.75 ml, with attached capillary graduated in 0.005 ml subdivisions on 1.400 ml. Before being charged, the solution was degassed by vacuum pump at about 25 mmHg and flushed with dry nitrogen frequently, while evacuating.

Once the solution was loaded, the meniscus rose at first to reach thermal equilibrium. After the onset of the polymerization, it rose a little bit more for a few seconds. This phenomenon is ascribed to the thermal expansion of the polymerization reaction in which the heat of polymerization is evolved. Therefore, we started the dilatometry measurements from the time when the meniscus came again to the

original position. This warm up period is estimated to be 5.7 minutes in this experiment. Then the meniscus starts to drop in the course of polymerization. As the conversion approaches 10%, the reaction is stopped.

The polymerization rate is then calculated from the change in volume for the conversion of monomer into polymer.

$$\Delta V = \frac{C_o V_o f}{\rho_p} - \frac{C_o V_o f}{\rho_m} = C_o V_o f \left(\frac{1}{\rho_p} - \frac{1}{\rho_m}\right), \tag{1}$$

where

C_o is the initial concentration of the monomer,

V_o is the initial volume of the solution,

ρ_p is the density of the polymer, and

ρ_m is the sensity of the monomer.

Then, the fractional conversion becomes:

$$f = \frac{\Delta V}{C_o V_o} \left(\frac{1}{\rho_p} - \frac{1}{\rho_m}\right)^{-1} . \tag{2}$$

The contraction in volume which occurs during addition polymerization of styrene is the result of the reduction of intermolecular distance between monomer units as they enter the polymer units. One might thus describe the rate of polymerization in terms of volume change, which in turn corresponds to the rate of monomer consumption at any instant as follows:

$$\frac{V_o - V_t}{V_o - V_f} = \frac{M_o - M}{M} . \tag{3}$$

Where

V_o is the monomer volume at any instant,

V_f is the final volume of monomer,

M_0 is the initial monomer concentration, and

M is the monomer concentration at any instant.

- Evaluation of the Reaction Environment

The thermal polymerization of styrene was conducted in the dilatometer at 70°C. The conversion curves are demonstrated in Fig 1. Its rate is measured to be about 0.0078 mol/l hr, which is very close to the literature values 0.0089 mol/l hr, 0.0082 mol/l hr and 0.0067 mol/l hr [69].

Thermal styrene polymerization in the presence of nitroxides was also performed at 70°C. The result illustrated that the influence of nitroxides is not significant. The involvement of nitroxides in thermal polymerization causing additional initiation is found insignificant. As soon as the initiating radicals are generated, they will be inactivated immediately. As seen in Fig 1, their induction period is very small. Thus, these nitroxides only slightly participate in the polymerization reaction at a very slow rate. The literature value of addition reaction of nitroxides to the double bond in styrene molecule is 10^{-6} l/mol s at 60°C [52]. In this work, we disregard this slow reaction in kinetic calculations.

Fig 1 also demonstrates that the addition reaction of mono-, bi-, and tri-radical nitroxides to the styrene molecule is fairly slow. The biradicals tend to react a little faster than mono- and tri-radicals. This may be explained, according to Ruban and his coworkers [56], that the local magnetic field of the second odd electron changes the adiabatic nature within the reacting cell. As a result, the fast initiation reaction causes the polymerization at a higher rate eventually. Nonetheless, such a catalytic effect was not observed in the case of triradical and polymeric radical (PMSO).

One can also see the polymerization curves with AIBN at the concentration of 0.02M and 0.0056 M in Fig 1. As compared to the thermal rate, the initiated is much faster than the uninitiated. At the early stage of reaction, the 0.02 M AIBN reaction is 15 times faster than the thermal, whereas the 0.0056 M is 8 times faster. This work adopts 0.02 M of AIBN as initiator concentration so as to minimize the possible error from the uncertain thermal mechanism for ongoing calculations.

Equation (28) in Chapter 2 allows us to calculate the initiator efficiency for the polymerization environment in this study. The equation is:

$$R_p = k_p [M] \left(\frac{f k_{di} [AIBN]}{k_t}\right)^{1/2}. \quad (4)$$

At 70°C, the following values are obtained from literature:

k_p = 14714.5 mol/l min,

k_{di} = 2.83 x 10^{-3} min^{-1}, and

k_t = 2.39 x 10^9 mol/l min.

As the initiator concentrations are 0.02 M and 0.0056 M, the polymerization rate is equal to 0.01537 and 0.00807 M/min respectively. Therefore, the obtained efficiencies **f** are 70.5 and 72.2. The difference is not very large. It may be attributed to the calculation and experimental error. The literature values for f can range from 0.4 to 0.8. During this study, the validity of **f** was frequently checked and found consistent all the time. For our calculation, the averaged f is 0.7135.

7.2.2 Inhibitor effects in initiated polymerization

Conversion curves of the styrene polymerization initiated by AIBN (0.02M) in the presence of TEMPO are depicted in Fig 2. The induction period is found linearly proportional to the inhibitor concentration. During this period, the meniscus in dilatometer stays motionless. This indicates that the polymerization is almost completely halted. The identical shapes of curves are observed for other concentrations of TEMPO between 1.98 mM and 0.16 mM.

Other conversion curves are also demonstrated in Figures (7)-(11). The summary of their induction periods with respect to concentration of inhibitor is illustrated in Fig (3)-(5). The slope for the triradical is 45.45 min/mM, 31.05 min/mM for the biradical and 14.48 min/mM for HPTPO. The triradical is about 3.14 times more effective than the monoradical, whereas the biradical is about 2.15 times.

The increased effectiveness is not very large. One may suppose that the first spin combination with alkyl radical increases the weight of the molecule and thereby the frequency of the collisions with other molecules for this heavy molecule

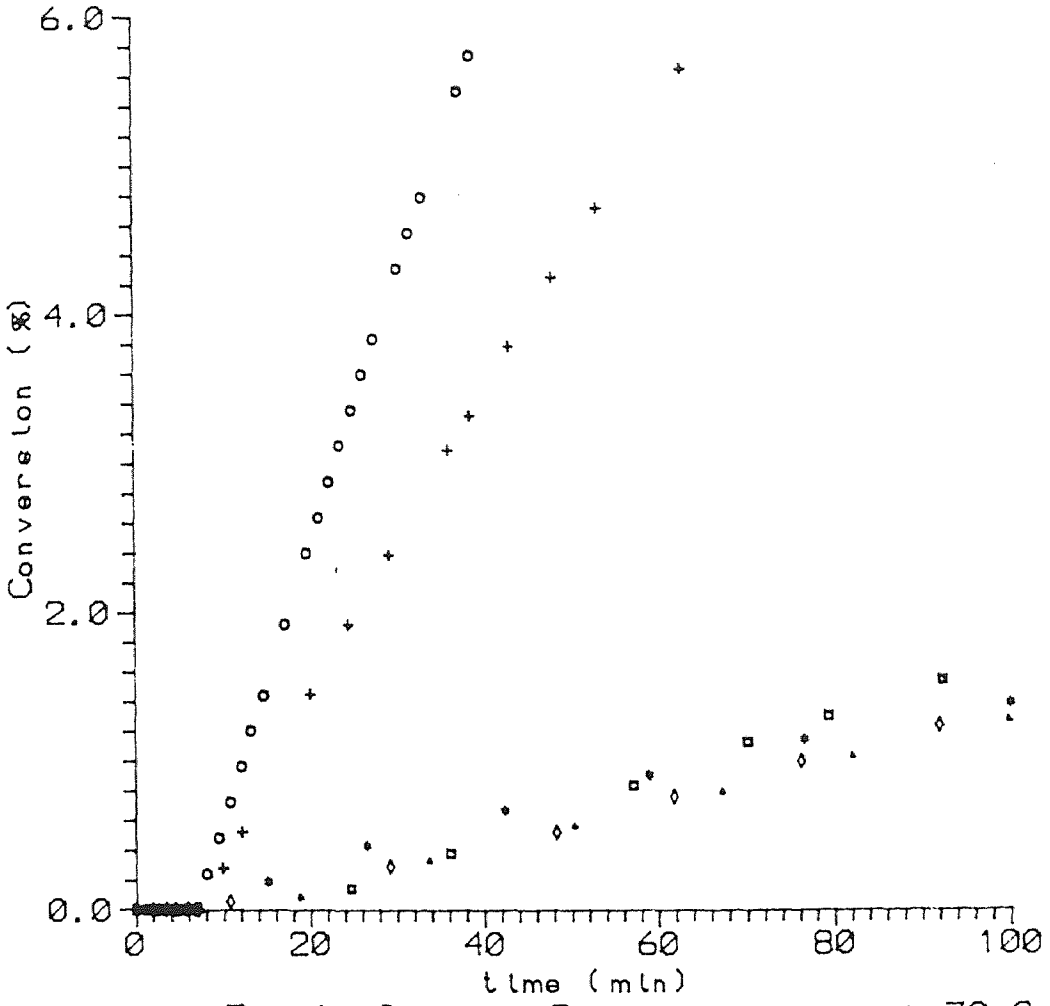

Fig 1: Styrene Polymerization at 70 C at the following conditions:

***** Thermal only
◊◊◊◊◊ with the addition of TMPO (4.9 mM)
ooooo with the addition of AIBN (21 mM)
+++++ with the addition of AIBN (5.6 mM)
□□□□□ with the addition of biradical (2 mM)
***** with the addition of triradical (2 mM)

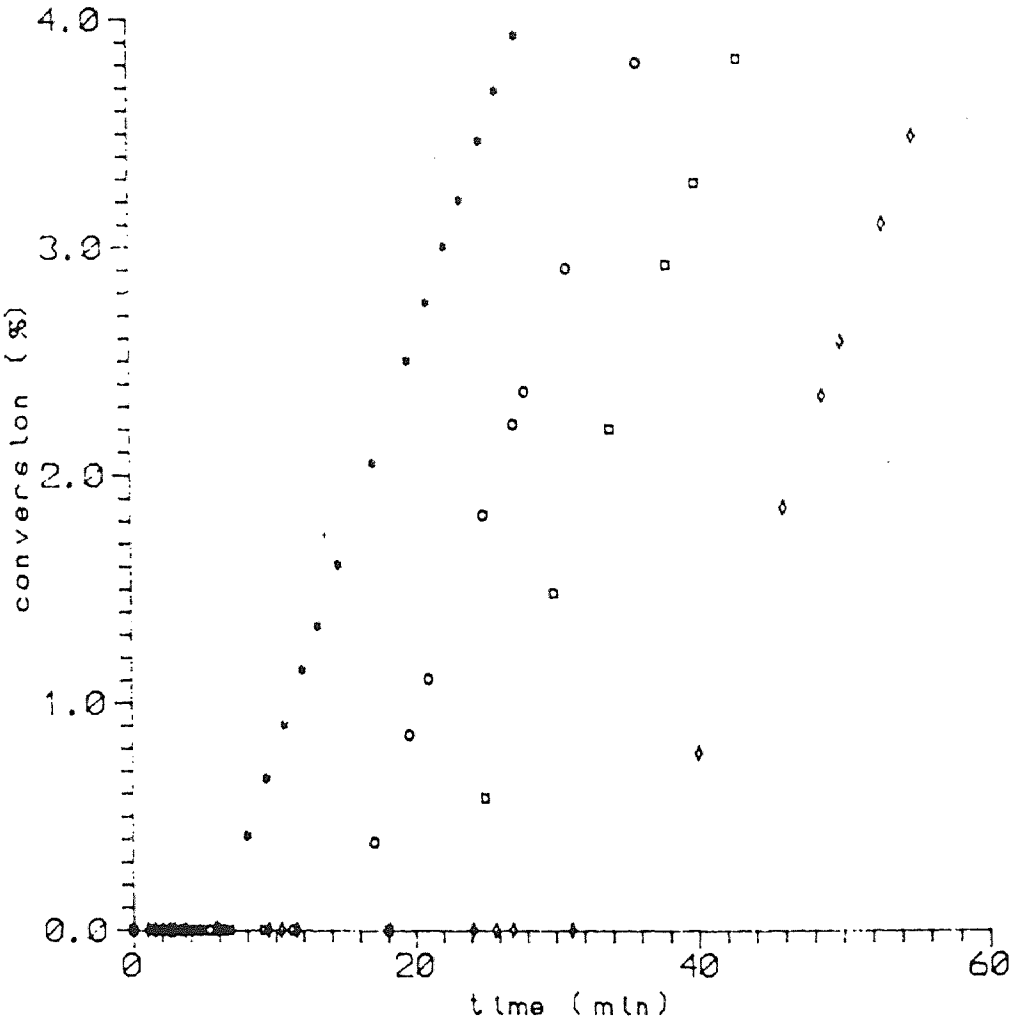

Fig 2: Styrene Polymerization Inhibited by TEMPO at 70 C (0.02 M AIBN)

• • • • • AIBN (0.02M)
▫ ▫ ▫ ▫ ▫ TEMPO (1.56 mM)
◊ ◊ ◊ ◊ ◊ TEMPO (2.345 mM)
○ ○ ○ ○ ○ TEMPO (1.02 mM)

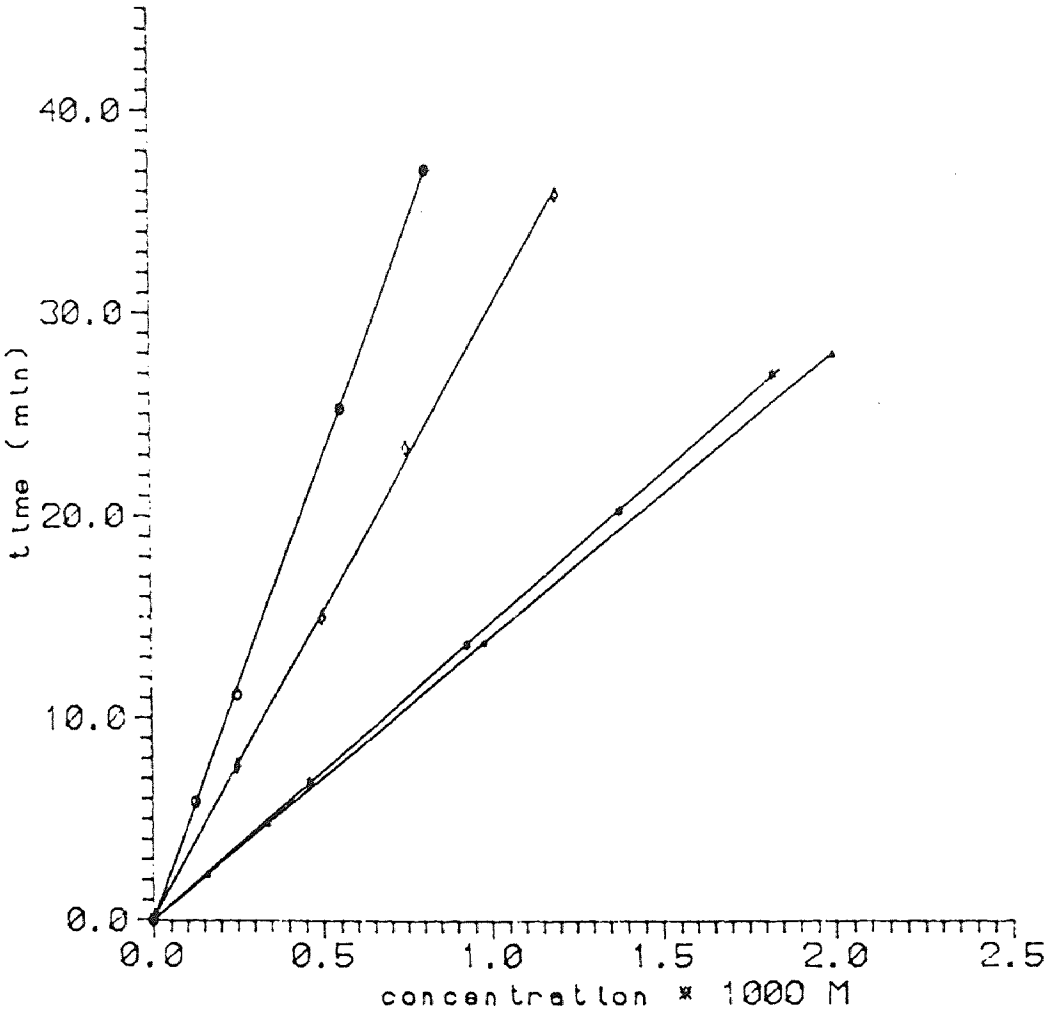

Fig 3: Dependence of Induction Period on Nitroxide Concentration

HPTPO
Biradical
Triradical
TEMPO

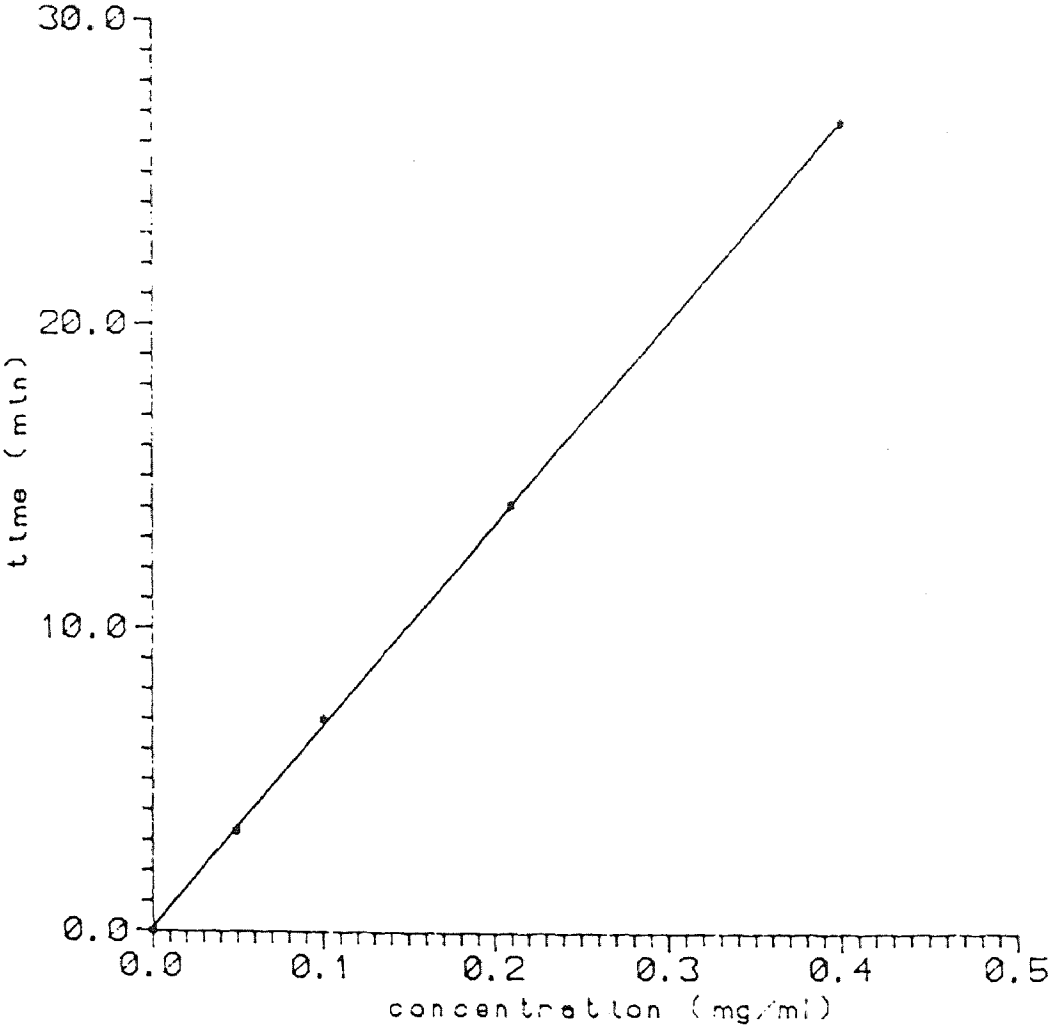

Fig 4: The Dependence of Induction Period on Concentration of Polyradical Nitroxides (PMTMPO)

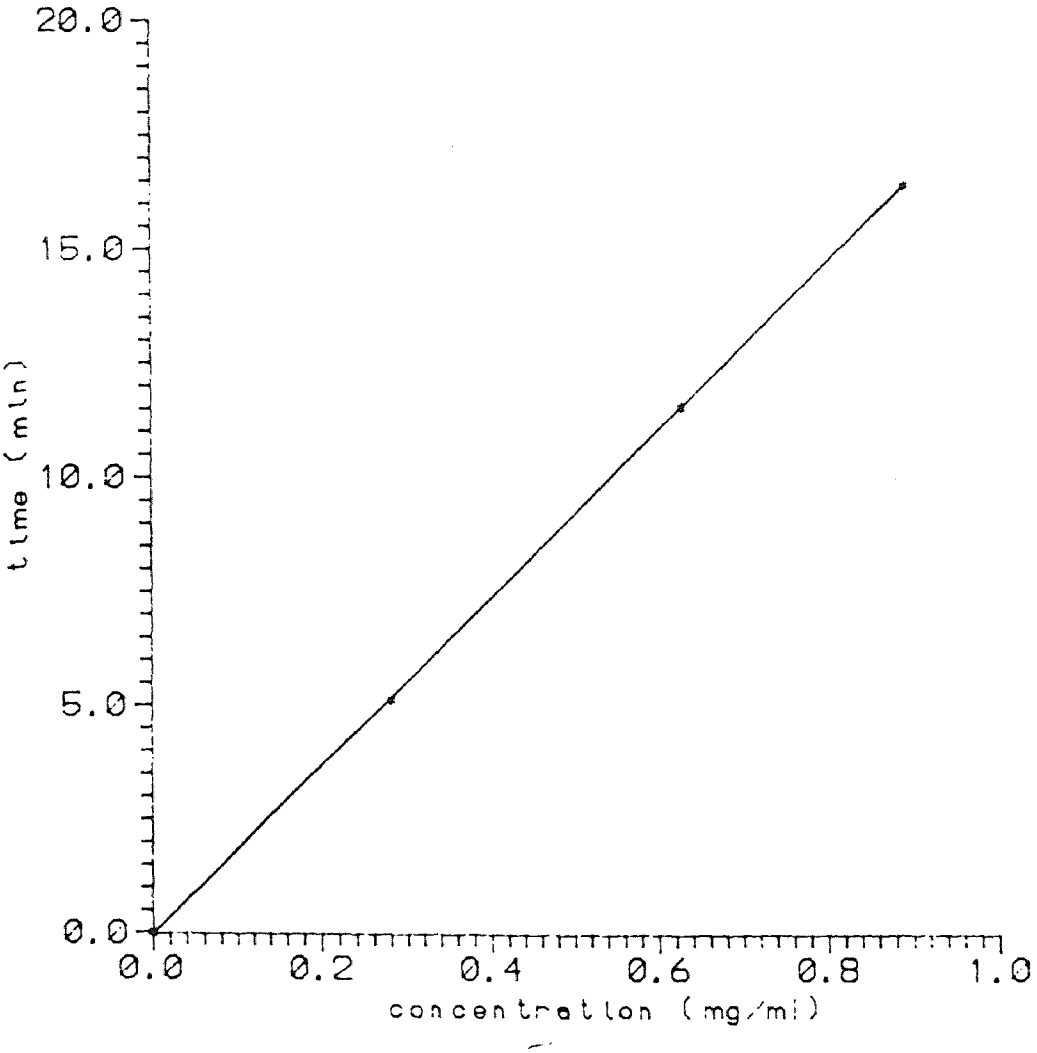

Fig 5: The Dependence of Induction Period on the Concentration of Polyradical Nitroxides (PMSO)

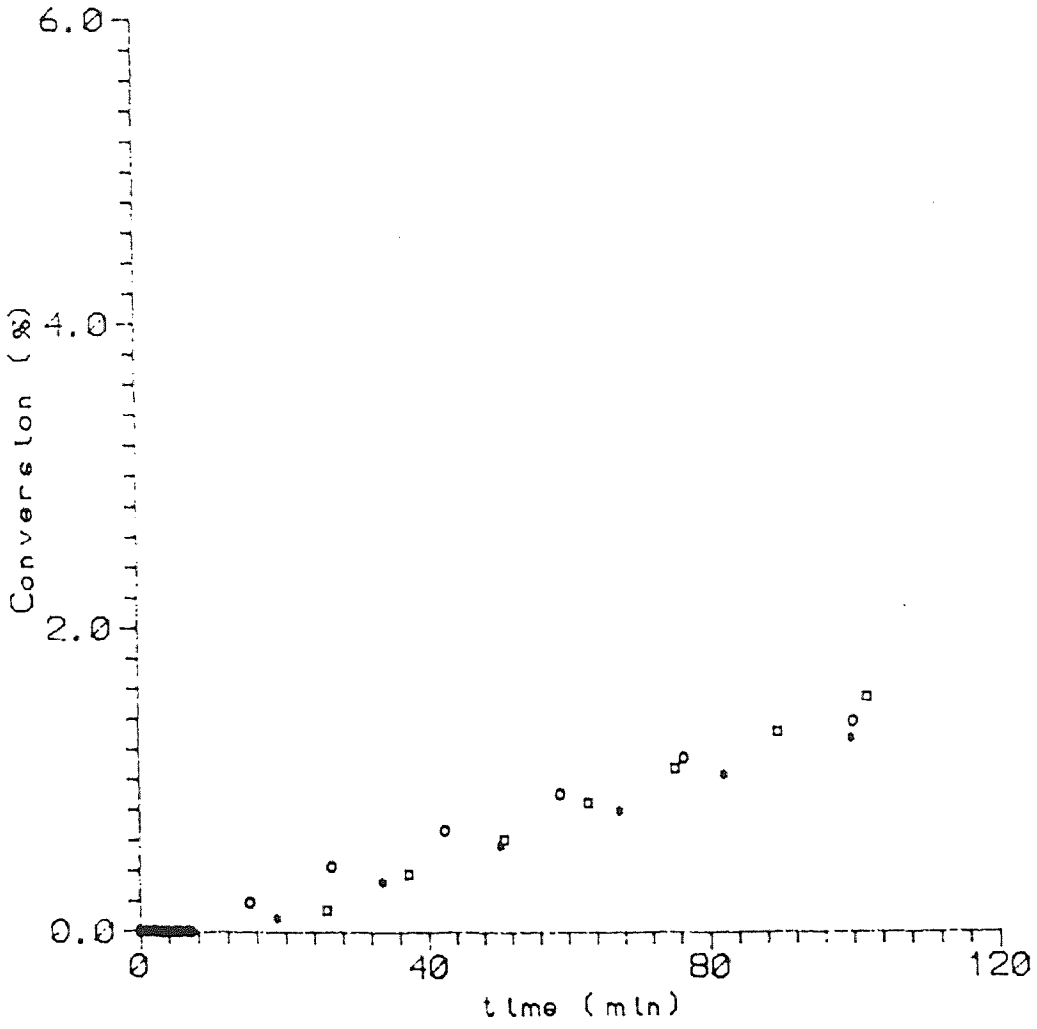

Fig 6: Thermal Polymerization Inhibited by Polyradical Nitroxides at 70 C

•••••PMSO (0.00012 g/ml)
ooooopure styrene
▫▫▫▫▫PMTMPO (0.000214 g/ml)

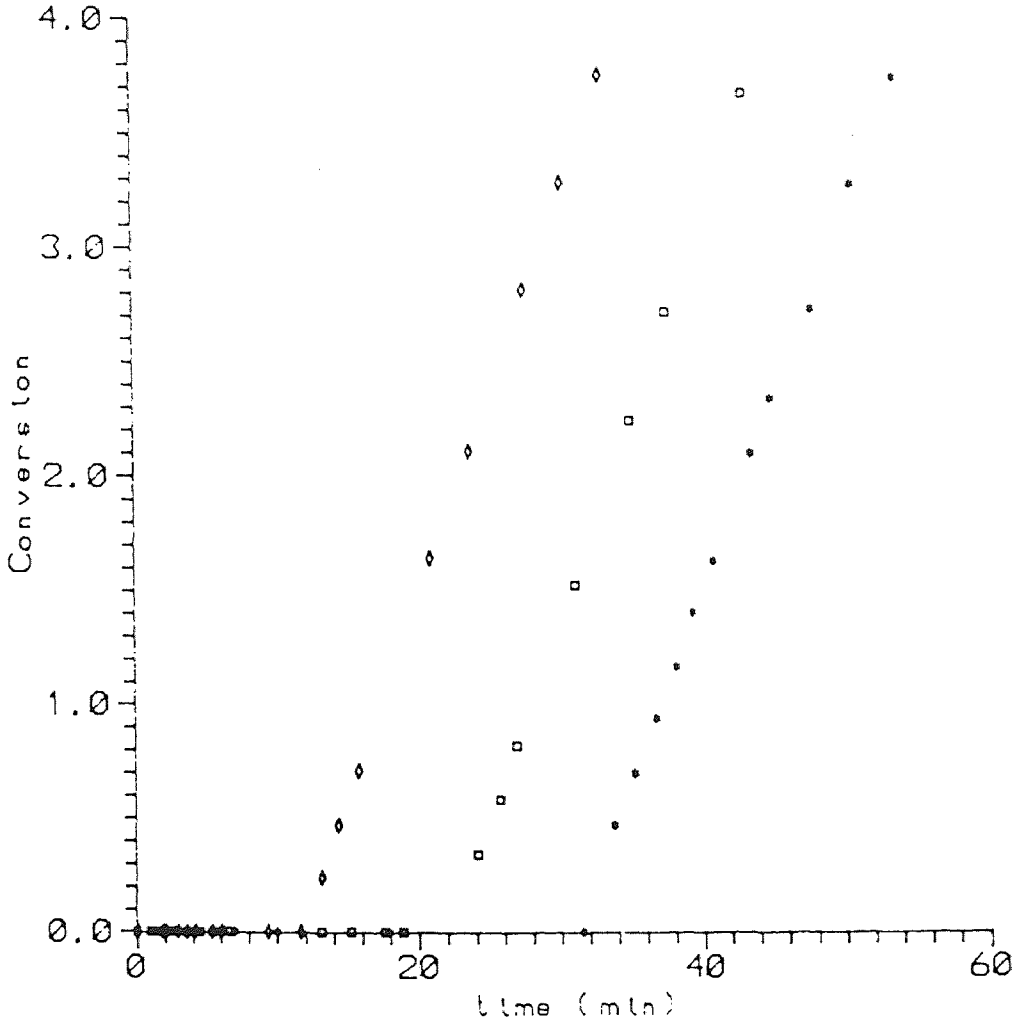

Fig 7: Styrene Polymerization Initiated by AIBN at 70 C with the Addition of HPTPO at following Concentrations:

***** 1.83 mM
▫▫▫▫▫ 1.38 mM
◊◊◊◊◊ 0.46 mM

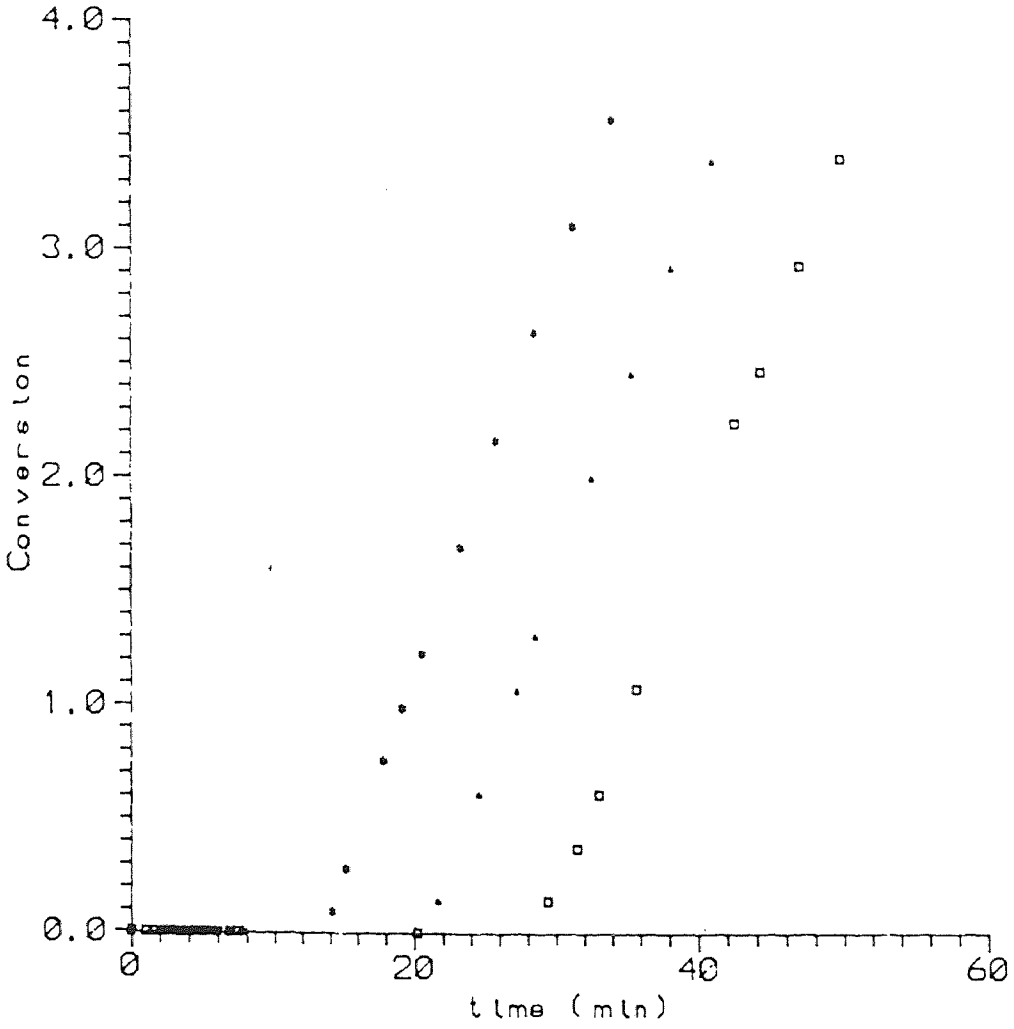

Fig 8: Styrene Polymerization Initiated by AIBN with the Addition of Biradical at following concentrations:

•••••0.5 mM
▫▫▫▫▫0.75 mM
•••••0.25 mM

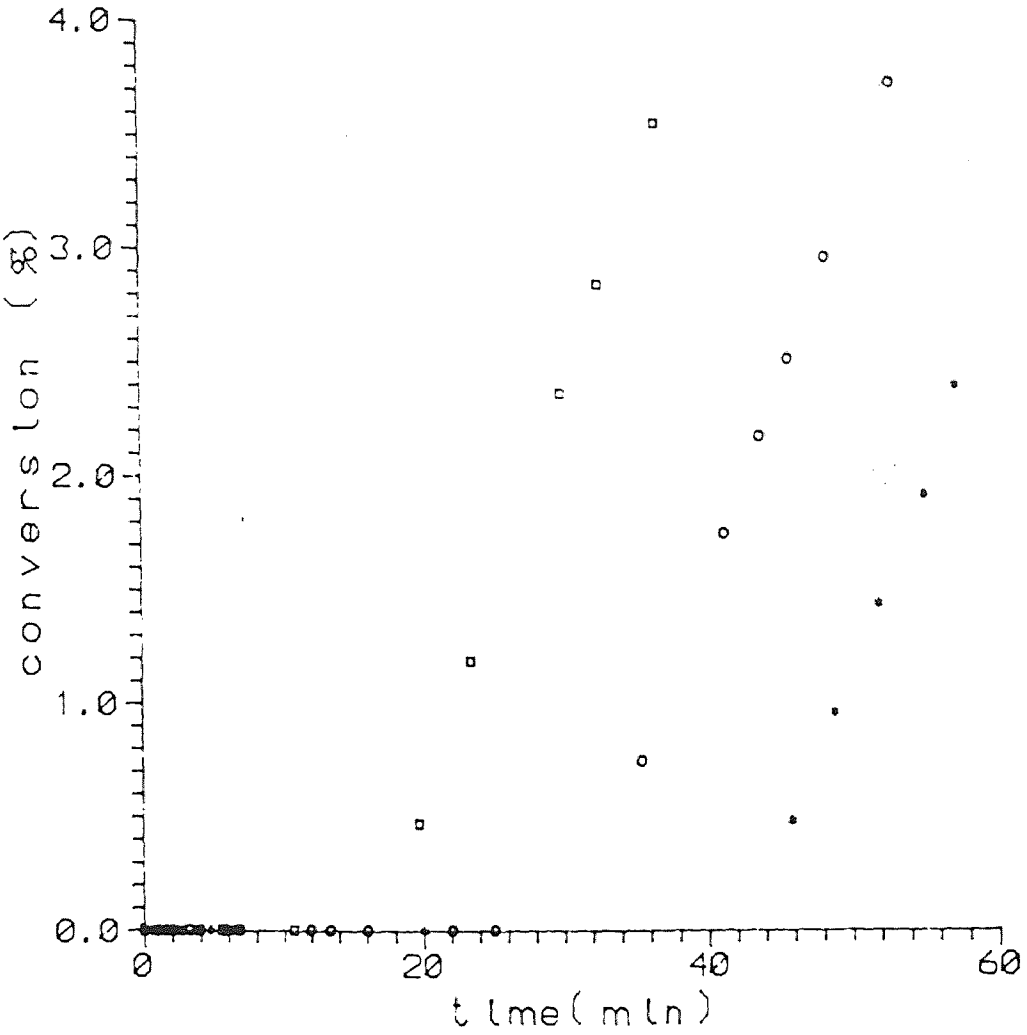

Fig 9: Styrene Polymerization Initiated By AIBN with the addition of Tritadical at the following Concentration:

•••••0.815 mM
▫▫▫▫▫0.251 mM
ooooo0.556 mM

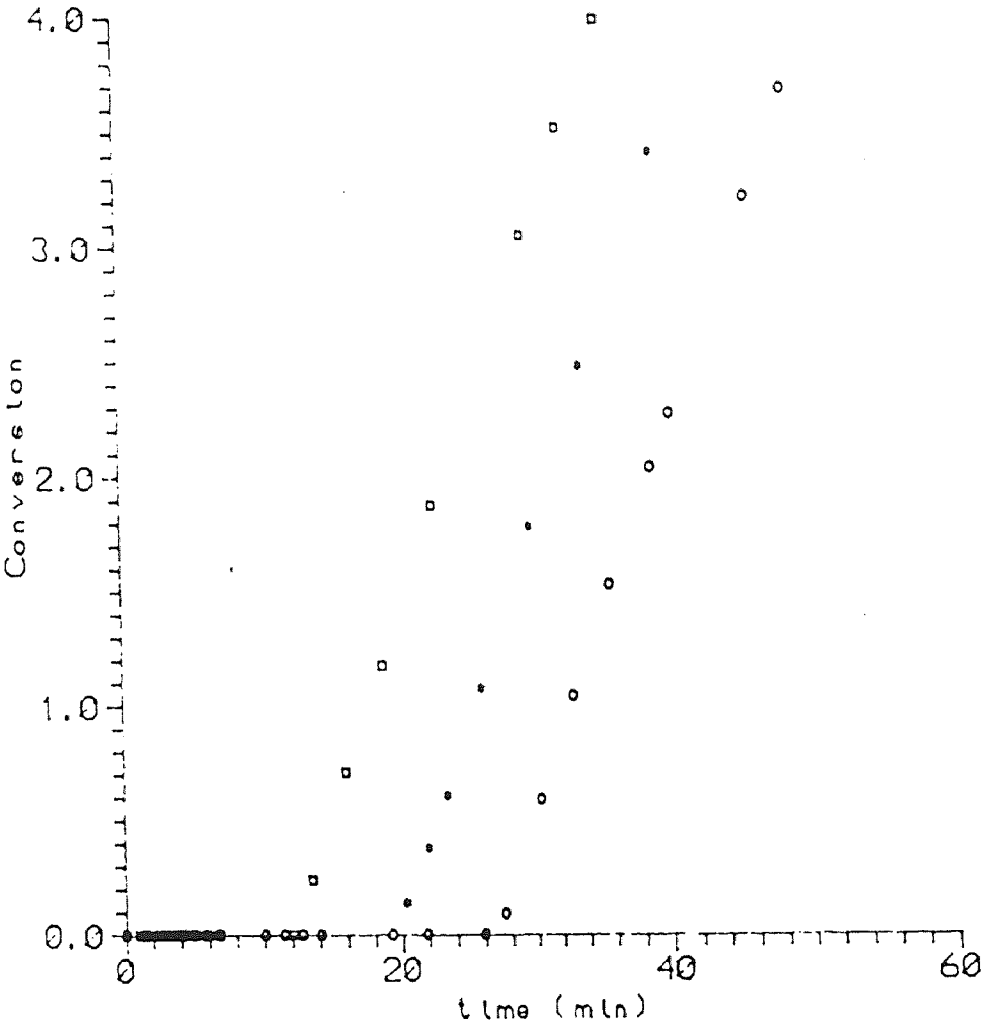

Fig 10: Styrene Polymerization Initiated by AIBN with the addition of PMTMPO at the following concentrations:

••••• 0.215 mg/ml
▫▫▫▫▫ 0.107 mg/ml
ooooo 0.318 mg/ml

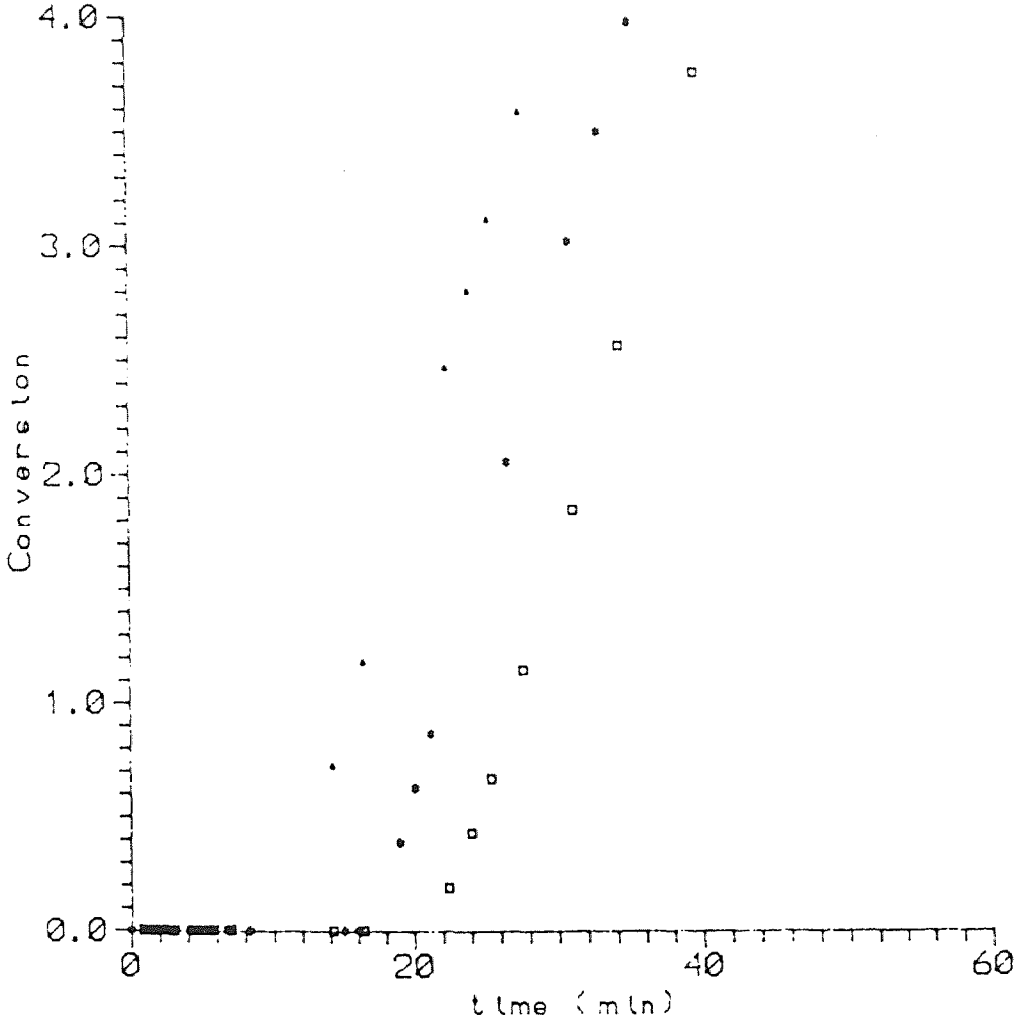

Fig 11: Styrene Polymerization Initiated by AIBN at 70 C with the Addition of PMSO at the following concentrations:

• • • • • 0.638 mg/ml
▫ ▫ ▫ ▫ ▫ 0.89 mg/ml
• • • • • 0.28 mg/ml

decreases. Therefore, their scavenging capability is reduced correspondingly. But the weight increase does not influence their inhibitory property significantly.

This may be also explained in a way that the probability of the disproportionation of the bi- and tri-radical with active radicals is relatively higher and then more nitroso compounds are formed:

$$R^{\cdot} + X \longrightarrow R - N = O + RH \qquad (5)$$

where x represents nitroxyl radicals

Low *et al.* [55] discovered the same effect and later concluded that the involvement of iminoxy radical into styrene polymerization to form nitroso compound is responsible for this phenomenon. Since each nitroso compound can terminate two kinetic chains, the inhibitory capability per unit nitroxyl center is more than one.

The inhibitory effect of polymeric free radicals on the polymerization was also examined. Their kinetic curves are shown in Fig 10 and Fig 11. These macromolecules also exhibit clear inhibition periods. The period increases with the amount of polyradicals (PMTMPO and PMSO) added to the monomer (styrene). As can be seen, no polymerization takes place during the inhibition period. After complete consumption of the inhibitor, polymerization starts at the rate of the unhibited process. Nonetheless, their killing ability is found proportional to the number of the available nitroxyl centers within a single molecule. As compared with TEMPO whose slope is 14.2 min/mM, theirs are 15.2 for PMTMPO and 15.8 for PMSO. The effectiveness is found higher than TEMPO in terms of each nitroxyl inhibitory center within single molecules. The reason could be either due to the experimental error or due to the formation of nitroso compounds. Consequently, the inhibitory coefficient is higher regardless of their being heavier.

- Nitroxides analysis in the course of polymerization

Solution of nitroxides are red colored. The UV/VIS scanning, shown in Fig 12, illustrates that their characteristic absorption occurs between 355 and 500 nm and their corresponding end products in solution are colorless, and do not absorb in this region. Using this method to detect the concentration of nitroxides is very con-

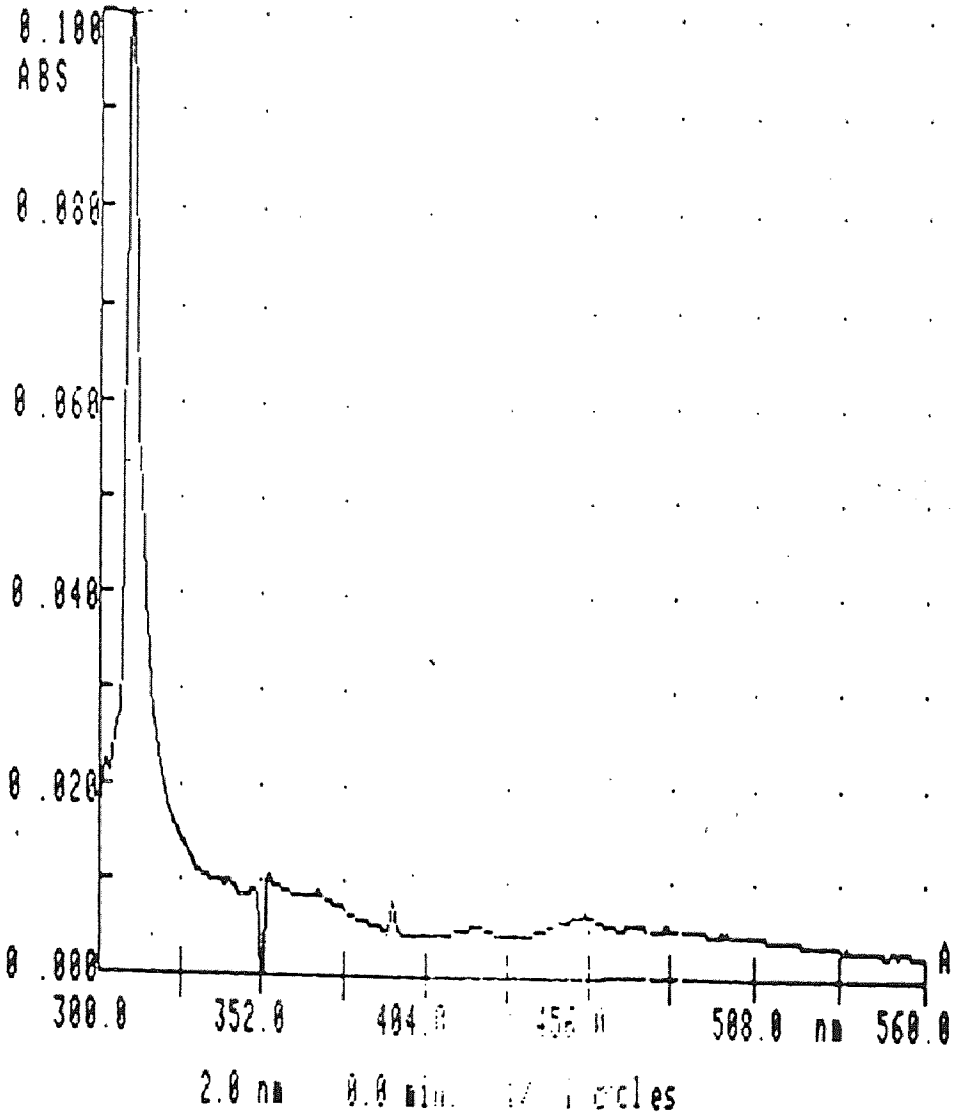

Fig 12: UV/VIS Scanning Curve for HPTPO in Styrene
in Reference to Pure Styrene.

venient as compared to the use of the ESR. Not only is it more time saving but also the real time measurements are highly desirable. VIS detection allows concentration measurement as low as 10^{-5} mol/l, whereas ESR can go down to 10^{-8} mol/l but it is very easy to get saturation if nitroxide concentration is lower than 10^{-5} mol/l. On the other hand, the real time measurement of radical concentration on ESR is more difficult. The signal can be easily masked from the presence of the short life active radicals such as initiating and propagating radicals.

7.3 Kinetic Treatment for Inhibited Polymerization

- Previous Kinetic Model

In chapter 2, we have discussed some kinetic models for the calculation of inhibition constant. Most of them require the information of monomer concentration during the inhibition period. Some inhibitors such as nitroxides are very effective. They must be almost completely consumed before the monomer can be polymerized. As the end of induction period is reached, the approach to the final uninhibited rate of polymerization is sharp, and the change of the curve of $\ln([M]_o/[M])$ versus time occurs in a short space of time. Therefore, reasonable points from the graph are hard to take.

Another assumption that these models have made is the steady state condition being kept at any instant during the inhibition period. Since the decomposition rate of AIBN is solvent independent, the primary radical is generated at a constant rate. The concentration of active radicals should be gradually increased as the inhibitor molecules are consumed. If the inhibitor is very strong, the concentration of active radicals may be kept very low longer. The polymerization rate is proportional to the concentration of active radicals. Therefore, its rate should be increased simultaneously as the inhibitor is consumed. The assumption that the concentration of propagating radicals remains the same all the time during the inhibition period may be taken as an approximation, but the concentration is not a constant value at this time.

To my knowledge, almost every kinetic model considers the inhibitor consumption in accordance with a linear law at a rate lower than that of initiation. Many re-

searchers have also supported this assumption based on experimental data. However, let us consider the following general equations for inhibited polymerization.

$$\frac{dr}{dt} = \omega_i - k_z r z - 2 k_t r^2 \quad , \text{ and} \tag{6}$$

$$-\frac{dz}{dt} = k_z r z \quad . \tag{7}$$

If the consumption rate is linear, then

$$-\frac{dz}{dt} = k_z r z = \text{constant} = \varphi \quad . \tag{8}$$

Therefore, $$r = \frac{\varphi}{k_z z} \quad . \tag{9}$$

Differentiating equation (9), in conjunction with equations (6) and (7)and simplifying, we obtain:

$$(\omega_i - \varphi) k_z^2 z^2 - (2k_t + k_z) \varphi^2 = 0 \quad , \tag{10}$$

which gives

$$z = \frac{\varphi}{k_z} \left(\frac{2k_t + k_z}{\omega_i - \varphi}\right)^{1/2} \quad . \tag{11}$$

From equation (11), the inhibitor concentration at any instant is also constant which is impossible. It is in contradiction to the initial assumption, that is, the inhibitor is consumed in a linear rate. The experimental data of the inhibitor consumption with respect to time appears to be linear. But it is not a fully linear relationship.

- Proposed Kinetic Model

The polymeric radicals may react with any free active radicals in the reaction medium. All these reactions will result in the formation of a polymer molecule and other new radicals. The polymer molecules are formed as a result of a primary reaction between polymeric radicals or between polymeric radicals and a scavenging molecule X.

The general kinetic model is presented as follows:

Initiation

3 M	$\longrightarrow$	$2M_1^{\cdot}$	rate = $3\ k_{it}\ m^3$
AIBN	$\longrightarrow$	$2\ I^{\cdot}$	rate = $2\ f\ k_{di}$ [AIBN]
$I^{\cdot}$ + M	$\longrightarrow$	$M_1^{\cdot}$	rate = k_{ii} [$I^{\cdot}$] m

Propagation

$R^{\cdot}$ + M	$\longrightarrow$	$R^{\cdot}$	rate = $k_p\ r\ m$

Termination

$R^{\cdot}$ + $R^{\cdot}$	$\longrightarrow$	X	rate = $2\ k_t\ r^2$
$R^{\cdot}$ + $Z^{\cdot}$	$\longrightarrow$	X	rate = $k_z\ r\ z$

Their corresponding differential equations may be written as follows:

$$-\frac{d\,m}{dt} = 3\,k_{it}\,m^3 + k_{ii}\,m\,[I^{\cdot}] + k_p\,r\,m \quad , \tag{12}$$

$$\frac{d\,r}{dt} = 3\,k_{it}\,m^3 + k_{ii}\,[I^{\cdot}]\,m - k_z\,r\,z - 2\,k_t\,r^2 \quad , \tag{13}$$

$$\frac{d\,[I^{\cdot}]}{dt} = 2\,f\,k_{di}\,[AIBN] - k_{ii}\,[I^{\cdot}]\,m \quad , \text{ and} \tag{14}$$

$$-\frac{d\,z}{dt} = k_z\,r\,z \quad . \tag{15}$$

at the initial conditions:

r = 0 m = 8.269 mol/l (AIBN) = 0.02 mol/l

$(I^{\cdot}) = 0$ $z = z_o$

- Assumptions

As discussed previously, nitroxides are very strong inhibitors. They have a clear inhibition period during which no polymerization takes place. Therefore, we may assume

$$m = m_o \qquad \text{as} \quad 0 \le t \le \tau \quad \text{(induction period)}$$

Since AIBN has already proved to be a constant and reliable initiator, the $[I^{\cdot}]$ may reach equilibrium immediately as soon as the thermal equilibrium is reached. Equation (14) then equals to 0, which gives:

$$2 f k_{di} [AIBN]_o = k_{ii} [I^{\cdot}] m_o \quad . \tag{16}$$

Therefore, the overall equations can be simplified to be:

$$\frac{dr}{dt} = \omega_i - k_z r z - 2 k_t r^2 \quad , \text{ and} \tag{17}$$

$$-\frac{dz}{dt} = k_z r z \quad . \tag{18}$$

where $\omega_i = 3 k_{it} m^3 + 2 f k_{di} [AIBN]_o$

$= 8.07 \times 10^{-5}$ mol/l min.

- Estimation of Rate Parameters

The DBCLSF routine is used to solve this nonlinear least squares problem. This subroutine is written by following the algorithm of the modified Levenberg-Marquadt. A finite-difference Jacobian program is also provided in the routine. DIVPAG is

used to solve this system of differential equations with initial values by using the Adams-Moulton or Gear method. During calculations, a tolerance of 10^{-15} is assigned to give consistent results for the concentration variable and the instantaneous rates to six significant figures. These routines are available in IMSL libraries on the NJIT Tesla system.

It is important that computations are carried out to a level of precision such that rounding errors do not make a significant contribution to the results. To check that precision was satisfactory, a double - precision version of the two above routines was used. The range and precision of the real values and integers for VAX 6430 is shown in Table 1. The results of the computations carried out at least kept six significant figures and therefore rounding errors were not a problem. The computed concentration of inhibitor and time curves are then fitted to its experimental values by adjusting the parameters K_Z, ω_i. The objective functions are defined as the sum of squared residuals between experimental and computed values of inhibitor concentrations. Thus

$$SSR = \sum_{i=1}^{n} (Z_{expt} - Z_{calc})^2,$$

where "i" is the counter of inhibitor values.

Table 2: The range and precision of values stored in VAX 6430

Range of Values		
Integer	Real (D, G format)	
2147483647	1.7D38	0.9D308
-2147483637	0.29D-38	0.29D-308

The computational searches for a minimum sometimes are locally confined. The minimum is not well defined and those values of the valuable parameters at the minimum are dependent on their initial values. These values can be scattered in the range of more than 100% difference. Moreover, the rate of free radical polymeriza-

tion somewhat relies on the reaction environment. Therefore, ω_i is initialized at the value where dr/dt = 0 as t = 0 in equation (23).

The approach to finding the minimum would be to systematically search a variety of dimensional spaces depending on the number of the parameters. However, this would be very costly in computation time on Tesla. To become possible in the tight schedule on the VAX system, the rate constant of ω_i is constrained within 30% of literature value.

- Estimation of Experimental Nitroxides Concentration, Time Profile

During the early stage of collecting the absorbance, time data the reaction mixture is heating up to the temperature of the thermostat. While the reaction mixture is heating up, the absorbance, time profile is affected by thermal expansion of the solvent and by the reaction of polymerization. In order to simplify the kinetic treatment of the data, the temperature rising is assumed to be following an exponential function. Consequently, the equivalent value of the absorbance in the equivalent reaction is calculated by the following approximation:

$$A_1 = A_2 \frac{\rho\,(T_1)}{\rho\,(T_2)} \quad , \tag{19}$$

where ρ stands for the density of the solvent at a temperature and the subscripts 1 and 2 refer to the actual reaction temperature and 70°C respectively.

To simplify the computational studies on the concentration versus time values spaced by regular time intervals were obtained by graphical interpolation of the experimental concentration of nitroxide versus time profile.

- Computational Results

When monoradical nitroxides are used as inhibitors, the kinetic model considered is:

$$\frac{dr}{dt} = \omega_i - k_z r z - 2 k_t r^2 \quad , \text{ and} \tag{20}$$

$$-\frac{dz}{dt} = k_z r z. \tag{21}$$

Since nitroxides are very strong inhibitors, the polymerization is not actually started until the concentration of inhibitor is almost completely consumed, that is, the r is very small. Therefore:

$$\frac{dr}{dt} = \omega_i - k_z r z \ . \tag{22}$$

Adding equations (21) and (22) gives:

$$-\frac{d(z-r)}{dt} = \omega_i \ . \tag{23}$$

After integrating equation (23) at initial concentration: $z = z_o$, $r = 0$ as $t = 0$, we have

$$r = \omega_i t - z_o + z \ . \tag{24}$$

In conjunction with equation (21), the final equation becomes:

$$-\frac{dz}{dt} = k_z r \ (\omega_i \ t - z_o + z) \ , \tag{25}$$

where $\omega_i = 3 k_{it} m^3 + 2 f k_{di} [AIBN]_o$.

The nitroxide concentration decreases as polymerization proceeds. Its data of disappearance rate was fitted to find the best value of k_z. The value of k_z obtained from the computer calculation is $(2.6 \pm 0.1) \times 10^4$ l/mol sec.

When biradical nitroxides are used in the system, an additional equation is introduced. The detailed model equations are as follows:

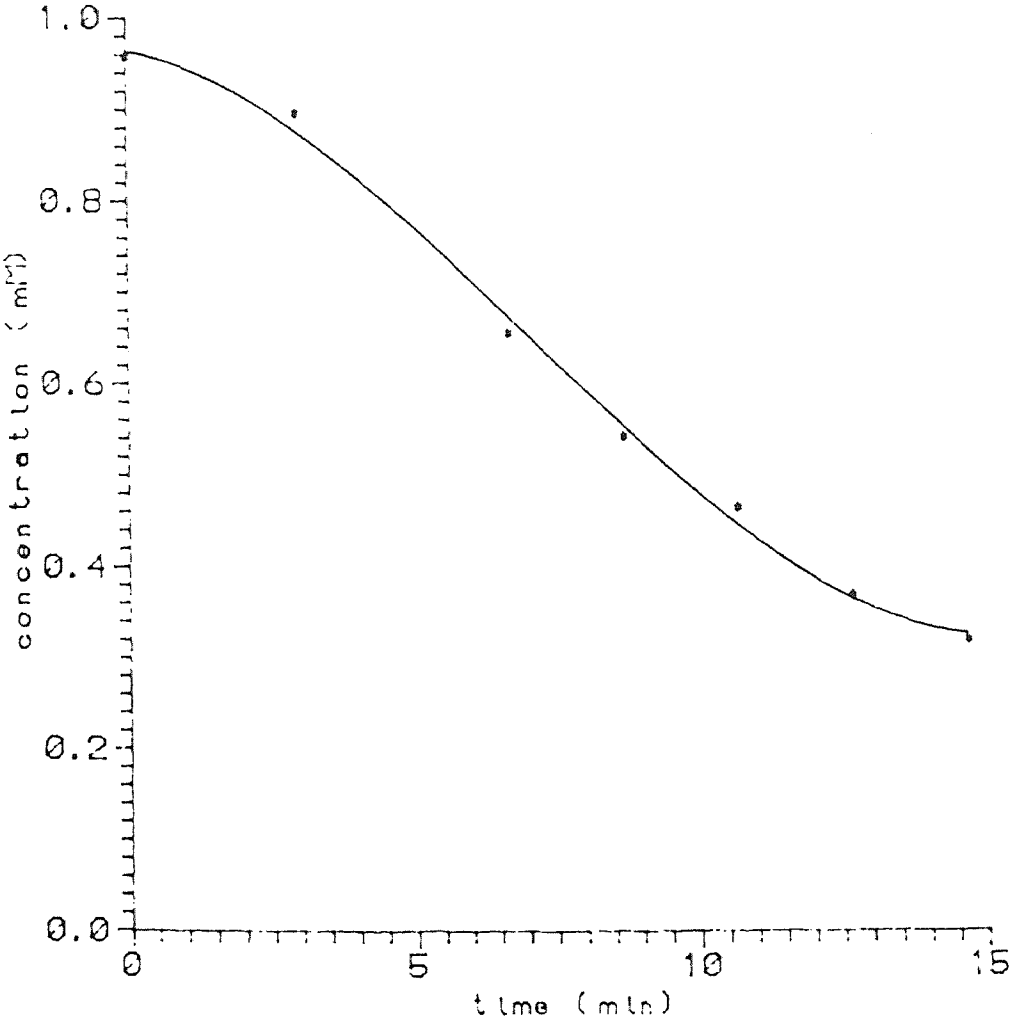

Fig 13: HPTPO Disappearance Rate in Styrene Polymerization Initiated By AIBN at 70 C

••••• Experimental points
_____ Model values

$$\frac{dr}{dt} = \omega_i - k_{z2} r z_2 - k_{z1} r z_1 - 2 k_t r^2 \quad , \tag{26}$$

$$-\frac{dz_2}{dt} = k_{z2} r z_2 \quad , \text{ and} \tag{27}$$

$$-\frac{dz_1}{dt} = k_{z1} r z_1 - k_{z2} r z_2 \quad . \tag{28}$$

Similar assumptions are applied to these rate equations. When adding equation (28) to the doubled equation (27) and equation (26), we obtain:

$$-\frac{d(z_1 + 2z_2 - r)}{dt} = \omega_i \quad . \tag{29}$$

Integrating equation (29) at initial condition r = 0, $z_1 = 0$ and $z_2 = z_{2o}$ as t = 0, we have

$$r = \omega_i t - 2z_o + z_1 + 2z_2 \quad . \tag{30}$$

When combined with equations (27) and (28), the same programs are used to evaluate the rate constants of k_{z1} and k_{z2}. The results are demonstrated in Figure 14, where k_{z1}, k_{z2} are $(2.4 \pm 0.1) \times 10^4$ and $(2.8 \pm 0.1) \times 10^4$ l/mol sec respectively.

In the case of triradicals, the model equations considered are:

$$\frac{dr}{dt} = \omega_i - k_{z3} r z_3 - k_{z2} r z_2 - k_{z1} r z_1 - 2 k_t r^2 \quad , \tag{31}$$

$$-\frac{dz_3}{dt} = k_{z3} r z_3 \quad , \tag{32}$$

$$\frac{d z_2}{dt} = k_{z3} r z_3 - k_{z2} r z_2 \ , \text{ and} \tag{33}$$

$$\frac{d z_1}{dt} = - k_{z1} r z_1 + k_{z2} r z_2 \ . \tag{34}$$

Similar strategies are utilized and the results are:

$$r = \omega_i t - 3 z_o + z_1 + 2 z_2 + 3 z_3 . \tag{35}$$

Combined with equations (33) and (34), the computational results obtained for the rate constants are $k_{z3} = (2.9 \pm 0.1) \times 10^4$, $k_{z2} = (2.6 \pm 0.1) \times 10^4$, and $k_z1 = (2.5 \pm 0.1) \times 10^4$ l/mol sec.

In view of the ratio of the stepwise rate constants, we found that the first spin is 1.16 more reactive than the second spin for biradical, whereas the first spin is 1.16 more and the second is 1.06 more reactive than the third spin. Their differences are small. As their overall induction period are considered together, we found that these multiradical inhibitors behave practically equivalent to their corresponding monoradical nitroxides. Therefore, it is believed that same kinetic behavior can be extended to interpret the inhibiting characteristics of the polymeric nitroxides in inactivating propagating radicals, providing that the adding of polymeric inhibitors does not affect the viscosity of the reaction medium.

7.4 Relaxivity Measurements

The nitroxyls of monomers were dissolved in water at three different concentrations of 11, 6 and 1 mM. One percent of polyradicals in methylene chloride was added to 1% Tween-50 in water. The two phase solution was sonicated and then centrifuged. The resultant milk-like suspension solution when analyzed showed that five ppm of polynitroxides were suspended. On the other hand, one percent of oligomers in CH_2Cl_2 were added to bovine plasma at three different concentrations of 100, 200

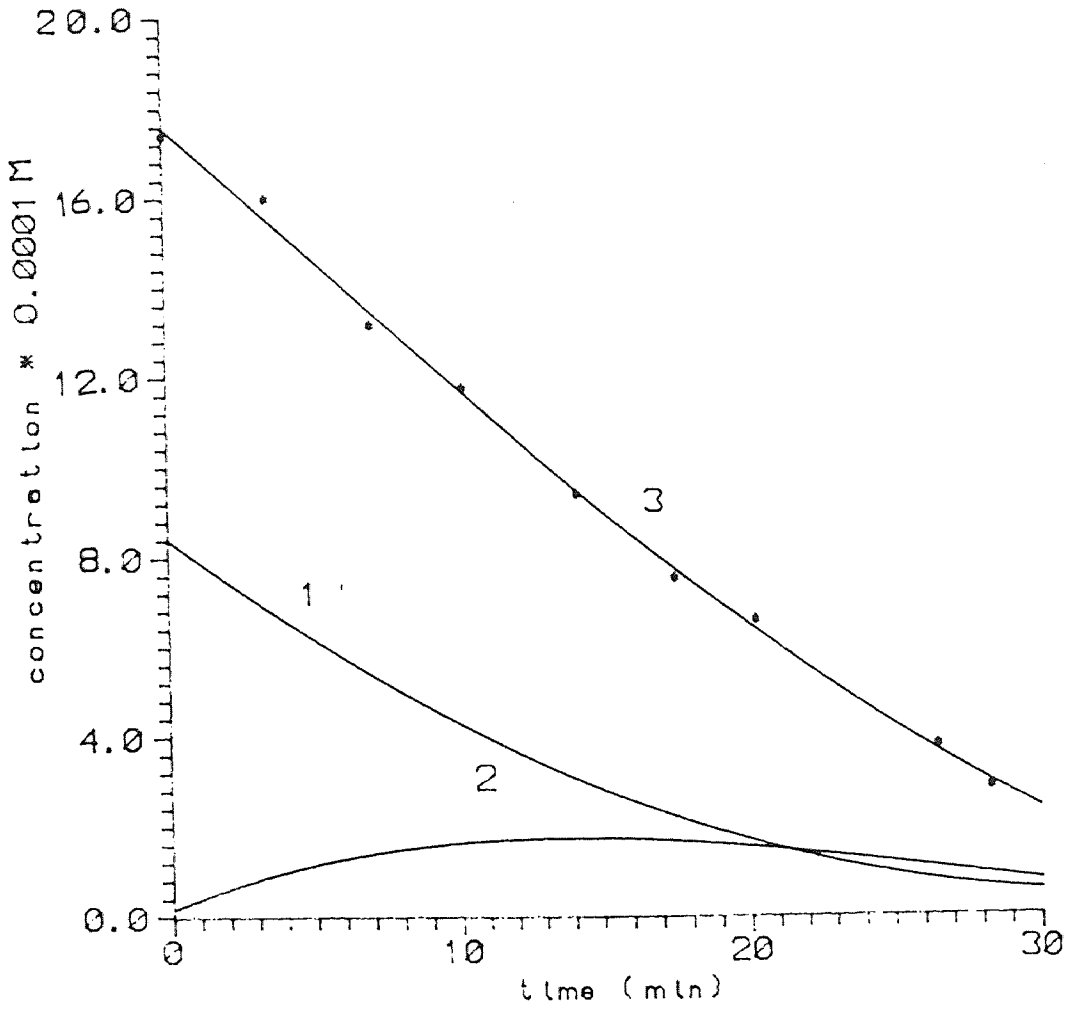

Fig 14: Biradical Disappearance Rate in Styrene Polymerization Initiated by AIBN at 70 C

1. Biradical Disappearance Rate
2. Corresponding Monoradical Disappearance
3. Combined Spins Disappearance Rate
   (*: experimental points)

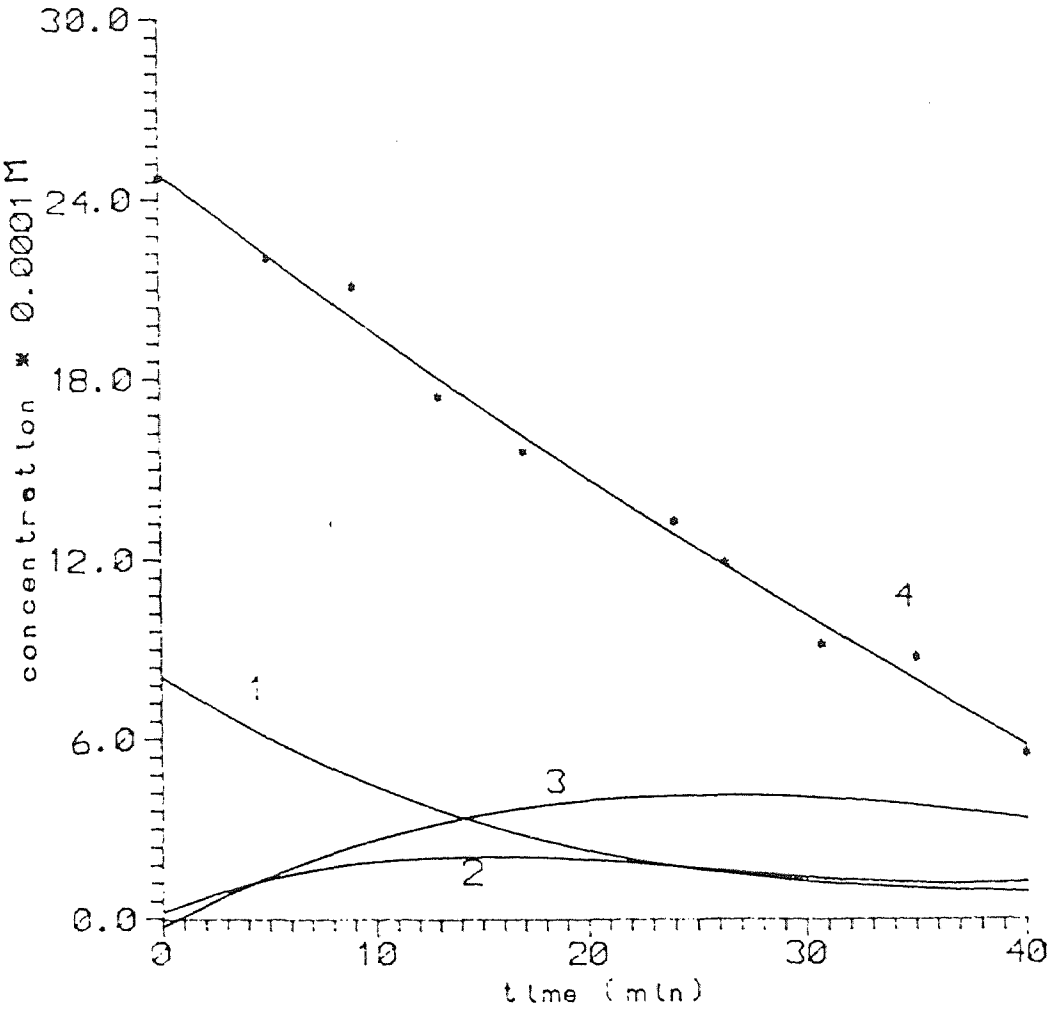

Fig 15: Triradical Disappearance Rate in Styrene Polymerization Initiated by AIBN at 70 C

1. Triradical Disappearance Rate
2. Corresponding Biradical Disappearance
3. Corresponding Monoradical Disappearance
4. Combined Spins Disappearance Rate
(*: experiment points; -: model values)

and 300 ppm. The two phase mixture was then sonicated and the oligomers were found completely suspended. Relaxation was measured on a Varian VXR400 NMR. Spin-lattice relaxation times (T_1) were determined by an Inversion-Recovery (IR) method and spin-spin relaxation times (T_2) were measured by a CPMG (Carr-Purcell Meiboom-Gill) technique.

Theoretically for a pure liquid T_2 can be obtained from the following equation:

$$\text{Log } I = \text{Log } I_o - t/T_2,$$

where I is echo amplitude at t, and I_o is equilibrium magnetization. But the experimental data for polynitroxides does not follow the above equation. As seen in Fig 16, T_2 seems to deviate more at longer echo times from the linear theoretical log plot. This effect may be due to the field inhomogeneity caused by nonhomogeneous insertion of nitroxides in the polymer backbones.

Hence T_2 was corrected by the following equation, taken from Ehman and coworkers [63]:

$$I = M(O) \exp[-(TE/T_2)-(j^2G^2DTE^3/12] \quad , \tag{36}$$

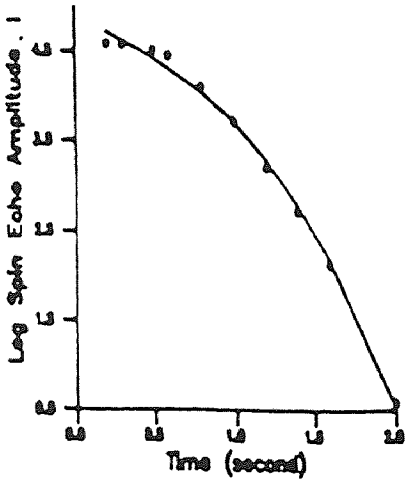

Fig 16: Spin echo intensity data for T_2 relaxation time for aqueous nitroxyl emulsion. Solid line illustrates least square fit to the equation (37). '*' is the experimental measurement.

where M(O) is the amplitude with zero echo delay, j is the gyromagnetic ratio and D is the diffusion coefficient. Using a simplified form and a nonlinear Marquart algorithm for curve fitting, we obtained A_1,A_2 and A_3, and T_2 is simply $-1/A_2$.

$$I = A_1 \exp[A_2 TE + A_3 TE^3] \quad , \tag{37}$$

In aqueous solution, proton relaxation times can be described by relaxivity and they are defined by the following relationships:

$$1/T_{1o} = 1/T_{1p} + 1/T_{1s}, \qquad 1/T_{2o} = 1/T_{2p} + 1/T_{2s}, \tag{38}$$

$$1/T_{1p} = K_1 * [P], \qquad 1/T_{2p} = K_2 * [P], \tag{39}$$

where T_{1o} and T_{2o} are the observed relaxation times of the two compounds, T_{1s} and T_{2s} are the relaxation times of solvents, T_{1p} and T_{2p} are relaxation times contributed to paramagnetic compounds, and K_1 and K_2 are the relaxivities of the paramagnetic compounds.

Table 3: Relaxivity of monomers in water (1/sec mM)

monomer	K1	K2
HPTPO	0.12	2.2
TEMPO	0.14	1.2

7.5 Experimentation on Imaging Characteristics of Nitroxides

7.5.1 Intensity Measurements on NMR

Relaxivity is strongly affected by chemical structure and each paramagnetic compound has a characteristic set of relaxivities. The data in Table 2 show that TEMPO has more capability to catalyze the relaxation times of the bulk water($k_2/k_1 = 1.2$)

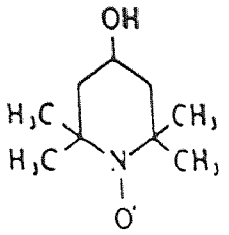

(I)

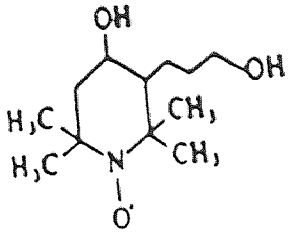

(II)

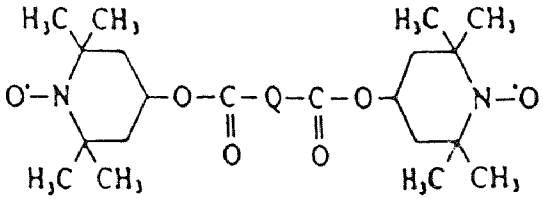

Q = — (III)

$(CH_2)_4$ (IV)

$(CH_2)_8$ (V)

$p\text{-}C_6H_4$ (VI)

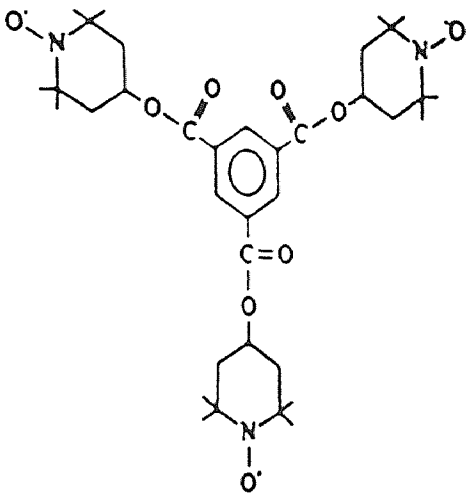

(VII)

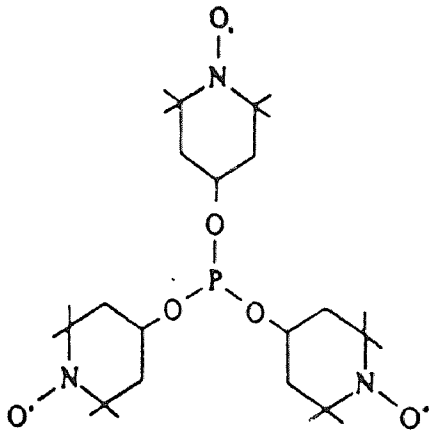

(VIII)

Fig 17: List of Compound Studied in a Clinical MRI Measurement.

than HPTPO ($k_2/k_1 = 2.2$). Not surprisingly, in substances like HPTPO with two hydroxyl groups and having more affinity with water, when T_1 is shortened (local magnetic field that accelerated phase loss is altered), T_2 is shortened simultaneously.

Two polynitroxides were further prepared, PMTMPO and PMSO to examine the hypothesis that polyradical paramagnetic centers will result in greater enhancement of MRI and offer much greater safety for an equivalent contrast enhancement. At 5ppm of emulsion in water, their T_1/T_2, 1.43/0.4 sec for PMTMPO and 2.04/1.2 sec for PMSO demonstrated that these linear polyradical centers tended to fold back. The resulting interference between the paramagnetic centers reduces overall effectiveness as contrast enhancement. This complex relationship of the folded multiple nitroxyl centers with their effects on T_1 and T_2 and signal intensity are polymer structure dependent, and is a subject of future work. It can be concluded that intensity response is not proportionally enhanced by increasing the number of paramagnetic centers.

ESR spectra (Figures 10b and 11b in Chapter 6) also illustrate that PMSO has less compacted nitroxyl centers, and enhancement is much better than PMTMPO, whose nitroxyl radicals are all entangled. But they both are much more resistant to *in vivo* bioreduction into hydroxylamine , are nontoxic at effective doses, and provide chemical flexibility in utilization either alone or as coupling agents to other biological molecules. Inorganic ions are being used extensively as contrast agents, but they also have drawbacks. The field of polynitroxides as contrast agents is relatively new. Polynitroxides may be better substitutes than heavy metals such as gadolinium.

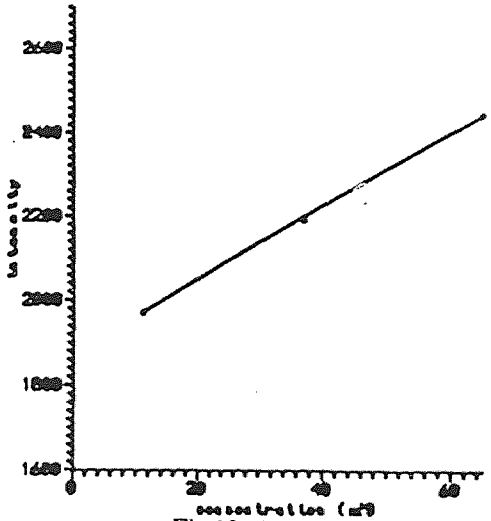

Fig 18: Compound (1) Intensity

As indicated earlier, the intensity enhancement is dependent on distribution of paramagntic centers which in turn depends on the structure of the polymer. Also the contrast enhancement is dependent on the medium in which the paramagnetic compounds are dispersed. Both polynitroxides were dispersed in cow plasma. The measurements of T_1 ratio between plasma and water indicated that cow plasma is two times more effective than water. The next step would be to chemically alter the polymer structure ad obtain a better distribution of the paramagnetic centers.

7.5.2 Signal Intensity on MRI

Preliminary examination on the relaxivities of nitroxides on NMR led us to design well distributed nitroxyl centers within nitroxide molecules. Their structures are shown and renumbered in Fig 17. The EPR spectra of HPTPO, compounds III and VII are illustrated in Figures 6c, 7b and 8b in Chapter 6. All the stable individual nitroxyls possess three well defined lines at room temperature. Nonetheless, the EPR spectra of the multinitroxides III and VII possess different characteristic features depending on the effect of conformational electronic exchange through the spatial interaction of the nitroxyl groups. From the spectra in Figures 7b and 8b (Chapter 6), we can observe that their nitroxyl paramagnetic centers do not interefere with one another. The downward shifts are due to the presence of at least one other nitroxide within the same molecule. Each of their paramagnetic centers can individually function as an image enhancing center to the surrounding protons.

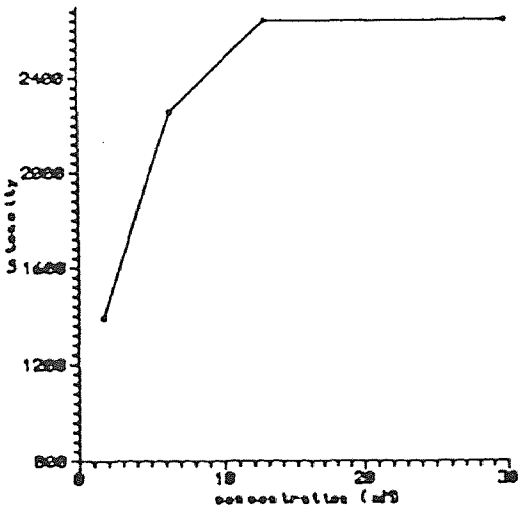

Fig 19: Intensity Response of Compound II

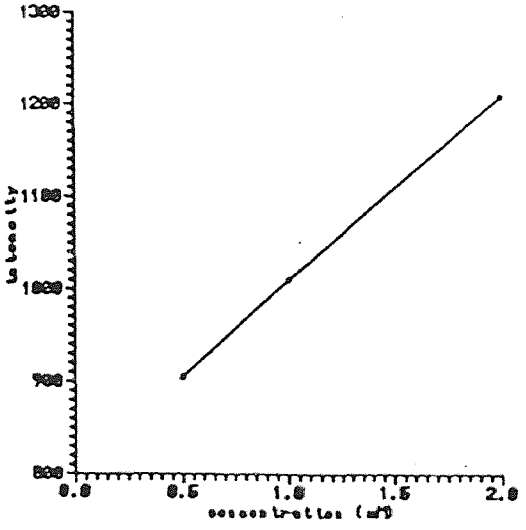

Fig 20: Intensity Response of Compound VIII

Different concentrations of these nitroxides (shown in Fig 17) are prepared in the vials for the clinical MRI measurements. These nitroxyl molecules do significantly enhance image contrast at very low concentration. Figure 21 shows a typical profile analysis on several samples. These images are individually read and compared. The results are listed in Table III and Figures 18, 19 and 20 where the dots represent the prepared concentrations. Many soluble nitroxides are cell permeant and tend to localize in the intracelluar compartment which contains 80% of the tissue water content. Water molecules can directly access the paramagnetic centers. This greatly helps in increased contrast.

Table 4: Intensity for biradicals and triradical

Compounds	Relative Intensity
III	1069
IV	1030
V	825
VI	893
VII	721

The intensity enhancement is dependent upon not only the distribution of the paramagnetic centers, but also the amount of their availability in the aqueous environment. TEMPO and HPTPO are both water soluble. The intensity (SI) of TEMPO is proportional to its concentration in water as shown in Figure 18 for the range 10-60 mM concentration. At 60 mM, its intensity response is 2448, whereas HPTPO is 2655 at 30 mM. Figure 19 demonstrates HPTPO intensity response with respect to concentration. Up to a concentration less than about 7 mM, the relationship is linear. At higher concentrations, it tends to reach equilibrium, i.e., maximum. Presumably at even higher concentrations, it would decline. HPTPO response is higher than TEMPO. For the compounds III-VII, due to their limited solubility in water, their intensity responses are finite. Compound VIII is found to be more soluble. Its response is measured and again an initial linear relationship is observed as shown in Figure 20. However, compounds III-VIII response may be strengthened

upon increasing of their solubility in water, for example, by hydroxylation of the carbonyl group into hydroxyl or introducing more polar functional groups into these molecules.

The comparison of nitroxides to iron and manganese standards (Figure 21) was also performed on MRI. The intensity of $FeCl_3$ at 2.5 mM is almost equal to that of TEMPO at 10 mM and HPTPO at 6mM. With the increase of free radicals in solution, the image intensity is proportionally increased.

The photograghs below (Fig 21) are prints from MRI negatives. Therefore, darker areas represent intensity. These results encourage us to further develop drugs with multiple nitroxyl cneters within single molecules. At lower concentrations of these multinitroxyls, the intensity will be greatly improved if the obstacle of their dissolution in water is overcome.

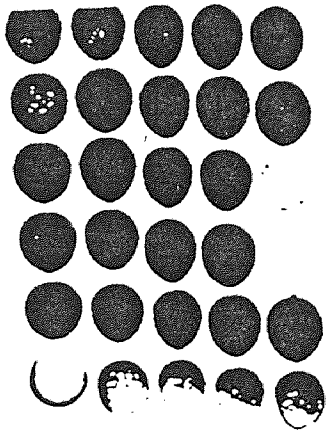

Fig 21: Contrast Image of All Compounds

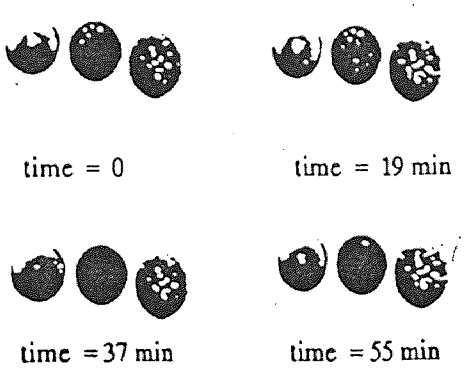

Fig 22: Image of Biomass Beads on MRI. Left to right, Liver, Yeast, and Bacterial Beads.

Such contrast agents are not improved by simple addition of nitroxyl centers to a given molecule. On the basis of compounds I and II, it is proposed that the OH group contributes to the intensity by rendering the functional group more polar. This effect induces nitroxyl paramagnetic centers more proximate to water protons, decreases their relaxation times and enhances image capability.

A gel-bead method (Figure 22) to characterize nitroxide behavior was tested with the immobilized liver enzyme, yeast and bacteria in 1 mM, 6mM and 12mM of HPTPO and conducted on MRI with respect to time. This system was adopted as a tool to characterize the behavior of nitroxides in biological systems hypothetically.

The characteristics of these three entrapped biological moieties are relatively similar. Initially, the individual image contrast of the liver microsomal beads was observed clearly at time equal to zero and later it vanished. The liver beads "disappeared" quickly, indicating high permeation. The contrast of yeast beads disappeared after 55 minutes of equilibration time. The contrast of bacterial beads remained after 55 minutes of equilibration. This behavior is complicated and needs further study.

The purpose here is only to demonstrate techniques to aid imaging studies which we are undertaking at the Biotechnology Laboratory of New Jersey Institute of Technology. Rigorous controls and detailed studies are further required. However, one explanation of non-diffusion in bacterial beads is as follows: during the MRI measurement the nitroxide imaging agents diffuse into the beads slowly and the image contrast of the beads appears and then starts disapperaing as their concentration equilibrates and finally loses contrast efficiency. These beads retain their physical integrity and they physically do not disappear. The liver beads are perfused most rapidly and soon contrast faded out. The contrast image of the bacterial consortium is retained most effectively in this examination. The bacteria may tend to either reject the diffusion of nitroxides or react slowly with the diffused nitroxides. The local concentration of nitroxides within these beads was never disturbed during 55 minutes of equilibration time. It is, however, too early to speculate on an active biological mechanism without further study.

CHAPTER 8
CONCLUSIONS

- The inhibition effect for the monoradical nitroxides studied on the styrene polymerization at 70°C was found to be practically independent of their substituents.
- Nitroxides are very effective inhibitors in styrene polymerization. No significant side reactions are observed in this study. Their inhibited polymerizations accompany an induction period during which no polymerization occurs. Its length is proportional to the concentration of inhibitors.
- At the beginning of the inhibited polymerization, the initiating radical concentration is very low due to the effect of inhibitor in higher concentration. As the inhibitor is consumed, radical concentration becomes higher. Finally the inhibitor loses its effect and the stationary polymerization resumes. The use of nitroxides as inhibitors does not affect the polymer molecular weight.
- The inhibiting behavior of stable mono-, bi- and tri-radical nitroxides was studied as well. When multiple nitroxyl molecules are used as inhibitors, the first spin tends to behave more reactively than the other spins. But their differences are small.
- These nitroxyl molecules do significantly enhance image contrast at very low concentration. The effect on MRI signal is dependent on their concentrations. Almost all compounds respond linearly to their concentrations, except for HPTPO whose linearity can only be observed at concentration lower than 7 mM.
- The intensity enhancement is also dependent on the distribution of paramagnetic centers. At very close distances of nitroxyl centers on the same molecule, the interradical interference causing a reduction in signal intensity is observed.

- HPTPO and TEMPO are water soluble. Their imaging enhancement capability is found to be better than the others.
- On MRI examination, the liver alginate beads demonstrated higher perfusion to their surrounding nitroxides than the yeast and bacterial beads, whereas the contrast image of bacterial beads was retained the longest. The mechanism requires further study.

BIBLIOGRAPHY

1. Yanaguchi, M., Miyazawa T., Takata T., and Endo T. "Application of Redox System Based on Nitroxides to Organic Synthesis." *Pure & Appl. Chem.* 62(1990): 217-222.

2. Volodarsky, L. "Advances in the Chemistry of Stable Nitroxides." *Pure & Appl. Chem.* 62(1990): 177-181.

3. Rozantsev, E. G. Free Nitroxyl Radical. New York: Plenum Press, 1970.

4. Kaufman, L., Crooks, L. E., Margulis, A. R. Nuclear Magnetic Resonance Imaging in Medicine. New York: Igaku-Shoin, 1981.

5. Brasch, R. C. "Work in Progress: Methods of Contrast Enhancement for NMR Imaging and Potential Applications." *Radiology* 147(1986): 781-787.

6. Ebdob, J. R. "Thermal Polymerization of Styrene - A Critical Review." *Br. Polym. J.* 3(1971): 9-12.

7. Mayo, F. R. "The Dimerization of Styrene." *J. Am. Chem. Soc.* 90(1968): 1289.

8. Badgasar'yan, Kh. S. Theory of Free Radical Polymerization. Translated from the Russian Second Edition by J. Schmorak, New York: Israel Program fc Scientific Translations, 1966.

9. Elster, A. D. Magnetic Resonance Imaging. Philadelphia: J. B. Lippincott Company, 1986.

10. Mayo, F. R. "Chain Transfer in the Polymerization of Styrene." *J. Am Chem. Soc.* 75(1953): 6133.

11. Flory, P. J. Principles of Polymer Chemistry. New York : Cornell University Press, 1953.

12. Walling, C., Free Radicals in Solution. New York : Wiley, 1957.

13. Flory, P. J., *J. Am. Chem. Soc.* 59(1937): 241.

14. Zimm, B.H. and Bragg, J.K. *J. Polymer Sci.* 9(1952): 476.

15. Sato, T., M. Abe, and T. Ostu *Makromol. Chem.* 178 (1977): 1267.

16. Bengough, W. J. *Chem. Ind.* 1955, 599.

17. Lewis, F. M. and M. S. Matheson *J. Am. Chem. Soc.* 71(1949): 747.

18. Overberger, C. G., M. T. O'shaughnessy and H. Shalit "The Preparation of Some Aliphatic Azo Nitriles and their Decomposition in Solution." *J. Am. Chem. Soc.* 71(1949): 2661.

19. Blackley, D. C. and H. W. Melville *Makromol. Chem.* 18 (1956): 16.

20. Moroni, A. F. "Uber den Einflub des Losungsmittels beim Thermischen Zerfalldes Azoisobuttersauredinitrils." *Makromol. Chem.* 105 (1967): 43-49.

21. Van Hook, J. P., and A. V. Tobolsky "The Thermal Decomposition of 2,2'-azo-bis-iosbutyronitrile." *J. Am. Chem. Soc.* 80(1958): 779.

22. Levy, S. A. Experimental and Computational Studies of Radical Scavenging and Polymerisation Inhibition. Dissertation, West Yorkshire, United Kingdom: University of Liverpool, 1987.

23. Hammond, G. S., J. N. Sen and C. E. Boozer *J. Am. Chem. Soc.* 77(1955): 3294.

24. Kerr, J. A. Rate Processes in the Gas Phase. Chap. 1 in Free Radicals. Vol I. New York: Wiley, 1973

25. Matheson, M. S., E. E. Auer, E. B. Bevilacqua, and E. J. Hant "Rate Constants on Free Radical Polymerization III." *J. Am. Chem Soc.* 71 (1949): 497.

26. Penchev, P. *Makromol Chem.* 177(1976): 413.

27. O'Driscoll, K. F. and H. K. Mahabadi "Spatially Intermittent Polymerization." *J. Polym. Sci. Polym. Chem. Ed.* 14(1976): 869.

28. Bamford, C. H., Barb, W. G., Jenkins, A. D., & Onyon, P. F. The Kinetics of Vinyl Polymerization by Radical Mechanisms. London : Butterworths, 1958.

29. Weissberger, A. Technique of Organic Chemistry. Vol. VIII, Part II, Chapter XX New York: Interscience Publishers, 1963.

30. North, A. M. Kinetics of Free Radical Polymerization. Oxford: Pergamon Press, 1966.

31. Odian, G. Principles of Polymerization, in Chapter 3 Radical Chain Polymerization. New York: John Wiley & Sons, 1981.

32. Eastmond, G. E. Free-Radical Polymerization. Chapter 2. New York: Elsevier, 1976.

33. Gol'dfein, M. D. Kinetics and Mechanism of the Radical Polymerization of Vinyl Monomers. Saratov, SSR: Izd. Saratov Gos. Univ., 1986

34. Kozhevnikov, N. V. Candidate's Thesis in Chemical Sciences. Saratov: Izd. Saratov Gos. Univ., 1977

35. Koenig, T. and H. Fischer Cage Effects. Chapt 4 Vol I. New York:Wiley, 1973.

36. Maybod, H. and M. H. George "Effect of Oxygen on Acrylonitrile Radical Polymerization: Application of Microwave Plasma Detector." *J. Polym. Sci. Polym. Lett. Ed.* 15(1977): 693.

37. George, M. H.and A. Ghosh *J. Polym. Sci. Polym. Chem. Ed.* 16(1978): 981.

38. George, M. H. Styrene. New York: Mercel Dekker, 1967.

39. Bartlett, P. D. and H. Kwart "Dilatometric Studies of the Behavior of Some Inhibitors and Retarders in the Polymerization of Liquid Vinyl Acetate." *J. Am. Chem. Soc.* 72(1950): 1051.

40. Hiatt, R. R. Bartlett, P. D. *J. Am.* Chem. Soc. 81(1959): 1149.

41. Billingham, N. C., A. J. Chapman and A. D. Jenkins "Vinyl Polymerization in the presence of Copper Salts." *J. Polym. Sci., Polym. Chem. Ed.* 18(1980): 827.

42. Bamford, C. H., W.G. Barb and F. F. Onyon Kinetics of Vinyl Polymerisation by Radical Mechanisms. Moscow: Inostr. Lit., 1961.

43. Gladyshev, G. P. Polymerisation of Vinyl Monomers. Alma-Ata, USSR: Izd. Akad. Nauk Kazakh., 1964.

44. Bagdasar'yan, Kh. S. Theory of Radical Polymerisation. Moscow: Izd. Nauka, Moscow, 1966.

45. Gladyshev, G. P. and V. A. Popov, Radical Polymerisation at Advanced Stages of the Reaction. Moscow: Izd., 1974.

46. Huyser, E. S. Free-Radical Chain Reactions. New York: Wiley-Interscience, 1970.

47. Barlett, I. and H. Kwart, *J. Amer. Chem. Soc.* 72(1950): 1051.

48. Miura, Y. and M. Nishigaki *Macromol. Chem.* 124(1969): 211

49. Pokhodenko, A. D. Phenoxy-Radicals. Kiev.: Izd. Naukova Dumka, 1969.

50. Bevington, J. C. and N. A. Ghenem, *J. Amer. Chem. Soc.* 2(1956): 3506.

51. Rozantsev, E. G. and V. D. Sholle Organic Chemistry of Free Radicals. Moscow: Izd.Khimiya, 1979.

52. Rozantsev, E. G., M. D. Gol'dfein, and A. V. Trubnikov "Stable Radicals and the Kinetics of the Radical Polymerization of Vinyl Monomers." *Uspekhi Khimii.* 55(1988): 1881-1897.

53. Ruban, L. V., A. L. Buchachenko, M. B. Neiman, and Yu. V. Kokhanov, "Kinetics of Addition of Nitroxide Mono- and Bi-radicals to Olephines." *Vysokomol. Soed.* 8A(1966): 1624.

54. Trubnikov, A. V. Abstract of Candidate's Thesis in Chemical Sciences. Saratov: Izd. Saratov. Gos. Univ., 1982.

55. Low, H., J. Paterson, J. Tedder, and J. Walton "Homosolvolysis." *J. Amer. Chem. Soc., Chem. Comm.* 171(1977).

56. Young, I. R., D. R. Bailes, M. Burl. "Initial clinical evaluation of a whole body nuclear magnetic resonance (NMR) tomography." *J. of Compt. Assist. Tomog.* 6(1982): 1-18

57. Kaufman, L., L. E. Crooks Nuclear Magnetic Resonance Imaging in Medicine. New York: Igakn-Shoin, 1981

58. Christiensen, H. E. Registry of Toxic Effects of Chemical Substances. Rockwille, MD: U. S. Department of HEW, NIOSH, 1975.

59. Browning, E. Toxicity of Industrial Metals. New York: Appleton-Century Crofts, 1969.

60. Levine, W. G. The Chelation of Heavy Metals. Oxford: Permangon Press,1984.

61. Valvis, I., D. Lischik, D. Shen, and S. Sofer, "In Vitro Synthesis of Nitroxies Free Radicals by Hog Liver Microsomes." *Free Radical Biology & Med.* 9(1990): 345-353.

62. Valvis, I., D. Lischik, D. Shen, and S. Sofer "Biooxidation of Diphenylamine by Hog Liver Microsomes." *Process Biochem. Intern.* 6(1990): 79.

63. Ehman, R. L., R. C. Brasch, M. T. McManara, U. Erikkson, G. Sosnovsky, J. Lukszo, and S. W. Li "Diradical Nitroxyl Spin Label Contrast Agents for Magnetic Resonance Imaging : A Comparison of Relaxation Effectiveness. " *Inves. Radio.* 2(1986): 125-131.

64. Zhang, Y. K. Studies on Nitroxides. Master Thesis. Beijing, China: Institute of Chemistry, Academia Sinica, 1987.

65. Shen, D. K. "Studies on Modified Polypropylene Fibers, Properties of Fiber Spun from a Polyblend of Polypropulene and a Copolymer of Styrene and 2,2,6,6-tetramethyl-4-piperidinylmethacrylate." *Polym. Comm. (China)* 5(1979): 285.

66. Shen, D. K. and L. Zhu "Synthesis of Polymeric Nitroxides and its Inhibition of Olephine Monomers." *Polym. Comm. (China)* 5(1982): 388.

67. Lakhwala, F. S. Doctoral Dissertation. Newark, New Jersey: New Jersey Institute of Technology, 1990.

68. Stork, G., A. Brizzolara, H. Landesman, J. Szmuszkovicz and R. Terrell "Enamine Alkylation and Acylation of Carbonyl Compounds." *J. Am. Chem. Soc.* 85(1963):207-221.

69. Mayo, F. R., R. A. Gregg, and M. S. Matheson "Chain Transfer in the Polymerization of Styrene VI." *J. Am. Chem. Soc.* 73(1951):1691-1699.

70. Ruban, L. V., A. L. Buchachenko, M. B. Neiman and Yu. V. Kokhanov "Inhibition of Radical Polymerization with Nitroxides Mono- and Biradicals." *Vysokomol. Soed.* 8A(1966): 1624.

71. Ogan, Marc D., R. C. Brusch "Annual Reports in Medical Chemistry." p.277 (1985).

72. Schulz, G. A., Dinglinger A., and Husemann E. Z. Phys. Chem., 43B(1939): 385.

73. Parat, F., and Kirchner K. *Naturwissenschaften* 45(1958): 129.

74. Van Hook, J. P., and A. V. Tobolsky *J. Am. Chem. Soc.*, 80(1958): 779.

75. Bretts, J., F. S. Dainton and K. J. Ivin *Trans. Faraday Soc.*, 58(1962): 1203.

76. Gee, G. and H. W. Melville *Trans. Faraday Soc.*,40(1944): 240..

77. Tseitlin, P. G. and Medvedev S. S. *Zhfkh*, 18(1944): 13.

78. Tudos, F., Shimandi L. and Azori M. *Vysokomol. Soed.*, 4(1962): 1431.

79. Tudos, F., and Shimandi L. *Vysokomol. Soed.*, 4(1962): 1271.

80. Bevington, J. and H. Troth *Trans. Farad. Sci.*, 59(1963): 1348.

81. Gomberg, M. *Ber.*, 33(1900): 3150.

82. Mayo, F. R. and R. A. Gregg *J. Amer. Chem. Soc.*, 70(1948): 1284.

83. Goldschmidt, S. and J. Bader *Annalen*, 392(1912): 186.

84. Yarmolyuk, B. M., O.M. Polumbrik, and G. F. Dvorko,Symposium,"Reactivity of Organic Compounds." *Izd. Tartu. Univ. Tartu*, 10(1973): 893.

85. Tudos, F., T. Bereznikh, and M. Azori *Acta Chim. Acad. Sci. Hung.*, 24(1)(1960): 91.

86. Zhulin, V. P., A. G. Squashina, and E. G. Rozantsev *Izv. Akad. Nauk SSSR, Ser. Khim.*, 7(1977): 1511.

87. Zhulin, V. P. and A. G. Stashina *Izv. Akad. Nauk SSSR, Ser. Khim.*, 11(1977): 2586.

88. Trubnikov, A. V., M. D. Gol'fein and A. D. Stepukhovich *Vysokomol. Soed.*, 25B(1983): 495.